Moritz Bürgler, BSc

Reaction intensification for the valorization of fatty acids with (co-immobilized) P450 BM3 and glucose dehydrogenase

MASTER´S THESIS

to achieve the university degree of

Diplom-Ingenieur

Master´s degree programme: Biotechnology

submitted to

Graz University of Technology

Institute of Biotechnology and Biochemical Engineering

Supervisor

Univ.-Prof. Dipl.-Ing. Dr.techn. Bernd Nidetzky

Dipl.-Biol. Dr.rer.nat. Alexander Dennig

Graz, January 2020

Eidesstattliche Erklärung

Ich erkläre an Eides statt, dass ich die vorliegende Arbeit selbständig verfasst, andere als die angegebenen Quellen/Hilfsmittel nicht benutzt, und die den benutzten Quellen wörtlich und inhaltlich entnommenen Stellen als solche kenntlich gemacht habe.

Graz, am ....

(Unterschrift)

Statutory Declaration

I declare that I have authored this thesis independently, that I have not used other than the declared sources / resources, and that I have explicitly marked all material which has been quoted either literally or by content from the used sources.

Graz, ...

(signature)

Kurzfassung

Fettsäuren (FS) fallen in großem Maßstab aus Abfällen der Agrikultur und Industrie an und stellen eine billige Ressource für die enzymbasierte Produktion von wertvollen chemischen Bausteinen dar. Cytochrom P450 Monooxygenasen sind vielversprechende Enzyme für die Valorisierung von FS, da sie ein breites Substratspektrum abdecken und häufig selektiv hydroxylieren. Ein außergewöhnliches Enzym ist P450 BM3 von *Bacillus megaterium,* da es unabhängig von anderen enzymatischen Redoxpartnern arbeitet (nur NAD(P)H und O_2 sind notwendig) und eine vergleichsweise hohe Aktivität aufweist. Entscheidende Faktoren für die Anwendung dieses Enzyms sind eine präzise Prozesskontrolle, inklusive der Versorgung von O_2 und Reduktionsäquivalenten (NAD(P)H). Diese Arbeit behandelt die Prozessintensivierung für die Umsetzung des wasserunlöslichen Modelsubstrates Dodecansäure (C12:0) in die entsprechenden ω-Hydroxy-Dodecansäuren (C12:0-OHs). Freie Enzyme (zellfreie Extrakte von Z_P450 BM3 and Wt_P450 BM3) wurden mit co-immobilisierten Enzymen auf Basis der Reaktionsrate, der Umsetzung und *in-operando* Kopplungseffizienzen verglichen. Initiale Reaktion mit Z_P450 BM3 und Z_GDH oder co-immobilisierten Enzymen erzielten volle Umsetzung von 40 mM C12:0 (8 g L^{-1}). Unter operativen Bedingungen wies Z_P450 BM3 allerdings unzureichende Bindungsstabilität zum Trägermaterial auf, was das Recycling des Katalysators limitiert. Da FS aufgrund ihrer geringen Wasserlöslichkeit dazu tendieren als Feststoff auszufallen, wurde die Durchführung von Fed-Batch Reaktionen untersucht. Ein interessantes und zu unserem Wissen kaum behandeltes Konzept in der Biokatalyse ist die O_2-abhängige Zugabe des organischen Substrates. Mithilfe dieser Reaktorführung und unter Verwendung von Wt_P450 BM3 konnten >99% (50 mL Maßstab) oder 90% Umsatz (500 mL Maßstab) von 80 mM (16 g L^{-1}) C12:0 erreicht werden. Für die 50 mL Reaktion betrug die initiale Raum-Zeit-Ausbeute (RZA) 1.7 g L^{-1} h^{-1}. Über die gesamte Reaktionszeit (28 h) konnte ein RZA von 0.56 g L^{-1} h^{-1} erreicht werden. Im Vergleich zu bereits publizierten P450 BM3 katalysierten C12:0 Umsetzungen wurde der Produkttiter mehr als verdoppelt. In der präparativen Aufarbeitung der Produkte ohne Chromatographie wurden exzellente Ausbeuten (79 bis 92%) und eine hohe GC-Reinheit (80 bis 92%) erreicht. Aufgrund von Überoxidation in den präparativen Reaktionen wurden kinetische Paramater für C12:0-OHs mit verschiedenen P450 BM3 Präparationen bestimmt und mit Parametern für C12:0 verglichen. Gemessene NADPH und O_2 Verbrauchsraten waren zwei bis drei Mal niedriger und K_m Werte zwei bis vier Mal höher in Reaktionen mit C12:0-OHs im Vergleich zu Reaktionen mit C12:0. Diese Resultate erklären die Limitierung für eine maximale Substratladung in den präparativen Reaktionen, da bei sehr hohen Produkttitern C12:0 und C12:0-OHs um das aktive Zentrum der P450 BM3 konkurrieren. Zusammengefasst, das etablierte Reaktionssystem stellt die Basis für weitere Reaktionsintensivierung dar und schafft Zugang zu potentiellen chemischen Bausteinen für die Herstellung von Biopolymeren im präparativen Maßstab.

Abstract

Fatty acids (FAs) occur to a large extend in agriculture, domestic and industrial waste and represent a cheap resource for the selective enzyme catalysed production of valuable compounds, for example hydroxy FAs. Especially, cytochrome P450s were identified as promising candidates for FA valorisation, as they cover a wide substrate spectrum and can hydroxylate selectively. An extraordinary candidate for this purpose is P450 BM3 from *Bacillus megaterium*, a self-sufficient monooxygenase (no additional redoxpartners required) displaying high catalytic activity. A prerequisite and often still limiting factor for a successful application of this monooxygenase is a precise process control including supplementation of sufficient O_2 and the reduction equivalents NAD(P)H. This work deals with the intensification for the conversion of the water-insoluble model substrate dodecanoic acid (C12:0) into a mixture of ω-hydroxy dodecanoic acids (C12:0-OHs). Cell free extracts of Wt_P450 BM3 and Z_P450 BM3 were benchmarked against a co-immobilizate of Z_P450 BM3 and Z_GDH in terms of the reaction rate, the conversion and the *in-operando* coupling efficiency. Initial reactions in batch-mode resulted in full conversion of 40 mM C12:0 (8 g L^{-1}) with co-immobilized and free Z_P450 BM3 and Z_GDH. However, Z_P450 BM3 did not fulfil an important pre-requisite for immobilized enzymes, a long-term binding stability on the carrier under operational conditions. Therefore, the co-immobilizate could not be reused if reactions with longer reaction times (>6 h) were conducted. The usability of a fed-batch mode for higher substrate titers was investigated, as FAs exhibit a low solubility limit and tend to form solid particles in water. An interesting and to the best of our knowledge underexplored concept for oxygenase biocatalysis is an O_2 concentration dependent substrate feed (here C12:0). Applying this feeding strategy resulted in >99% conversion (50 mL scale) or 90% conversion (500 mL scale) of 80 mM (16 g L^{-1}) C12:0 with Wt_P450 BM3. An initial space-time-yield (STY) of 1.7 g L^{-1} $h^{-1}$and an overall STY of 0.56 g L^{-1} h^{-1} (28 h reaction time) could be achieved on a preparative scale of 50 mL. In comparison to previously described P450 BM3 catalysed C12:0 hydroxylations, the product titre could be more than doubled without the need for expensive additives/solubilizers. Preparative isolation of the products yielded C12:0-OHs with excellent isolated yields (79 to 92%) and high GC purities (80 to 92%) in a single organic extraction step. As significant overoxidation of the products (C12:0-OHs) was observed, kinetic parameters for the isolated C12:0-OHs and different P450 BM3 preparations were measured and compared to parameters for C12:0. Determined NADPH and O_2 consumption rates were 2- to 3-fold lower and K_m values were 2- to 4-fold higher for P450 BM3 catalysed C12:0-OHs reactions compared to C12:0 reactions. These findings explain the defined limit (80 mM) for conversion of C12:0 since over longer reaction times C12:0 and C12:0-OHs compete for the active centre of P450 BM3. Concluded, the established system provides the basis for additional reaction intensification and provides access to potential building blocks e.g. for biopolymer production.

Acknowledgements

First, I would like to thank Prof. Dr. Bernd Nidetzky for giving me the opportunity to work on this interesting topic at the interface of biotechnology and bioprocess engineering. I greatly benefited from your instructive comments and suggestions during the meetings and institute seminars.

Furthermore, I am deeply grateful to Dr. Alexander Dennig for his supervision during the whole thesis. I am particularly grateful for your guidance throughout the project and for providing me scientific expertise and ideas. The frequent discussions greatly contributed to the outcome of this project.

In the following, I would like to thank Dr. Juan Bolivar for sharing his expertise in oxygen related topics and the helpful instructions in the oxygen analytics and in the application of the respective instruments and programmes.

I would like to thank Sabine Schelch and Stefanie Gross Belduma for guiding me through the HPLC measurements. At this point I also would like to thank the entire institute team, on the one hand for all science related discussion, and on the other hand for the welcoming atmosphere at the institute and all off-topic chats.

Finally, I would like to thank my entire family and my friends for accompanying me through the last years. The success of this project greatly benefited from your motivating quotes and support.

Table of contents

1 Introduction 1

1.1 The role of P450s in fatty acid activation and valorization 1

1.2 Prep-scale examples in literature for the conversion of fatty acids by P450 BM3 3

1.3 Oxygen in biocatalysis: current strategies in controlling bioprocesses with O_2 5

1.4 Enzyme immobilization for preparation of heterogeneous catalysts 7

1.5 Immobilisation of P450 BM3 8

1.6 Aim of this thesis 10

2 Material and methods 11

2.1 Materials 11

2.1.1 Chemicals 11

2.1.2 Enzymes 12

2.1.3 Growth media and supplements 12

2.1.4 Bacterial strain 13

2.1.5 Laboratory devices 13

2.2 Analytics 15

2.2.1 Carbon monoxide titration for the determination of active P450 BM3 15

2.2.2 Photometric assay for the determination of GDH activity 15

2.2.3 GC-FID and GC-MS analysis 16

2.2.4 Determination of gluconic acid (GlcA) concentration via HPLC 18

2.2.5 K_La value determination 20

2.2.6 SDS-PAGE 22

2.3 Enzyme expression and preparation of cell free extracts (CFEs) 23

2.3.1 Expression of P450 BM3 23

2.3.2 Expression of Z_GDH 23

2.3.3 Preparation of cell free extracts (CFEs) of P450 BM3s and Z_GDH 23

2.4 Co-Immobilization of Z_P450 BM3 and Z_GDH on ReliSorb^{TM} SP400 24

2.4.1 Preparation of enzyme solutions 24

2.4.2 Co-immobilization of enzymes 24

2.5 Purification of P450 BM3 25

2.6 Preparative scale reactions to produce C12:0-OHs 26

2.7 Preparative isolation of C12:0-OHs 27

2.8 Determination of kinetic key parameters of P450 BM3 28

3 Results and discussion 31

3.1 Expression and immobilization of enzymes 31

3.1.1 Optimized immobilization process for Z_{Basic2}-tagged enzymes 31

3.1.2 Co-immobilization of Z_P450 BM3 and Z_GDH on g-scale 33
3.1.3 Single step immobilization of Z_P450 BM3 34
3.1.4 36
3.1.5 Storage stability of immobilized enzymes 36
3.2 Preparative scale reaction to convert dodecanoic acid 39
3.2.1 Relevance of pH stabilization and O_2 supply in the P450/GDH coupled reaction 39
3.2.2 Establishing a robust reaction platform for oxyfunctionalization 42
3.2.3 Oxygen concentration dependent substrate feed 57
3.2.4 Preparative isolation of C12:0-OHs 72
3.2.5 Relevance of product overoxidation for the whole process 73
3.3 Determination of kinetic parameters of varying P450 formulations 75
3.3.1 Purification of enzymes 75
3.3.2 Overview of determined kinetic parameters 76
4 Summary and conclusion 78
5 Appendix 82
5.1 Storage stability of co-immobilizate 82
5.2 Testing of carrier reusability 83
5.3 NAD(P)H oxidation reactions with CFE 83
5.4 Foam composition analysis 86
5.5 Influence of DMSO and EtOH on the conversion C12:0 86
5.6 Technical summary for oxygen dependent substrate feed reactions 88
5.7 Preparative scale isolation of C12:0-OHs 92
5.8 Purification of Wt_P450 BM3 and Z_P450 BM3 96
5.9 Michaelis-Menten plots 97
6 References 101

List of figures

Figure 1: Catalytic cycle for cytochrome P450s. 2

Figure 2: Reaction scheme for the envisioned preparative-scale conversion of dodecanoic acid with P450 BM3 supported by glucose dehydrogenase (GDH). 3

Figure 3: Recycling study with co-immobilized Z_P450 BM3 and Z_GDH. 4

Figure 4: Requirements for a general immobilization strategy 8

Figure 5: Schematic representation of the immobilization of a Z_{Basic2}-tagged enzyme on ReliSorb^{Tm} SP400. 9

Figure 6: Calibration curve for C12:0 (left) and C12:0-OHs (right) for GC-FID analysis. 17

Figure 7: Calibration curve for C12:0 for GC-MS analysis. 17

Figure 8: Representative chromatograms of a C12:0 conversion via the P450 BM3/GDH reaction system for GC-FID (top) and GC-MS (bottom) analysis. 18

Figure 9: Chromatograms of samples containing 15 mM GlcA (left) and 15 mM Glc (right). 19

Figure 10: Chromatograms of samples containing 15 mM GlcA (left) and 15 mM Glc (right). 19

Figure 11: Calibration curve for HPLC analysis and quantification of GlcA. 19

Figure 12: Increase of O_2 concentration monitored in a 50 mL reactor (glass beaker) for k_La determination. 21

Figure 13: Determination of the k_La for a 50 mL reactor. 21

Figure 14: General set-up for the preparative scale production of C12-OHs with the P450 BM3/GDH reaction system. 27

Figure 15: Immobilization efficiency for Z_P450 BM3 (loaded in three steps) and Z_GDH (loaded in one step) at varying pH values. 32

Figure 16: Immobilization efficiency of Z_P450 BM3 (loaded in three steps) and Z_GDH (loaded in one step) at varying NaCl concentrations. 33

Figure 17: ReliSorb^{Tm} SP400 before (left) and after the immobilization (right) of Z_P450 BM3 and Z_GDH. 33

Figure 18: Immobilization efficiencies for the preparation of the co-immobilizate on g-scale. 34

Figure 19: SDS-PAGE to monitor the storage stability of the co-immobilizate in liquid (A) and the respective carriers in solution (B). 36

Figure 20: Analysis of storage stability of BM3/GDH on ReliSorb^{Tm} SP400 via SDS-PAGE. 37

Figure 21: Conversion of 2 mM C12:0 catalyzed by the co-immobilizate after zero weeks (0 W) and one week (1 W) storage at 4°C. 37

Figure 22: Activity study for the co-immobilizate stored at -20°C. 38

Figure 23: Reaction scheme for the catalyzed reaction by the P450 BM3/GDH system to convert C12:0. 39

Figure 24: Change in pH in the Z_P450 BM3/Z_GDH system overtime. 40

Figure 25: Influence of aeration (21% O_2) on the formation of C12:0-OHs. 41

Figure 26: Influence of aeration (21% O_2) on the change in pH in the Z_P450 BM3/Z_GDH system. 41

Figure 27: Time courses for the products (C12:0-OHs), the substrate (C12:0), the consumed KOH and the O_2 concetration for a reaction with 2 µM Z_P450 BM3 and 6.8 U mL^{-1} Z_GDH. 43

Figure 28: Time courses for the products (C12:0-OHs), substrate (C12:0), consumed KOH and O_2 concetration for a reaction with 2 µM Z_P450 BM3 and 6.8 U mL^{-1} Z_GDH (free). 43

Figure 29: C12:0 distributon between ReliSorb™ SP400 and the water phase. 46

Figure 30: Comparison of the product formation and substrate consumption for clogged and not clogged particles. 47

Figure 31: NADH (right) and NADPH (left) consumption of immobilized Z_GDH and spiked free Z_GDH. 50

Figure 32: SDS-PAGE for analysis of *in-operando* binding stability of Z_P450 BM3 and Z_GDH on ReliSorb™ SP400.. 52

Figure 33: Influence of reaction components (NaCl, C12:0), stirring and different buffer systems/bulk phases on the binding stability of Z_P450 BM3 and Z_GDH on ReliSorb ™ SP400. 53

Figure 34: Initial experiment for oxygen dependent substrate feed to convert C12:0 on preparative scale. 57

Figure 35: Time course for the O_2 concentration and C12:0 and C12:0-OHs concentration during conversion of 80 mM C12:0 with 2 µM Wt_P450 BM3 and 1.9 U mL^{-1} GDH (DSM).. 61

Figure 36: Influence of silicone antifoam on the initial product formation rate. 62

Figure 37: Wt_P450 BM3 titration experiment 63

Figure 38: Adaption of the self-assembled gassing unit for the 500 mL reaction. 64

Figure 39: Time course for the O_2 concentration, the product formation and the KOH consumption for an 80 mM C12:0 conversion at 500 mL scale. 65

Figure 40: Comparison of the relative overoxidation product (%) to the coupling efficiency (%). 69

Figure 41: Flow scheme for the separation of solid particles from the reaction bulk and subsequent extraction and GC-FID analysis. 72

Figure 42: Reaction scheme for overoxidation reaction catalysed by P450 BM3 and GDH yielding dihydroxylated fatty acids (other routes potentially forming ketones are not shown here) [62]. 74

Figure 43: Conversion of C12:0-OHs by the Wt_P450 BM3/GDH (DSM) system. 75

Figure 44: SDS-PAGE for collected fractions during purification of Wt_P450 BM3 (left) and Z_P450 BM3 (right). 76

Figure 45: Conversion experiments for the liquid stored carrier (A1 and A2) and the lyophilized carrier (B1 and B2) after zero and one week (W) of storage at 4°C. 82

Figure 46: Course of oxygen concentration and the GC-MS chromatogram after 5.5 h reaction time for a reaction with reused co-immobilizate (previous reaction ran for 23 h reaction, 20000 TTN_{P450}). 83

Figure 47: Consumption of NADH in 1 mL reactions containing 10 U mL^{-1} Z_GDH CFE, 300 µM NADH, 50 mM KPi (pH 7.5) and 0 or 5 mM benzaldehyde. 83

Figure 48: Consumption of NADPH in 1 mL reactions containing 10 U mL^{-1} Z_GDH CFE, 300 µM NADPH, 50 mM KPi (pH 7.5) and 0 or 5 mM benzaldehyde. 84

Figure 49: Conversion of 5 mM benzaldehyde by 5 U mL^{-1} Z_GDH CFE to detect ADH background activity from *E. coli* enzymes. 85

Figure 50: Conversion of 5 mM acetophenone by 5 U mL^{-1} Z_GDH CFE to detect ADH background activity from *E. coli* enzymes. 85

Figure 51: Composition of the foam flushed upwards by the O_2-stream after 4 h of gassing (>82% C12:0). 86

Figure 52: Influence of the co-solvent and pulse-feeding on the conversion of C12:0 by Wt_P450 BM3 (2 µM)/Z_GDH (7 U mL^{-1}) reaction system. 87

Figure 53: Time course for the conversion of 40 mM C12:0 (here: >99%) with free Z_P450 BM3 (2 µM) and Z_GDH (10.8 U mL^{-1}). 88

Figure 54: Time course for the conversion of 40 mM C12:0 (here: 96.5%) with the co-immobilizate (2 µM Z_P450 BM3/10.8 U mL^{-1} Z_GDH. 89

Figure 55: Time course for the conversion of 48 mM C12:0 with the co-immobilizate (2 µM Z_P450 BM3/8.8 U mL^{-1} Z_GDH) (75% GC-area product). 90

Figure 56: GC-MS chromtogram obtained after the preparative extraction of a 36 mM C12:0 reaction (50 mL) with free Z_P450 BM3. 92

Figure 57: GC-MS chromtogram obtained after the preparative extraction of a 40 mM C12:0 reaction (50 mL) with co-immobilizate. 92

Figure 58: GC-FID chromtogram obtained after the preparative extraction of a 40 mM C12:0 reaction (50 mL) with free Wt_P450 BM3. 92

Figure 59: GC-FID chromtogram obtained after the preparative extraction of a 80 mM C12:0 reaction (50 mL) with free Wt_P450 BM3. 93

Figure 60: GC-FID chromtogram obtained after the preparative extraction of a 40 mM C12:0 reaction (50 mL) with free Z_P450 BM3. 93

Figure 61: GC-FID chromtogram obtained after preparative extraction of a 40 mM C12:0 reaction (50 mL) with co-immobilizate. 93

Figure 62: GC-FID chromtogram obtained after the preparative extraction of the water phase of a 48 mM C12:0 reaction (50 mL) with co-immobilizate. 94

Figure 63: GC-FID chromtogram obtained after the preparative extraction of the carrier of a 48 mM C12:0 reaction (50 mL) with co-immobilizate. 94

Figure 64: GC-FID chromtogram for the preparative extraction (7 g material isolated) of the carrier of a 80 mM C12:0 reaction (500 mL) with free Wt_P450 BM3. 94

Figure 65: GC-FID chromtagogram of the removed solids from the 80 mM C12:0 reaction (500 mL)..95

Figure 66: Purification of Wt_P450 BM3 (top) and Z_P450 BM3 (bottom). 96

Figure 67: Determination of the O_2 consumption rate for different C12:0 (top) and C12:0-OHs (bottom) concentrations for purified Wt_P450 BM3. 97

Figure 68: Determination of the O_2 consumption rate for different C12:0 (top) and C12:0-OHs (bottom) concentrations for purified Z_P450 BM3. 98

Figure 69: Determination of the O_2 consumption rate for different C12:0 (top) and C12:0-OHs (bottom) concentrations for the co-immobilizate. 99

Figure 70: Determination of the O_2 consumption rate for different C12:0 (top) and C12:0-OHs (bottom) concentrations for Wt_P450 BM3 (CFE). 100

List of tables

Table 1: Selected relevant examples of P450 BM3 catalyzed conversions of fatty acids. 5

Table 2: Selected strategies to control O_2 in biocatalysis and related applications. 6

Table 3: List of applied chemicals 11

Table 4: List of applied enzymes 12

Table 5 List of used media including compound concentrations and supplements 12

Table 6: Bacterial strain used for protein expression 13

Table 7: List of laboratory devices 13

Table 8: Temperature program used for GC-FID and GC-MS analysis 16

Table 9: General composition of samples for SDS-PAGE analysis. 22

Table 10: General reaction composition of reactions for the preparative scale conversion of C12:0. 26

Table 11: Reaction set-up for the determination of v_{max} and K_m for conversion of C12:0. 29

Table 12: Reaction set-up for the determination of v_{max} and K_m for conversion of C12:0-OHs. 29

Table 13: Reaction set-up for the determination of the maximal NADPH consumption rate with C12:0 as substrate.. 29

Table 14: Reaction set-up for the determination of the maximal NADPH consumption rate with C12:0-OHs as substrate. 30

Table 15: Reaction set-up for the determination of the coupling efficiency for conversion of C12:0. 30

Table 16: Reaction set-up for the determination of the coupling efficiency for conversion of C12:0-OHs. 30

Table 17: Loaded nmole Z_P450 BM3 and Units Z_GDH on ReliSorb ^{Tm} SP400 at different pH values and NaCl concentrations. 32

Table 18: Comparison of loading three times 4 µM Z_P450 BM3 and one time 10.9 µM Z_P450 BM3. 35

Table 19: Composition of the 45 mL reactor to convert C12:0 on preparative scale 42

Table 20: Influence of Antifoam 204 and ReliSorb^{Tm} SP400 on the k_La. 44

Table 21: Summary of determined key reaction paramters obtained for the initial reaction with free enzymes and the co-immobilizate. 45

Table 22: Comparison of the oxygen background consumption for different enzyme preparations. . 49

Table 23: Influence of different co-solvents on the conversion and defoaming. 56

Table 24: Influence of ReliSorb^{TM} SP400 and silicone antifoam on the k_La value. 58

Table 25: Comparison of feed intervals for free Wt_P450 BM3, free Z_P450 BM3 and the co-immobilizate. 60

Table 26: Comparison of k_La values for the 50 and 500 mL reaction, respectively. 64

Table 27: Determination of *in-operando* coupling efficiencies via GlcA concentration (50 mL and 500 mL reaction) and oxygen transfer rate (OTR, 16.0 mM h^{-1} for 500 mL reactoion) for Wt_P450 BM3. 66

Table 28: Determination of in-operando coupling efficiencies via GlcA concentration measurements in reaction with free Z_P450 BM3 and the co-immobilizate. 68

Table 29: Summary of determined key reaction parameters for reactions with oxygen dependent substrate feed. 71

Table 30: Summary of the preparative isolation of C12:OHs of various conducted reactions. 73

Table 31: Determined key kinetic parameters for different monooxygenase catalysts and C12:0 and C12:0-OHs as substrate. 77

Table 32: GC-MS temperature program for evaluation of the ADH background reactions in the Z_GDH CFE. 84

Table 33: Fed-strategies for the substrate pulsing experiments for investigation of the co-solvent influence. 86

Table 34: Key reaction parameters for a 40 mM C12:0 conversion with free Z_P450 BM3 (50 mL scale). 88

Table 35: Key reaction parameters for a 40 mM C12:0 conversion with co-immobilizate (50 mL scale). 88

Table 36: Key reaction parameters for a 48 mM C12:0 conversion with co-immobilizate (50 mL scale). 89

Table 37: Key reaction parameters for the conversion of 80 mM C12:0 conversion with Wt_P450 BM3 (50 mL scale). 90

Table 38: Key reaction parameters for the conversion of 80 mM C12:0 with Wt_P450 BM3 and Z_GDH (500 mL scale). 91

Abbreviations

Abs	Absorption
ALA	δ -aminolevulinic acid
DMSO	Dimethyl sulfoxide
DTT	Dithiothreitol
C12:0	Dodecanoic acid
C12:0-OHs	ω-Hydroxy dodecanoic acids (ω-1, ω-2 and ω-3)
EtOAc	Ethyl acetate
EtOH	Ethanol
GC-FID	Gas chromatographer coupled to flame ionization detector
GC-MS	Gas chromatographer coupled to mass spectrometry
GDH (DSM)	Glucose dehydrogenase purchased from DSM
Glu	Glucose
GlcA	Gluconic acid
GOX	Glucose oxidase from *Aspergillus niger*
IPTG	Isopropyl β-D-1-thiogalactopyranoside
KPi	Phosphate buffer
k_{cat}	Catalytic constant [s^{-1}]
LB	Lysogeny broth
MeOH	Methanol
NAD(P)	Nicotinamide adenine dinucleotide (phosphate)
SDS-PAGE	Sodium dodecyl sulfate polyacrylamide gel electrophoresis
TB	Terrific broth
TTN	Total turnover number [-]
Wt_P450 BM3	Cytochrome P450 fatty acid ω-hydroxylase from *Bacillus megaterium* (His-tagged)
Z_GDH	Glucose dehydrogenase (type IV) from *Bacillus megaterium* (Z_{Basic2}-tagged)
Z_P450 BM3	Cytochrome P450 fatty acid ω-hydroxylase from *Bacillus megaterium* (Z_{Basic2}-tagged)

1 Introduction

1.1 The role of P450s in fatty acid activation and valorization

In nature fatty acids occur predominately as triglycerides, phospholipids or cholesteryl esters and rather small amounts are available as free fatty acids [1]. Fatty acids consist of a hydrophilic carboxyl group and a hydrophobic carbon-hydrogen chain with varying chain lengths. They appear as saturated (no double bond) or unsaturated fatty acids (one or more double bonds in the aliphatic backbone) [2]. Fatty acids are renewables that have large potential in waste-to-values approaches as they accumulate to a large extend in the agricultural, industrial and domestic waste making innovative solutions for valorization inevitable [3].

Cytochrome P450 monooxygenases (CYPs, P450s) are a versatile group of oxidoreductases, that provide an enzymatic platform for chemical reactions including decarboxylation, hydroxylation and epoxidation [4, 5]. Their common name is derived from the change of absorption maxima from 420 to 450 nm, if carbon monoxide (CO) binds to the reduced and heme coordinated Fe^{2+} [6]. Especially, the hydroxylation of fatty acids displays an interesting reaction as the conventional chemical C-H bond activation requires harsh reaction conditions and high energy-demand typically with a lack of sterical control [7, 8]. Instead, P450s offer regio- and stereoselective hydroxylation of the α, β, and various ω-positions of fatty acids at mild reaction conditions [9, 10]. Hydroxy fatty acids represent basic compounds for a large list of industrial application within polymer chemistry, pharmaceuticals or cosmetics [11, 12]. A general catalytic cycle for P450s is shown in Figure 1. H_2O_2 can serve as oxidant via the peroxide shunt or electrons are provided by NAD(P)H and a NAD(P)H-dependent reductase for the homolytic cleavage of O_2 to form “compound 1” [13, 14]. A major drawback of many P450s is the lack of stability against H_2O_2 and inability for rapid conversion of H_2O_2 into reactive compound I, which finally results in decreased total turnover numbers (TTNs) [15, 16]. However, H_2O_2 is a cheap and already “activated” oxidant in comparison to O_2. Molecular oxygen requires two electrons from NAD(P)H for homolytic cleavage. Consequently, NAD(P)H recycling is needed on preparative scale reactions [17]. If “compound 2” is not reached, so called uncoupling of the catalytic cycle occurs in which reactive oxygen species (superoxide via the autoxidation shunt or H_2O_2 via the peroxide shunt) are formed. This results in loss of redox-equivalents and potentially destruction of the catalyst. Using H_2O_2 as oxidant avoids the uncoupling via the peroxide shunt. Additionally, the ferryl-oxo porphyrin “radical cation” presumably present in “compound 1” can accept additional electrons from NAD(P)H, resulting in an oxidase uncoupling, the release of H_2O and the formation of the “high spin” ferric state. All three possible uncoupling reactions lead to an imbalance in the formed product and consumed NADPH (mol mol^{-1}) [18]. Activation and cleavage of one molecule of O_2 requires oxidation of one

molecule of NAD(P)H to NAD(P)$^+$. The uncoupling can be quantitatively expressed in the coupling efficiency, which is defined as followed:

$$\text{coupling efficiency (\%)} = \frac{\text{mol product formed}}{\text{mol NAD(P)H consumed}} \times 100 \text{ or } \frac{\text{mol product formed}}{\text{mol } O_2 \text{ consumed}} \times 100$$

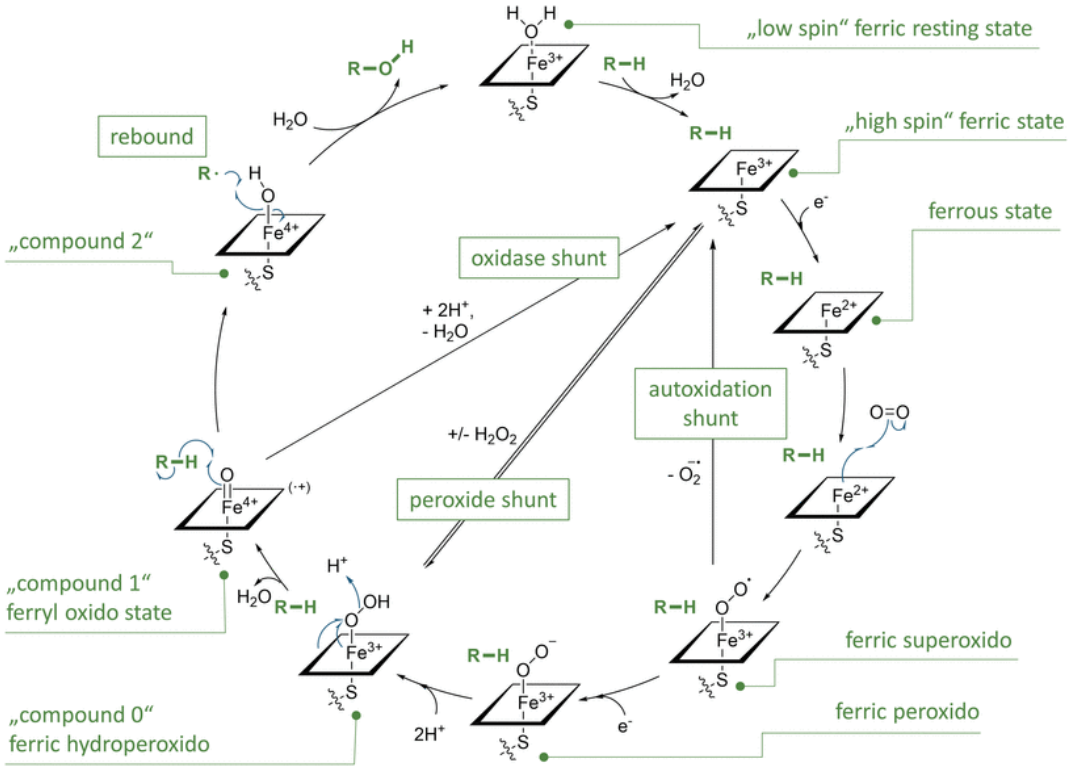

Figure 1: **Catalytic cycle for cytochrome P450s.** Figure taken from Hammerer et al (2018) [9].

P450 BM3 depicts an industrially and scientifically interesting enzyme as it introduces hydroxyl groups into a large variety of chemical compounds, including its natural substrates fatty acids. The enzyme catalyses the oxyfunctionalization of the fatty acids at the ω-positions [19, 20]. Compared to most other CYPs, P450 BM3 is a self-sufficient enzyme that contains a diflavin (FAD/FMN-containing) NADPH-reductase domain fused to the monooxygenase subunit within a single polypeptide. No other redox-partners are needed, which simplifies its application as compared to most multi-component redox systems [21]. For preparative-scale reactions and hence conversion of high-substrate loadings it is not feasible to provide the costly co-factor NAD(P)H in stoichiometric amounts [9]. Consequently, different regeneration systems were identified. The most prominent systems are based on the oxidation of cheap and renewable substrates (e.g. glucose, formate, phosphite) for subsequent reduction of NAD(P)$^+$ by enzymes such as glucose dehydrogenase (GDH), formate dehydrogenase (FDH) or phosphite dehydrogenase (PH) [22–24]. Figure 2 displays the reaction scheme for the conversion of fatty acids with P450 BM3 and the regeneration of NADPH based on a GDH.

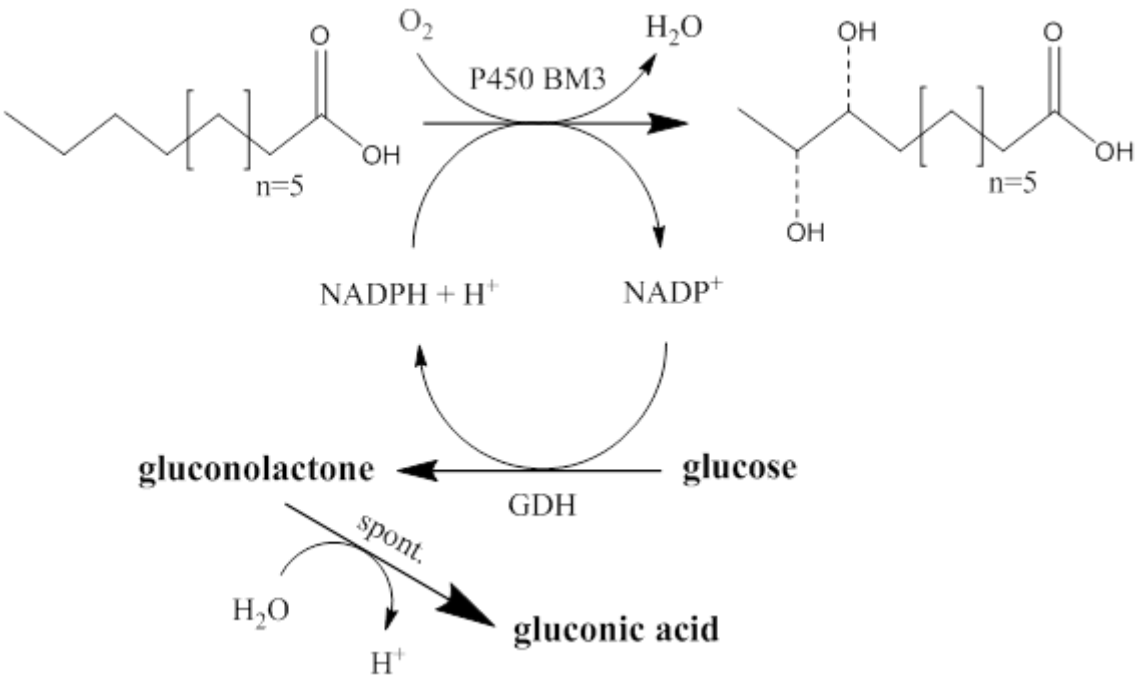

Figure 2**: Reaction scheme for the envisioned preparative-scale conversion of dodecanoic acid with P450 BM3 supported by glucose dehydrogenase (GDH).**

1.2 Prep-scale examples in literature for the conversion of fatty acids by P450 BM3

Examples for preparative scale P450 BM3 catalyzed oxyfunctionalization of fatty acids are rare in literature. The low solubility of fatty acids in water, the uncoupling of the P450 reaction and overoxidation have been major limitations for preparative scale production of mono-hydroxylated fatty acids in the past [9, 25]. Strategies to overcome the limited substrate solubility in water include the addition of co-solvents (EtOH, DMSO, etc.) or additives like cyclodextrins. However, the addition of co-solvents can have influences on the enzyme activity and stability dependent on the type and concentration [26]. Additionally, two-phase systems were applied were the substrate was dissolved and provided via an organic phase (e.g. dodecane), while the enzymatic reaction proceeds in the aqueous phase [27]. For the selection of the organic phase one should consider the ability of P450 BM3 and its variants to convert a wide range of organic compounds, including alkanes, alkenes, alkynes and aromatics [19]. Further challenges involve slow substrate transfer rates (surface to value problem) and distribution, which in particular limits reactions with high K_m values. Maurer et al (2005) reported 55% conversion of 100 mM tetradecanoic acid (C14:0) with a variant of P450 BM3 (CYP102A1 A74G/F87V/L188Q) reaching TTNs of 44000. The reaction was carried out in a two-phase system with dodecane (48 h reaction time). However, overoxidation was observed, resulting in a mixture of at least 25 different products. Further, a mono-phasic system containing 20 mM randomly methylated β-cyclodextrin (CAVASOL W7 M Pharma) to solubilize 44 mM C14:0 was tested. Conversion of 76% and TTNs of 50600 for the P450 BM3 could be reached in 48 h reaction time [28]. A comparable study for dodecanoic acid (C12:0) as substrate was conducted by Kühnel et al (2007) by using a NADH-dependent

P450 BM3 variant (CYP102A1 3mDS). Two-phase systems with isooctane, dodecane and DMSO and monophasic systems with a variety of co-solvents (DMSO, EtOH, methyl tert-butyl ether, Tween 80, acetonitrile and CAVASOL W7 M Pharma) were tested for the conversion of 50 mM C12:0 (48 h reaction time). The best results were achieved in the monophasic reaction system, when 20 mM CAVASOL W7 M Pharma were added. A conversion of 67% and a TTN of 66 700 were reported. For comparison, the same reaction with 2% DMSO as co-solvent reached 42% conversion and a TTN of 42000 [29]. Beside crude cell lysates, whole cell approaches were conducted to produce ω-hydroxy fatty acids from glucose *in-vivo*. An engineered *Escherichia coli* (*E. coli*) strain capable of producing free fatty acids (244.8 mg L^{-1} cell culture, in shake flasks) and expressing P450 BM3, reached up to 58.7 (in batch) and 548 mg (in fed-batch) hydroxy fatty acids (HFA) per litre of cell culture. The major of HFAs were 9-hydroxy decanoic acid, 11-hydroxy dodecanoic acid, 10-hydroxy hexadecenoic acid and 12-hydroxyoctadecanoic acid in the batch-conversion. 49.3% of the 58.6 mg L^{-1} hydroxy fatty acids were identified as 11-hydroxy dodecanoic acid, which corresponds to 140 µM 11-hydroxy dodecanoic acid [30]. Recently, co-immobilized P450 BM3 and GDH showed promising potential for the conversion of C12:0. In a recycling study 2 mM C12:0 were converted within 15 min for up to 9 cycles (Figure 3). This corresponds to the conversion of 8 mM C12:0 per h (1.6 g L^{-1} h^{-1}), a promising value for preparative scale reactions and further reaction intensification. TTNs of 18000 were reached for the P450 BM3. The reactions were carried out at rather small scale (5 mL) providing the fatty acid as homogenous substrate and without showing product isolation or down streaming. [31].

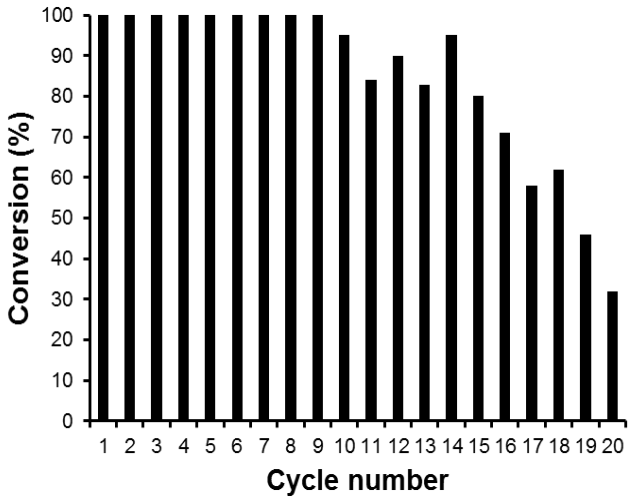

Figure 3: **Recycling study with co-immobilized Z_P450 BM3 and Z_GDH.** For each cycle 2 mM C12:0 were applied and 100% conversion were reached for the first 9 cycles. Each cycle lasted 15 min. Figure taken from Valikhani et al (2018) [31].

Table 1: **Selected relevant examples of P450 BM3 catalyzed conversions of fatty acids.**

Catalysts	Reaction system	Substrate	Co-solvent/additive	Conversion (%)	Ref
P450 BM3 (A74G/F87V/L188Q) and FDH	Two-phase batch	100 mM C14:0	Dodecane	55%	[28]
	Single-phase batch	44 mM C14:0	CAVASOL W7 M Pharma (20 mM)	76%	
CYP102A1 3mDS and FDH	Single-phase batch	50 mM C12:0	DMSO (2%)	42%	[29]
	Single-phase batch	50 mM C12:0	CAVASOL W7 M Pharma (20 mM)	67%	
Co-immobilized Z_P450 BM3 and Z_GDH	Single phase repeated batch	2 mM C12:0 per cycle (20)	EtOH	100% (cycle 1 to 9)	[31]

1.3 Oxygen in biocatalysis: current strategies in controlling bioprocesses with O_2

Due to the low solubility of O_2 in water (~250 µM) at ambient temperatures (25 °C) and pressure (1 atm), O_2 dependent reactions require constant and sufficient supply of the oxidant [32]. Especially, whole cell biocatalysis is limited by the competition of the target enzymatic reaction itself and respiration processes in the cell [33]. Oxygen transfer can be described via following equation, whereas the gas-liquid interphase displays the highest resistance:

$$\mathrm{dC_{O_2}/dt = k_L a * (C_{O_2 equ} - C_{O_2})}$$

- dC_{O_2}/dt … change of O_2 concentration in a defined time period t (µM min^{-1})
- k_L … mass transfer coefficient for O_2 (cm min^{-1})
- a … gas/liquid phase interface area per liquid volume (cm^2 cm^{-3})
- $C_{O_2 equ}$ … equilibrium concentration of O_2 in the liquid phase (µM)
- C_{O_2} … O_2 concentration at time point t (µM)

The volumetric mass transfer coefficient (k_La) is strongly dependent on the reactor geometry, the type of stirrer, the stirrer speed, the type of O_2 sparger unit, the O_2 mass flow rate and liquid properties, like viscosity or the surface tension [34, 35]. As k_La values are often insufficient for stirred tank reactors, different strategies are followed to enhance the available O_2 in the reaction. An interesting concept, including whole cell biocatalysis, makes use of the O_2 producing algae *Synechocystis* sp. PCC 6803 expressing an α-ketoglutarate-dependent dioxygenase (AlkBGT). The system is based on the light-

driven formation of O_2 by photosynthetic cleavage of H_2O and produces 1.8 µM (0.34 mg L^{-1}) hydroxy nonanoic acid methyl esters (H-NAME) per min from nonanoic acid methyl esters (NAME) under anaerobic conditions [36]. Besides enhancing the k_La value it is possible to enhance the driving force for the oxygen transfer ($C_{O2equ} - C_{O2}$) by applying pressurized or pure O_2 to increase C_{O2equ}. For example, co-immobilized glucose oxidase (GOX) and catalase were used in a continuous pressured reactor resulting in the conversion of 25 mM glucose into gluconic acid per min (4.9 g L^{-1} min^{-1}) [37]. A recent example for an O_2 dependent reaction in a stirred tank reactor was the conversion of 3,3,5-trimethyl-cyclohexanone to trimethyl-ε-caprolactones by TmCHMO at 30 mL, 1 L and 100 L scale. The reactor was run in fed-batch mode (30 mM h^{-1}, continuous substrate feed) and 3.4 g L^{-1} trimethyl-ε-caprolactones (CHLs) per h could be produced at 1 L scale. 92% conversion of the 240 mM applied substrate were reached. They reported solubilities of 100 to 130 mM for the substrate and up to 200 mM for the product in aqueous solution containing 10% methanol (MeOH) [38]. Kaluzna et al (2016) published a second example for a stirred tank reactor with bubbled oxygenation (100% O2). They showed the conversion of α-isophorone to 4-hydroxy-α-isophorone with a Wt_P450 BM3/GDH system on kg scale. Product concentrations of 10 and 6 g L^{-1} and STYs of 1.5 and 1.0 g L^{-1} h^{-1} could be achieved at 1 L scale and 100 L scale, respectively. Two consecutive batch reactors (100 L) reached conversions of 80 and 82% The batch at 1 L scale reached a conversion of 61% [39]. A summary of the described systems is shown in Table 2.

Table 2: **Selected strategies to control O_2 in biocatalysis and related applications.**

Catalyst	**Substrate**	**Reactor mode**	**O_2 supply**	**STY**	**Ref.**
Whole cells (*Synechocystis* sp. PCC 6803) expressing AlkBGT	Nonanoic acid methyl esters	Batch	in situ regeneration from H_2O (light driven)	0.34 mg L^{-1} min^{-1}	[36]
Co-immobilized GOX and catalase	Glucose	Continuous	pressure reactor and conversion of H_2O_2 by catalase	4.9 g L^{-1} min^{-1}	[37]
TmCHMO (cell broth)	3,3,5-Trimethyl-cyclohexanone	Fed-Batch	Bubble oxygenation (100% O_2)	3.4 g L^{-1} h^{-1}	[38]
WtP450 BM3/GDH (permeabilized cell slurry)	α-isophorone	Batch	Bubble oxygenation (100% O_2)	1.5 g L^{-1} h^{-1}	[39]

1.4 Enzyme immobilization for preparation of heterogeneous catalysts

In general, three different types of immobilization strategies are conducted to prepare enzyme-based heterogeneous catalysts: cross-linking, encapsulation and binding to supports. A bottleneck and time-consuming process in immobilization is the necessary extensive screening and optimisation of the immobilization conditions. In general, one immobilization strategy should be applicable to a broad variety of enzymes, but at least applicable to the same class of enzymes. This generality is often lacking. An overview of general immobilization requirements is shown in Figure 4. Immobilisation on solid supports is the most promising strategy for enzyme immobilization. However, compared to cross-linking and encapsulation its environmental impact is larger and the strategy is regarded as “less green” [40]. An advantage of immobilization is the protection of the enzyme by or within a microenvironment. Therefore, immobilized enzymes are often more resistant to environmental influences, like pH changes, higher temperatures or organic co-solvents. Additionally, immobilization provides the basis for advanced reactor designs, for example the application of enzymes in continuous reactions or the reusability of the expensive biocatalyst (recycling). A prerequisite for these applications is a stable (no leaching of enzyme from carrier) and active immobilizate. Further, the facilitated protein removal provides the basis for simplified product downstreaming. However, immobilized enzymes are often less active compared to free enzymes due to steric hindrance, inaccessibility of the active site for the substrate or conformational changes of the enzymes during the immobilization. This effect is described by the effectiveness factor η, the ratio between the activity of the immobilized enzyme and free enzyme. An ideal immobilizate would reach an η-value of 1. Additionally, limitations due to a restricted mass transfer might occur, which is in particular true for carriers with nanoporous structure [41, 42].

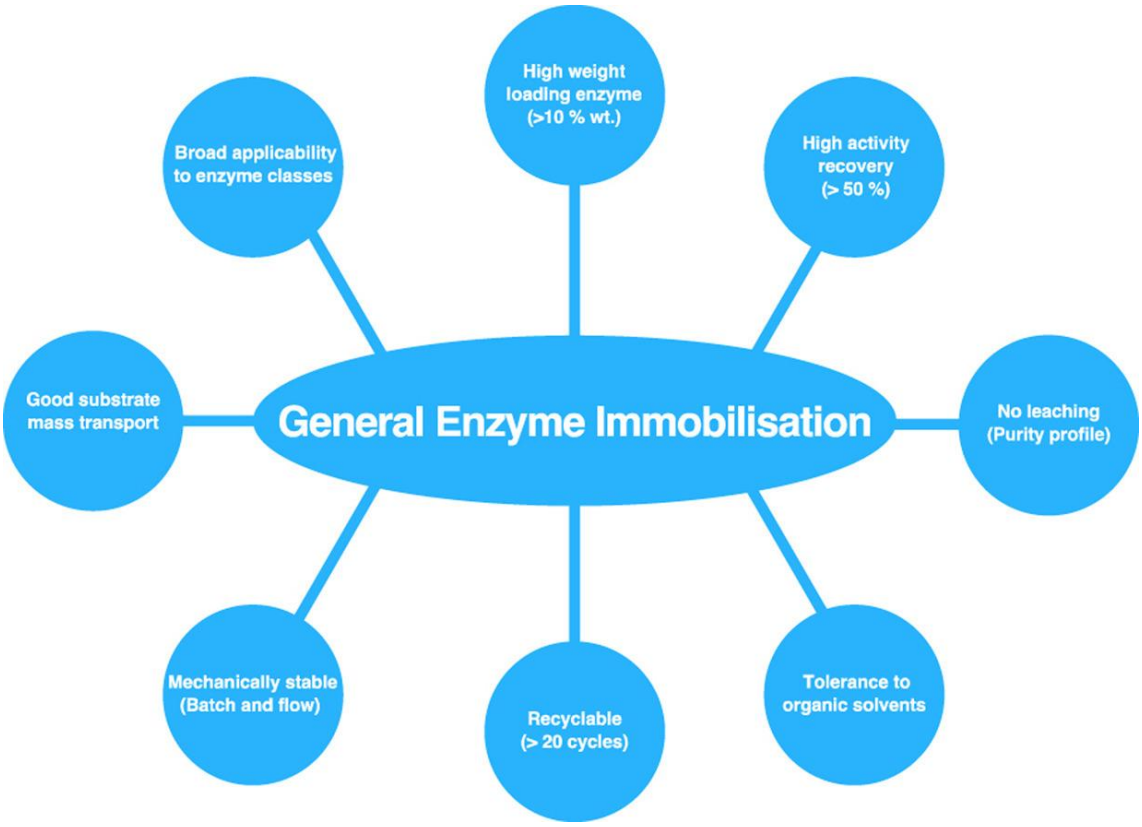

Figure 4: **Requirements for a general immobilization strategy.** Figure taken from Thomson et al (2019) [40].

1.5 Immobilisation of P450 BM3

Several attempts to immobilize P450 BM3 were conducted based on different immobilization strategies. A NADH-dependent P450 BM3 variant (R966D/W1046S) was covalently immobilized on glutaraldehyde activated super paramagnetic iron oxide nanoparticles (SPIONs) with 100% binding efficiency (2 nmol P450 BM3 per 40 mg SPIONs). The active SPIONs (η=0.6) were separable from the reaction bulk with a magnet [43]. Maurer et al reported the encapsulation of a P450 BM3 variant (A74G, F87V, L188Q) and a $NADP^+$-dependent FDH in a sol-gel matrix. The model substrate p-nitrophenoxydecanoic acid (10-pNCA) was used to determine the activity of immobilized P450 BM3 (0.89 U mg^{-1}) and free P450 BM3 (1.7 U mg^{-1}). This corresponds to a η -value of 0.52 [44]. Solé et al (2019) conducted a covalent co-immobilisation approach using agaroses with different functionalities (epoxy, amine and aldehyde). The highest retained activity for P450 BM3 (83%) and GDH (20%) could be reached with the epoxy-agarose with 30 U P450 BM3 per g of support. However, 50% activity loss (P450 BM3) were observed within 4 h of incubation in 1 M potassium phosphate buffer (pH 8) [45]. A non-covalent immobilization approach was carried out by immobilizing His-tagged P450 BM3 on controlled porosity glass coated with an organic polymer and chelated Fe(III) ions (EziG^{Tm}). However, compared to a selection of different enzymes including an alcohol oxidase, an alcohol dehydrogenase, an amine dehydrogenase, a carboxylic acid reductase and a reductive aminase, the maximum loadable P450 BM3 was very poor (>2% weight enzyme on carrier) and retained activity was rather low

(30 to 40%) [40]. Bolivar and Nidetzky (2012) described an alternative and mild immobilization strategy using a positively charged peptide module (Z_{Basic2}) fused to the target enzyme. The tagged enzyme can therefore bind to negatively charged nanoporous particles, surfaces and various materials (Figure 5) [46]. The 7 kDa large Z_{Basic2}-module did not influence the expression of the tagged D-amino acid oxidase from *Trigonopsis variabilis* (*Tv*DAO) and sucrose phosphorylase from *Leuconostoc mesenteroides* (*LmS*Pase) compared to the native enzymes [47]. Valikhani et al (2018) showed a successful preparation of a co-immobilizate containing up to 19.5 U Z_P450 BM3 (for the substrate anisole) and 700 U Z_GDH (for the substrate glucose) per g carrier (ReliSorb^{Tm} SP400). For single enzyme immobilizations, η-values of 0.48 for Z_P450 BM3 and 0.31 for Z_GDH were determined. The prepared co-immobilizate reached TTNs of up to 18000. In a recycling study sufficient *in-operando* stability of the co-immobilizate was observed [31].

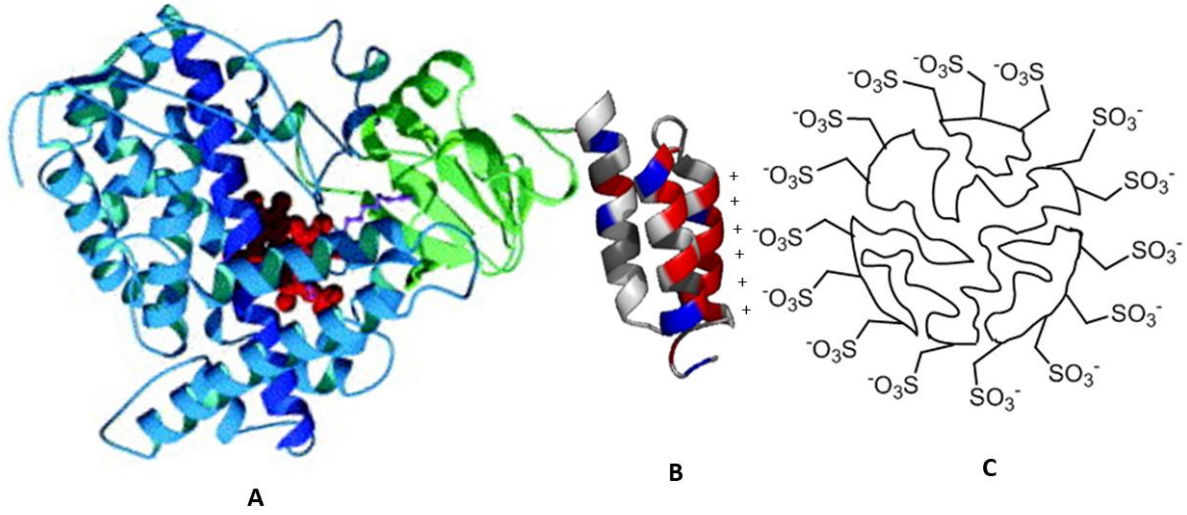

Figure 5: **Schematic representation of the immobilization of a Z_{Basic2}-tagged enzyme on ReliSorb^{Tm} SP400**. The enzyme (A) is covalently linked to the Z_{Basic2}-module (B). The arginine-rich Z_{Basic2}-module is positively charged (indicated by the red colour in the α-helices) at neutral pH and binds to the negatively charged sulphonic groups of the nanoporous carrier ReliSorb^{Tm} SP400 (C) via ionic interactions. Enzyme, Z_{Basic2}-module and the ReliSorb^{Tm} SP400 particle are not shown in scale. Figure taken and adapted from Munro et al (2002) (A) [21] and Bolivar and Nidetzky (2012) (B) [46].

1.6 Aim of this thesis

The aim of this project is to intensify reaction processes for monooxygenases as homogeneous and heterogeneous catalysts in fatty acid oxyfunctionalization. As starting point the established system by Valikhani et al (2018) [31] is tested under defined operative batch conditions (O_2 supplementation and pH controlled) and increased reaction scale. Co-immobilized Z_P450 BM3 and Z_GDH are benchmarked against cell free extracts of Z_P450 BM3 and Wt_P450 BM3. Dodecanoic acid is used as challenging (water-insoluble) model substrate for bioprocess design with heterogeneous substrates in aqueous solution. Operational stability, conversion rates, maximal substrate loading and *in-operando* coupling efficiencies for each enzyme preparation are investigated in depth. Reactor modes, including batch- and fed-batch conversions should be explored with the aim to increase product titers and STYs. The binding stability of the immobilized enzymes on the carrier is investigated for its potential for "in-flow catalysis". Product inhibition or overoxidation are not well understood or described for the application of monooxygenases. To overcome this, key kinetic parameters, including the O_2 and NADPH depletion rates, k_{cat}, K_m, k_{eff} and the coupling efficiency for C12:0 and C12:0-OHs are determined with selected monooxygenase preparations. Finally, products (C12:0-OHs) should be isolated on preparative scale and evaluated based on isolated yield, purity and potential overoxidation(s). To this end, this work should provide a deeper understanding for limitations in preparative application of monooxygenases and a guideline for process design.

2 Material and methods

2.1 Materials

2.1.1 Chemicals

Table 3: List of applied chemicals

Antifoam 204	FLUKA (Munich, Germany)
Dipotassium hydrogen phosphate	Roth (Karlsruhe, Germany)
DMSO	Roth (Karlsruhe, Germany)
Dodecanoic acid	Tokyo Chemical Industry (Tokyo, Japan)
Ethanol	Roth (Karlsruhe, Germany)
Ethyl acetate	Roth (Karlsruhe, Germany)
Gluconic acid	Sigma Aldrich (St. Louis, Missouri, United States)
Glucose monohydrate	Roth (Karlsruhe, Germany)
Hydrochloric acid	Roth (Karlsruhe, Germany)
Imidazole	Roth (Karlsruhe, Germany)
Methanol	Sigma Aldrich (St. Louis, Missouri, United States)
NADH disodium salt	Roth (Karlsruhe, Germany)
NADPH tetrasodium salt	Roth (Karlsruhe, Germany)
$NADP^+$ disodium salt	Roth (Karlsruhe, Germany)
1-Octanol	Sigma Aldrich (St. Louis, Missouri, United States)
Potassium dihydrogen phosphate	Roth (Karlsruhe, Germany)
Potassium hydroxide	Roth (Karlsruhe, Germany)
Silicone antifoam	Sigma Aldrich (St. Louis, Missouri, United States)
Sodium chloride	Roth (Karlsruhe, Germany)
Sodium dithionite	Sigma Aldrich (St. Louis, Missouri, United States)
Sodium dodecyl sulfate	New England Biolabs (Ipswich, Massachusetts, United States)
Sodium sulfate	Roth (Karlsruhe, Germany)
Sulfuric acid	Roth (Karlsruhe, Germany)
(Trimehtlysilyl)diazomethane	Sigma Aldrich (St. Louis, Missouri, United States)

2.1.2 Enzymes

Table 4: List of applied enzymes

	Activity	Source	Company
Lysozyme	≥35000 U mg^{-1}	Chicken egg white	Roth (Karlsruhe, Germany)
Catalase	2000 – 5000 U mg^{-1}	Bovine liver	Sigma Aldrich (St. Louis, Missouri, United states)
Glucose oxidase	150-200 U mg^{-1}	*Aspergillus niger*	Sigma Aldrich (St. Louis, Missouri, United states)

2.1.3 Growth media and supplements

All media components and supplements were purchased from Roth (Karlsruhe, Germany). Except for the δ -aminolevulinic acid, which was obtained from Sigma Aldrich (St. Louis, Missouri, United States). Media components were dissolved in water and autoclaved at 121 °C for 20 min. Supplements were prepared as 1000-fold concentrated stocks, sterile filtered (0.45 µM filters) and added after autoclaving.

Table 5 List of used media including compound concentrations and supplements

	Component	Final concentration in media
LB-Media	Tryptone	10 g L^{-1}
	Yeast extract	5 g L^{-1}
	NaCl	10 g L^{-1}
TB-Media	KH_2PO_4	2.31 g L^{-1}
	K_2HPO_4	12.54 g L^{-1}
	Tryptone	20 g L^{-1}
	Yeast extract	24 g L^{-1}
	Glycerol	4 mL L^{-1}
Supplements	δ -aminolevulinic acid	0.5 mM
	IPTG	0.2 mM
	Kanamycin	50 µg mL^{-1}
	Trace element solution	0.5 mg L^{-1} $CaCl_2 \cdot 2H_2O$, 0.18 mg L^{-1} $ZnSO_4 \cdot 7H_2O$, 0.1 mg L^{-1} $MnSO_4 \cdot H_2O$, 20.1 mg L^{-1} Na_2-EDTA, 16.7 mg L^{-1} $FeCl_3 \cdot 6H_2O$, 0.16 mg L^{-1} $CuSO_4 \cdot 5H_2O$

2.1.4 Bacterial strain

Table 6: Bacterial strain used for protein expression

Strain	Properties
Escherichia coli BL21(DE3)	str. B F^- ompT gal dcm lon $hsdS_B(r_B^-m_B^-)$ λ(DE3 [lacI lacUV5-T7p07 ind1 sam7 nin5]) $[malB^+]_{K-12}(\lambda^S)$

2.1.5 Laboratory devices

Table 7: List of laboratory devices

Analytical Balance ENTRIS® 224I-1S	Sartorius AG (Goettingen, Germany)
Balance LE224S	Sartorius AG (Goettingen, Germany)
WPA CO8000 Cell Density Meter	Biochrom WPA (Cambridge, UK)
Sterile workbench Bioair Auro 2000 Laminar Flow	EuroClone S.p.A. (Milan, Italy)
Rotary shaker CERTOMAT® BS-1	Sartorius AG (Goettingen, Germany)
Ultracentrifuge Sorvall® Evolution RC	Thermo Fisher Scientific (Waltham, Massachusetts, USA)
Vortex Reax 2000	Heidolph Instruments GmbH &Co.KG, (Schwabach, Germany)
Fisher Scientific* Model 705 Sonic Dismembrator	Thermo Fisher Scientific (Waltham, Massachusetts, USA)
Eppendorf Centrifuge 5415 R	Eppendorf AG (Hamburg, Germany)
Minisart® Single use filter unit 0.45 µm	Sartorius AG (Goettingen, Germany)
ÄKTAprime plus	Amersham BioSciences, GE Healthcare (Chicago, IL, USA)
HiTrap SP FF column, 5 mL	GE Healthcare Life Sciences (Chicago, Illinois, USA)
HisTrap HP protein purification column	GE Healthcare Life Sciences (Chicago, Illinois, USA)
Moisture Analyzer MA 100	Sartorius AG (Goettingen, Germany)
Varian Cary® 50 UV-Vis spectrophotometer	Varian Medical Systems Inc. (Palo Alto, California)
DeNovix DS-11 Spectrophotometer	DeNovix Inc. (Wilmington, North Carolina, USA)

GC-MS: 7890B GC – 5977A MSD	Agilent Technologies (Santa Clara, California, USA)
GC-FID: Hewlett Packard Series II	(Hewlett-Packard, Palo Alto, California, United States)
CP Chirasil-DEX CB (GC-column)	Agilent Technologies (Santa Clara, California, USA)
OXROB10 (Oxygen sensor)	Pyroscience GmbH (Aachen, Germany)
NuPAGE™ 4-12% Bis-Tris Gel	Invitrogen Thermo Fisher Scientific (Carlsbad, California, United States)
LDS Sample Buffer (4x)	Invitrogen Thermo Fisher Scientific (Carlsbad, California, United States)
Rotator SB3	Stuart equipment (Staffordshire, United Kingdom)
MCP-CPF Process IP65	IsmaTec (Wertheim, Germany)
Laborota 4000	Heidolph Instruments GmbH &Co.KG (Schwabach, Germany)
Christ ALPHA 1-4	B. Braun Biotech GmbH (Berlin, Germany)
IKA-WERK RW 20 / IKA RCT Basic	IKA (Staufen, Germany)
Lauda RE104/ Lauda E100	Lauda-Königshofen (Germany)

2.2 Analytics

2.2.1 Carbon monoxide titration for the determination of active P450 BM3

The molartiy of active P450 BM3 was determined via carbon monoxide (CO) titration [48]. An appropriate dilution of the P450 BM3 solution (in 50 mM KPi, pH 7.5) was mixed with a spatula tip of sodium dithionite ($Na_2S_2O_4$) to reduce the heme iron from Fe^{3+} to Fe^{2+}. An absorption spectrum from 400 to 600 nm was recorded. Afterwards, the solution was gassed with CO under the fume hood for 30 seconds and a second absorption spectrum was recorded. CO binds to the reduced Fe^{2+} and a shift in the absorption maxima from 420 to 450 nm occurs. Based on the differential spectrum of the not gassed and gassed sample and the extinction coefficient (ε = 91 mM^{-1} cm^{-1}) the molarity of active enzyme can be calculated with the following equation:

$$c\,(P450) = \frac{\Delta abs\,(450\,nm) - \Delta abs\,(500\,nm)}{\varepsilon} \times 1000 \times f \times d$$

- $c\,(P450)$ … concentration of active P450 (µM)
- Δabs … absorbance difference between the CO gassed and not gassed enzyme solution at 450 nm and 500 nm, respectively (-)
- ε … extinction coefficient (mM^{-1} cm^{-1})
- f … dilution factor of P450 solution (-)
- d … solution thickness (cm)

2.2.2 Photometric assay for the determination of GDH activity

Activity of glucose dehydrogenase (GDH) was determined spectrophotometrically based on the formation of NADPH. Therefore, 740 µL KPi buffer (50 mM, pH 7.5), 200 µL glucose solution (1 M in buffer) and 10 µL of an appropriate diluted enzyme solution were mixed in cuvettes. The solution was blanked at 340 nm and 50 µL $NADP^+$ (20 mM stock solution) were added to start the reaction. Based on the absorption change at 340 nm and the extinction coefficient of NADPH (ε_{340} = 6.22 mM^{-1} cm^{-1}) the GDH-activity was calculated with the following equation:

$$GDH\ activity\ (U\ mL^{-1}) = \frac{\Delta Abs}{\Delta t} \times \frac{V_{tot} \times f}{V_{\ enzyme} \times \varepsilon \times d}$$

- $\frac{\Delta Abs}{\Delta t}$ … change of absorption per time (min^{-1})
- V_{tot} … total reaction volume (mL)
- $V_{\ enzyme}$ … applied enzyme volume (mL)
- ε … extinction coefficient (mM^{-1} cm^{-1})
- f … dilution factor of GDH solution (-)
- d … solution thickness (cm)

2.2.3 GC-FID and GC-MS analysis

Sample preparation

Fatty acid substrate and products were extracted in a two-phase solvent extraction and quantified via GC-FID and GC-MS analysis. Samples (250 µL) were acidified with 25 µL (GC-FID) or 100 µL (GC-MS) 37% HCl to protonate fatty acids and hydroxy fatty acids and make them less soluble in the water phase. 500 µL ethyl acetate (EtOAc) containing 20 mM 1-octanol as internal standard (ISD) were added and mixed thoroughly by shaking. The water and organic phase were separated by centrifugation (4 °C, 16100 x g, 2 minutes) and the organic phase was transferred in a new reaction tube containing Na_2SO_4 to remove any residual water in the organic phase. Fatty acids and hydroxy-fatty acids in the organic phase were derivatized to yield the respective methyl esters. For this, 60 µL MeOH were mixed with 120 µL extracted sample in glass GC-vials containing 200 µL inlets. 10 µL (GC-FID) or 16 µL (GC-MS) trimethylsilyl-diazomethane were added, mixed by pipetting and the vial was closed immediately for GC measurement.

Measurement

A gas chromatograph coupled to a flame ionization detector (GC-FID) from HP Series II was used for detection and quantification of dodecanoic acid (C12:0) and ω-hydroxy dodecanoic acids (C12:0-OHs). An Agilent Technologies 7890B GC system equipped with a 5977A mass spectrometer (GC-MS) was utilized for identification and quantification of products. In both GC systems an Agilent HP-5 column (30 m x 320 µm, 0.25 µm film) was installed and H_2 (GC-FID) or helium (GC-MS) were used as carrier gases, respectively. Toluene and EtOAc were used for syringe washing. The applied temperature profiles are shown in Table 8. The inlet temperature was set to 275°C, the detector temperature to 300 °C for GC-FID analysis.

Table 8: **Temperature program used for GC-FID and GC-MS analysis**

	GC-FID	**GC-MS**
Start	100 °C	100 °C
Hold	100 °C for 5 min	100 °C for 5 min
Rise	40 °C per min until 320 °C	20 °C per min until 320 °C
End	320 °C for 0.5 min	320 °C for 0 min

Calibration curves

Calibration curves were measured for quantification of C12:0 and C12:0-OHs. C12:0-OHs were derived from the preparative isolation of the conducted reactions. 25 µL of stock solutions in the range of 200 to 1.5 mM of each analyte in DMSO (GC-FID) or EtOH (GC-MS) were mixed with 225 µL KPi buffer (50 mM, pH 7.5) and 25 µL (GC-FID) or 100 µL (GC-MS) 37% HCl. This samples were used in a two-phase

solvent extraction and derivatization for GC-FID/GC-MS analysis as described previously. Figure 6 depicts the calibration curve for C12:0 and C12:0-OHs for GC-FID analysis, Figure 7 for C12:0 for GC-MS analysis. For quantification, obtained peak areas for C12:0 and C12:0-OHs were divided by the internal standard (ISD, 1-octanol). The obtained results were used to calculate the analyte concentration based on the measured calibration curves. Representative chromatograms for GC-FID and GC-MS analysis of a C12:0 conversions with P450 BM3 are shown in Figure 8.

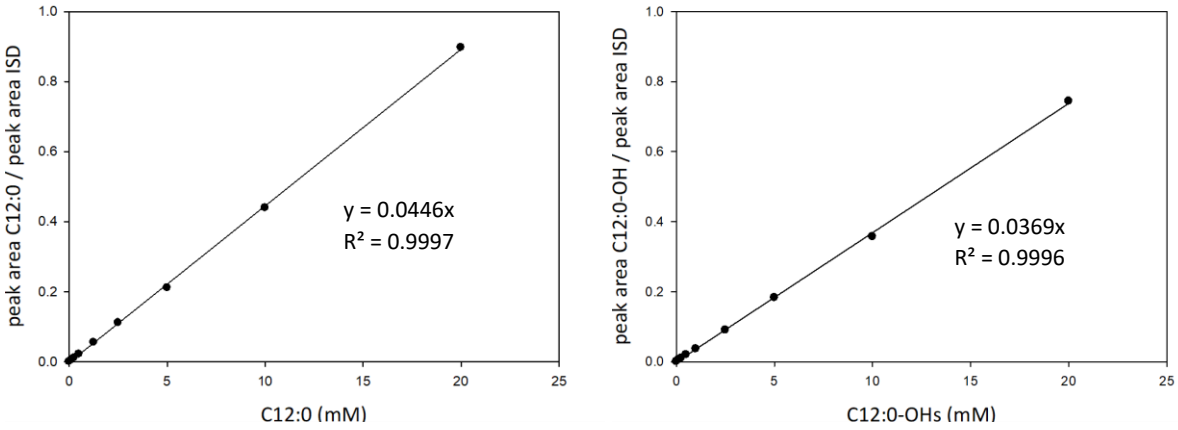

Figure 6: **Calibration curve for C12:0 (left) and C12:0-OHs (right) for GC-FID analysis.** The analyte concentration in mM is plotted against the quotient of the determined peak area of the analyte and the internal standard (ISD). A linear regression was performed and the respective equation and the determination coefficient (R^2) of the calibration curve are displayed.

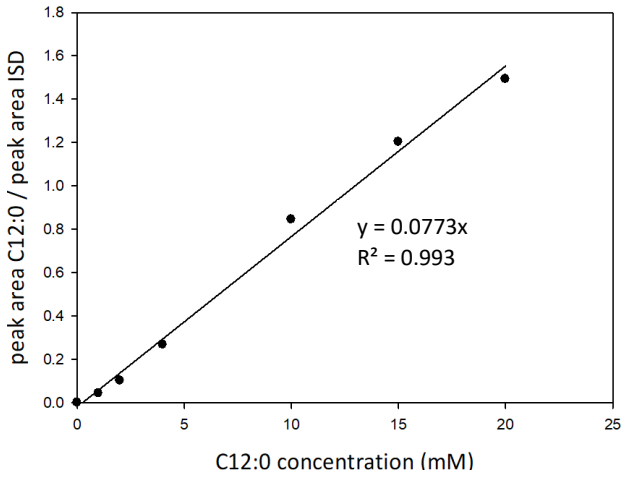

Figure 7: **Calibration curve for C12:0 for GC-MS analysis.** The analyte concentration in mM is plotted against the quotient of the determined peak area of the analyte and the internal standard (ISD). A linear regression was performed and the respective equation and the determination coefficient (R^2) of the calibration curve are displayed.

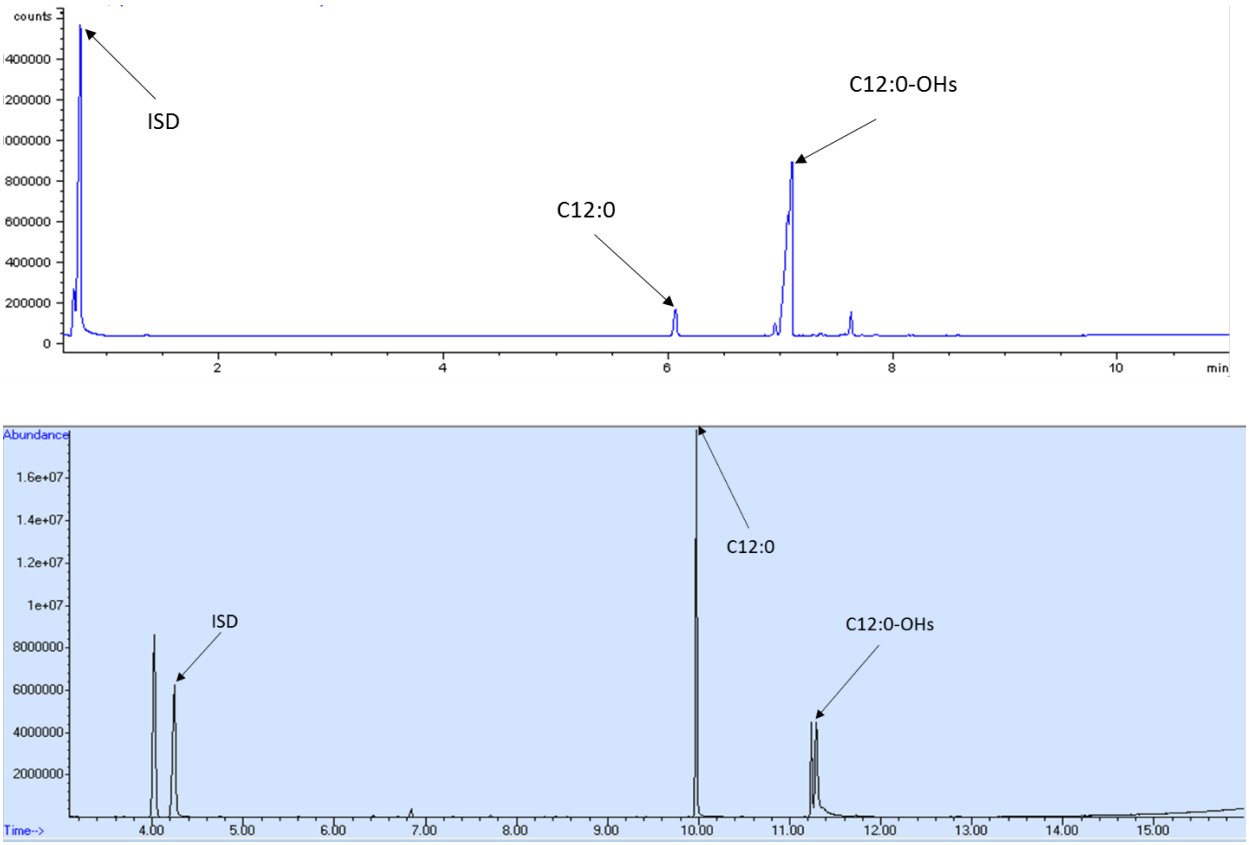

Figure 8: **Representative chromatograms of a C12:0 conversion via the P450 BM3/GDH reaction system for GC-FID (top) and GC-MS (bottom) analysis.** For GC-FID analysis, the retention times for C12:0 and C12:0-OHs are at 6.1 minutes and 7.1 minutes, respectively. For GC-MS analysis, the retention times for C12:0 and C12:0-OHs are at 9.9 minutes and 11.3 minutes, respectively. ISD = internal standard, 1-octanol

2.2.4 Determination of gluconic acid (GlcA) concentration via HPLC

Sample preparation and measurement

Samples (50 µL) were mixed with 50 µL 10% H_2SO_4 to stop the reaction. The acidified samples were diluted (1:10) with dH_2O and centrifuged for 30 minutes at 16100 x g. The supernatant (100 µL) was transferred into glass GC vials with 200 µL inlets and put to HPLC measurement.

Samples were analysed on a Merck Hitachi HPLC system equipped with a HPX-87H column, an UV detector (L-7400) and a RI detector (L-7490). The column oven was kept at room temperature (22 °C) and the flow rate was set to 0.6 mL min^{-1}. Water containing 5 mM H_2SO_4 was used as mobile phase in an isocratic mode. Ten µL sample were injected and the method run time was 30 minutes. With the present setup, it was not possible to separate GlcA and Glc. However, only GlcA was detectable via the UV-detector (Figure 9 and Figure 10). Consequently, all quantifications for GlcA were done via the UV detector.

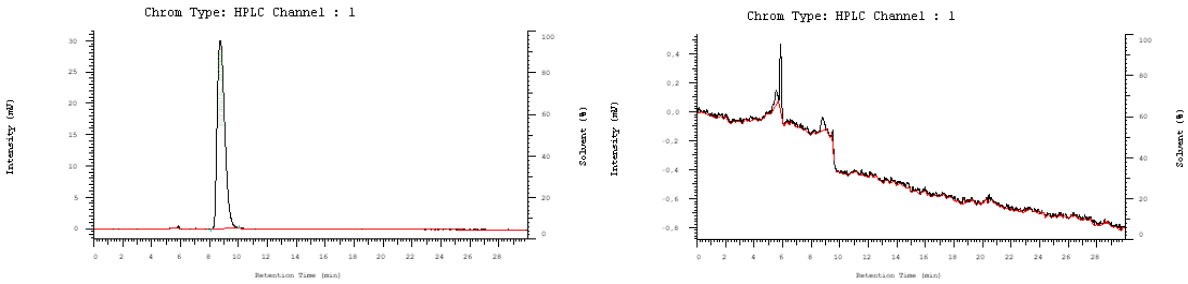

Figure 9: **Chromatograms of samples containing 15 mM GlcA (left) and 15 mM Glc (right).** An UV-detector was used for compound detection.

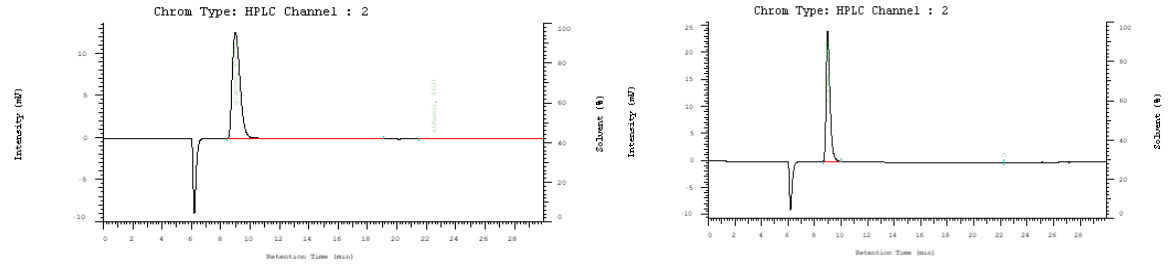

Figure 10: **Chromatograms of samples containing 15 mM GlcA (left) and 15 mM Glc (right).** A RI-detector was used for compound detection.

Calibration curve preparation

Calibration curves for glucose (Glc) and gluconic acid (GlcA) in the range of 0.5 to 15 mM were prepared. Figure 11 depicts the calibration curve for GlcA for HPLC analysis. The calibration curve for Glc cannot be used due to poor detection of the compound (data not shown).

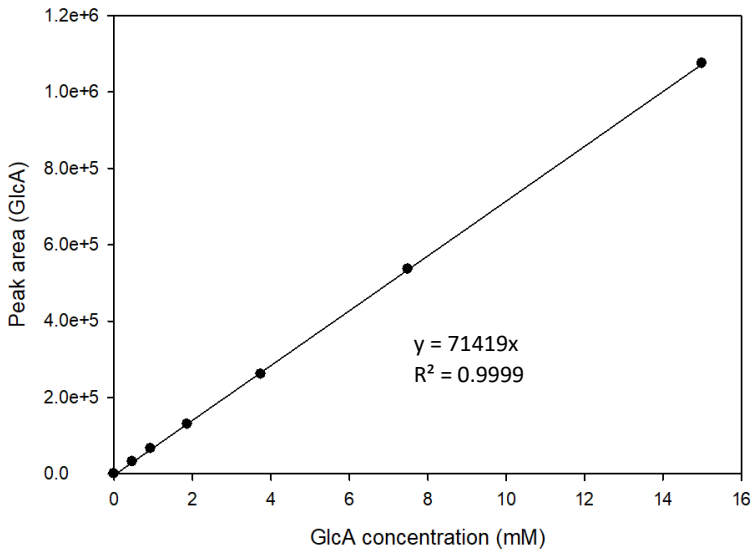

Figure 11: **Calibration curve for HPLC analysis and quantification of GlcA.** The GlcA concentration in mM is plotted against the determined peak area of the analyte. A linear regression was performed and the respective equation and the determination coefficient (R^2) of the calibration curve are displayed.

2.2.5 K_La value determination

The volumetric mass transfer coefficient for O_2 (k_La) was determined individually for different reactor set-ups. Therefore, reaction conditions excluding the respective enzymes were mimicked. To remove O_2 from the liquid phase the reactor was flushed with N_2 until the signal of O_2 reached 200 µmol L^{-1}. A defined stirring speed and volumetric mass transfer of O_2 were used to increase the O_2 concentration (100% O_2 at 1 bar pressure) until an equilibrium concentration was reached. The O_2 concentration was measured with an OXROB10 O_2 sensor and the PC-controlled (USB) fiber-optic oxygen meter FireStingO_2 (FSO2-x) from Pyro Science. Based on the measured values for each time point the k_La was determined with the following equations.

$$dC_{O_2}/dt = k_L a \times (C_{O_2 equ} - C_{O_2})$$

- dC_{O_2}/dt … change of O_2 concentration in a defined time period t (µM min^{-1})
- k_L … mass transfer coefficient for O_2 (cm min^{-1})
- a … gas/liquid phase interface area per liquid volume (cm^2 cm^{-3})
- $C_{O_2 equ}$ … equilibrium concentration of O_2 in the liquid phase (µM)
- C_{O_2} … O_2 concentration at time point t (µM)

Integrating from the time (t_0) at which the O_2 flow was started to any subsequent time (t) results in the following equation.

$$\ln\left(C_{O_2 equ} - C_{O_2}\right) = -k_L a \times (t - t_o)$$

Plotting ln ($C_{O2,equ} - C_{O2}$) against the time results in a linear curve. The absolute value of the slope equals the k_La. Figure 12 and Figure 13 display an exemplary determination of the k_La for a 50 mL reactor. O_2 was removed by pumping N_2 through the liquid. The experiment was performed at 25°C, under continuous stirring at 350 rpm and the O_2 flow rate was set to 25 mL min^{-1}. $C_{O2,equ}$ is 990 µM and the k_La was determined to be 31.2 h^{-1}. Consequently, the product of k_La and $C_{O2,equ}$ is the maximal oxygen transfer rate (OTR, 30.9 mM h^{-1}) and would correspond to the theoretical maximal reaction rate in the reactor system.

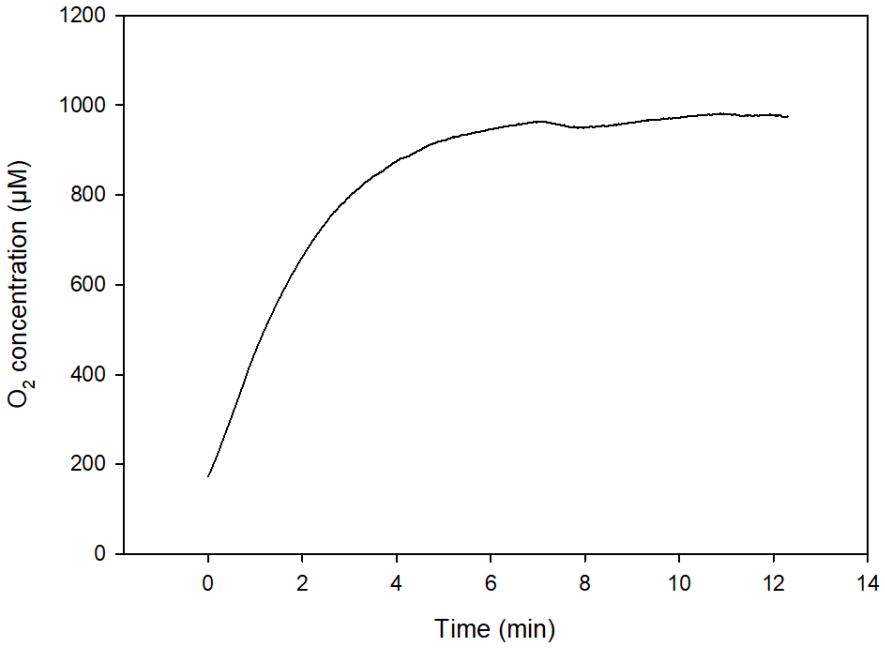

Figure 12: **Increase of O_2 concentration monitored in a 50 mL reactor (glass beaker) for k_La determination.** The time in minutes is plotted against the respetive oxygen concentration in µM. Based on the eqilibrium concentration ($C_{O2,equ}$,990 µM) and the oxygen concentration at different time points (C_{O2}), the k_La is calculated by plotting the time against ln ($C_{O2,equ} – C_{O2}$) (Figure 13).

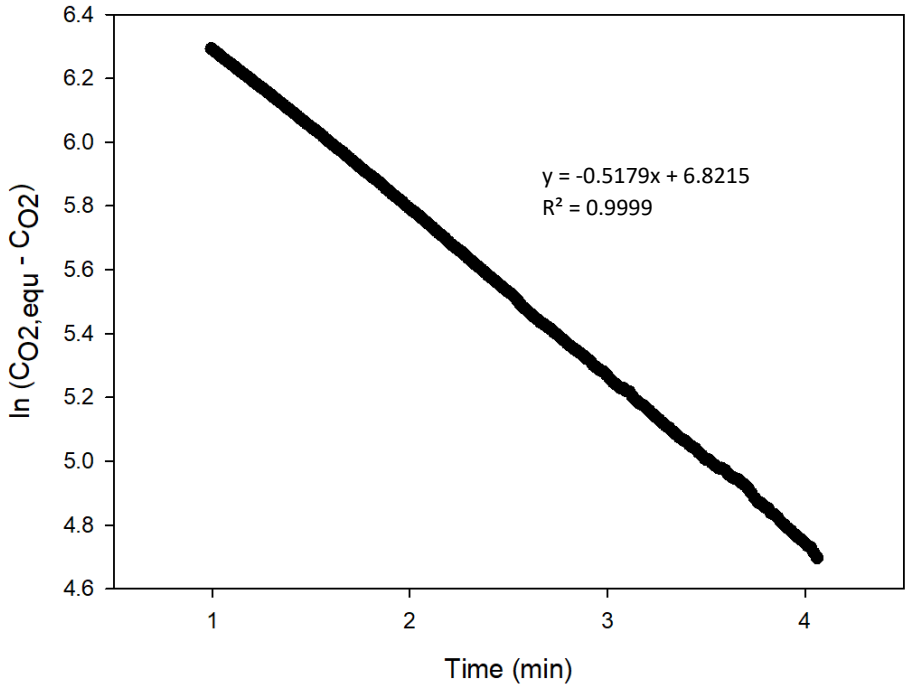

Figure 13: **Determination of the k_La for a 50 mL reactor.** The time in minutes is plotted against the ln ($C_{O2,equ} – C_{O2}$) (-). The respective slope of the linear curve corresponds to the k_La. For the selected reaction set-up (50 mL, 25 mL min^{-1}, 350 rpm) the k_La is 0.52 min^{-1}, which equals 31.2 h^{-1}.

2.2.6 SDS-PAGE

SDS-PAGE was used to verify the successful immobilization of proteins onto carrier materials and in order to check the purity of purified Wt_P450 BM3 and Z_P450 BM3. Further this method was used to determine the *in-operando* and storage stability of immobilized enzymes on ReliSorb™ SP400 (carrier material for Z_{Basic2}-tagged proteins). A general composition for liquid protein samples for SDS-PAGE loading is shown in Table 9. The samples were heated to 95 °C for 10 minutes. Afterwards, samples were centrifuged shortly to spin down condensed liquid on the tube lid. To determine the *in-operando* and storage stability of immobilized enzyme on ReliSorb™ SP400, the enzyme must be removed from the carrier. Therefore, a defined mass of carrier (~10 mg) was mixed with SDS-PAGE loading dye (5 µL per mg carrier) and incubated for 1 hour at 600 rpm and 90 °C in a thermomixer. After a short centrifugation (16100 x g, 2 min, 21°C), 10 µL of liquid sample were mixed with 9 µL dH_2O and 1 µL dithiothreitol (DTT). Depending on the slot number of the SDS-gel, either 10 µL (15 slots per gel) or 15 µL (10 slots per gel) sample were loaded on NuPAGE™ 4-12% Bis-Tris Protein Gels. For evaluation either the PageRuler™ Prestained Protein Ladder (4 µL) or the PageRuler™ Unstained Protein Ladder (4 µL) were loaded as standards on the gel. The SDS-PAGE was run for 60 minutes at 200 V in NuPAGE™ MOPS SDS Running Buffer. Finally, the gels were stained in a Coomassie Brilliant Blue solution (1 g dissolved in MeOH 50% (v/v) and acetic acid 10% (v/v)) and destained in a solution containing ddH_2O, MeOH and acetic acid in a ratio of 5:4:1 (v/v).

Table 9: **General composition of samples for SDS-PAGE analysis.**

	Volume (µL)
Protein sample	14
DTT	1
SDS-PAGE loading dye	5

2.3 Enzyme expression and preparation of cell free extracts (CFEs)

2.3.1 Expression of P450 BM3

Cell material of glycerol stocks containing *Escherichia coli* (*E. coli*) pET28a (+)_Wt_P450 BM3 or *E. coli* pET28a (+)_Z_P450 BM3 were used to inoculate an over-night-culture (ONC) for protein expression in 50 mL LB-medium containing kanamycin (50 µg mL^{-1}) in a baffled flask. On the next day, 2 mL of the ONC were transferred into baffled flasks each containing 200 mL TB-medium, 50 µg mL^{-1} kanamycin and 200 µL trace element solution. The culture was grown at 37 °C and 130 rpm. Protein expression was induced with IPTG (0.2 M) at OD_{600} of 0.8 to 1.0 for Wt_P450 BM3 and at OD_{600} of 1.8 to 2.0 for Z_P450 BM3. Additionally, the heme precursor ALA (0.5 M) was supplemented for efficient heme production. Wt_P450 BM3 was expressed at 30 °C for 20 hours and 110 rpm, Z_P450 BM3 was expressed at 18 °C for 40 hours and 110 rpm.

2.3.2 Expression of Z_GDH

Cell material from a glycerol stock containing *E. coli* pET28a (+)_Z_GDH was used to inoculate an ONC for protein expression (50 mL LB-medium with kanamycin (50 µg mL^{-1}) in a baffled flask). On the next day, 2 mL of the ONC were transferred into baffled flasks each containing 200 mL LB-medium and 50 µg mL^{-1} kanamycin. The culture was grown to OD_{600} of 0.8 to 1.0 at 37 °C and 130 rpm. Protein expression was induced with IPTG (0.2 M) followed by incubation at 25 °C and 110 rpm for 20 hours.

2.3.3 Preparation of cell free extracts (CFEs) of P450 BM3s and Z_GDH

The cells were harvested by centrifugation for 20 minutes at 8850 g rpm and 4 °C. The supernatant was removed, and the pellet was frozen over night at -20 °C. For cell disruption the pellet was resuspended in KPi Buffer (50 mM, pH 7.5) and lysozyme was added (1 mg mL^{-1}). The cell suspension was incubated at 37 °C for one hour. Afterwards, the cells were disrupted by sonication (2 seconds pulse, 4 seconds pause, 5 minutes pulse, 70% amplitude for P450 BM3 and 60% amplitude for Z_GDH). Cell debris was removed by centrifugation at 16100 x g and 4 °C for 30 (P450 BM3) or 20 minutes (Z_GDH), respectively. The supernatant was pooled in a round bottom flask, frozen in liquid N_2 and lyophilized. The active concentration for P450 BM3 and activity of Z_GDH in the lyophilized CFE was determined with the respective assays described in the section 0.

2.4 Co-Immobilization of Z_P450 BM3 and Z_GDH on ReliSorb™ SP400

2.4.1 Preparation of enzyme solutions

Obtained CFEs of Z_P450 BM3 and Z_GDH were dissolved in KPi buffer (50 mM, 250 mM NaCl, pH 7.5) to prepare the enzyme solution for immobilization. The amount of CFE was chosen to reach 4 µM Z_P450 BM3 and 50 U mL^{-1} Z_GDH in solution, respectively. Afterwards, the pH was set to 7.5 (with KOH) and the enzyme solutions were filtered using a 0.45 µm filter to remove any remaining particles that might interfere in the immobilization process.

2.4.2 Co-immobilization of enzymes

All incubation steps were done in an end-to-end rotator at 20 rpm and room temperature (22 °C). The ReliSorb™ SP400 carrier was separated from the enzyme solution and the washing buffer by centrifugation at 3220 x g for 2 minutes followed by a removal of the liquid phase.

ReliSorb™ SP400 was weighed in (100 mg per mL enzyme solution) and incubated in 1 mL KPi buffer (50 mM, 250 mM NaCl, pH 7.5) per 100 mg carrier. The carrier was separated from buffer. The buffer was replaced by enzyme solution followed by immobilization for one hour. Afterwards, the enzyme solution was separated from the carrier and the carrier was washed and incubated in KPi buffer (50 mM, 250 mM NaCl, pH 7.5) for five minutes. The loading of enzyme and washing step was repeated for three times in case of Z_P450 BM3 followed by a single loading and washing step for Z_GDH. For each loading step and each washing step the molarity of the Z_P450 BM3 solution and the activity of the Z_GDH in the supernatant were determined with the assays described in the section 2.2. The prepared carrier was used either immediately or after lyophilization. Based on the difference of measured active enzyme in solution, the loaded nmole Z_P450 BM3 and Units Z_GDH per g carrier were determined and an immobilization efficiency (%) was calculated with the following formula.

$$\text{Immobilization efficiency (\%)} = \frac{(C_0 - C)}{C_0} \times 100$$

- C_0 … concentration of active Z_P450 BM3 or Units Z_GDH in the loading fraction (µM or U mL^{-1})
- C … concentration of active Z_P450 BM3 or Units Z_GDH in the supernatant after loading (µM or U mL^{-1})

2.5 Purification of P450 BM3

The Wt_P450 BM3 and Z_P450 BM3 were purified for the determination of kinetic parameters. Cell disruption for Wt_P450 BM3 was performed as described previously using a 100 mM KPi buffer (pH 7.5, 300 mM KCl, 25 mM imidazole) for Wt_P450 BM3 and a 50 mM KPi buffer (pH 7.5) for Z_P450 BM3. The supernatant obtained after centrifugation was sterile-filtered using a 0.45 µm filter and the pH was re-set to 7.5.

The Wt_P450 BM3 was purified by affinity chromatography with a $NiSO_4$-His-Trap using the ÄKTA-system for pumping and UV-detection of proteins at 4°C. Buffer A (100 mM KPi, pH 7.5, 300 mM KCl, 25 mM imidazole) was used for the loading/binding of the Wt_P450 BM3 and Buffer B (100 mM KPi, pH 7.5, 300 mM KCl, 400 mM imidazole) for the elution. The entire process was performed with a flow rate of 2 mL min^{-1}. After loading the column, the resin was washed with Buffer A until a stable UV-signal was reached, followed by an isocratic elution of the Wt_P450 BM3 with Buffer B. The amount of active Wt_P450 BM3 in the elution fractions was determined via CO-titration and the fractions were loaded on a SDS-PAGE to verify purity of samples. The fractions were pooled and the purified Wt_P450 BM3 was re-buffered against Buffer C (100 mM KPi, pH 7.5, 300 mM KCl) via dialysis. Therefore, a dialysis tube with a cut-off of 8 kDa was filled with the Wt_P450 BM3 solution and put into 600 ml Buffer C for 24 hours. Buffer C was replaced twice by fresh solution of the same buffer. Finally, the enzyme solution was frozen in liquid nitrogen and lyophilized.

The Z_P450 BM3 was purified via ion exchange chromatography with pre-packed HiTrap SPFF columns using the ÄKTA-system for pumping and UV-detection of proteins at 4°C. Buffer D (50 mM KPi, pH 7.5) was used for equilibration of the column and loading of the Z_P450 BM3, Buffer E (50 mM KPi, 2 M NaCl, pH 7.5) for the elution of Z_P450 BM3. The elution was done with a gradient from 0 to 100% Buffer E in a total volume of 75 ml. The entire process was performed with a flow rate of 3 mL min^{-1}. The amount of active Z_P450 BM3 in the elution fractions was determined via CO-titration and the fractions were loaded on a SDS-PAGE to determine purity of protein samples. The fractions containing purified Z_P450 BM3 were pooled and re-buffered against Buffer E via dialysis. Therefore, a dialysis tube with a cut-off of 8 kDa was filled with the Z_P450 BM3 solution and put into 600 ml Buffer E for 24 hours. Buffer E was replaced only once during dialysis as a protein precipitation became visible overtime.

2.6 Preparative scale reactions to produce C12:0-OHs

Reactions for the conversion of C12:0 on preparative scale were performed at least at 45 mL scale for reliable installation of all sensor systems. The reactions were performed either in a double-walled reaction vessel (Wheaton) or a 250 mL beaker, respectively. The reactions were homogenously mixed via an IKA® RCT basic hotplate stirrer and a magnetic stirrer bar or an IKA® RW 20 digital overhead stirrer. The temperature was set to 25 °C by either connecting the double-walled reaction vessel (Wheaton) to a Brinkmann Lauda Ecoline RE104 Recirculating chiller or by tempering the beaker in a water bath, which was temperature controlled via the IKA® RCT basic hotplate stirrer. The 500 mL reaction was performed in an 800 mL beaker without temperature control (RT). For fed-batch strategies, the substrate was supplied either manually or automatically. A MCP-CPG piston pump from Ismatec® was used for the automatic supply of substrate in fed-batch mode. A general reaction composition is displayed in Table 10.

Table 10: **General reaction composition of reactions for the preparative scale conversion of C12:0**

Reactor components	**Concentration/stocks/catalyst loading**
P450 BM3 (Wt or Z_{Basic2})	Free (CFE) or immobilized, 2 µM
GDH (DSM or Z_{Basic2})	Free (CFE) or immobilized, 1.9 to 14 U mL^{-1}
Reaction buffer	50 mM KPi (pH 7.5, 0 or 250 mM NaCl)
C12:0	40 to 80 mM final concentration (stocks in EtOH and/or DMSO)
Glucose	200 or 300 mM (1 M stock in KPi buffer)
Bovine liver catalase	1 mg mL^{-1}
Antifoaming agent	Antifoam 204 (600 µL) or silicone antifoam (2 to 20 mg)

O_2 concentration in the liquid phase was constantly measured as described on page 20 for the k_La determination. Pure O_2 was supplied at a defined volumetric mass flow controlled via an EL-FLOW® select mass flow meter. As pH stabilization was necessary, a TitroLine Alpha titration device was used to keep the pH at 7.2 by pumping 5 M KOH into the reaction. A general reaction set-up is depicted in Figure 14.

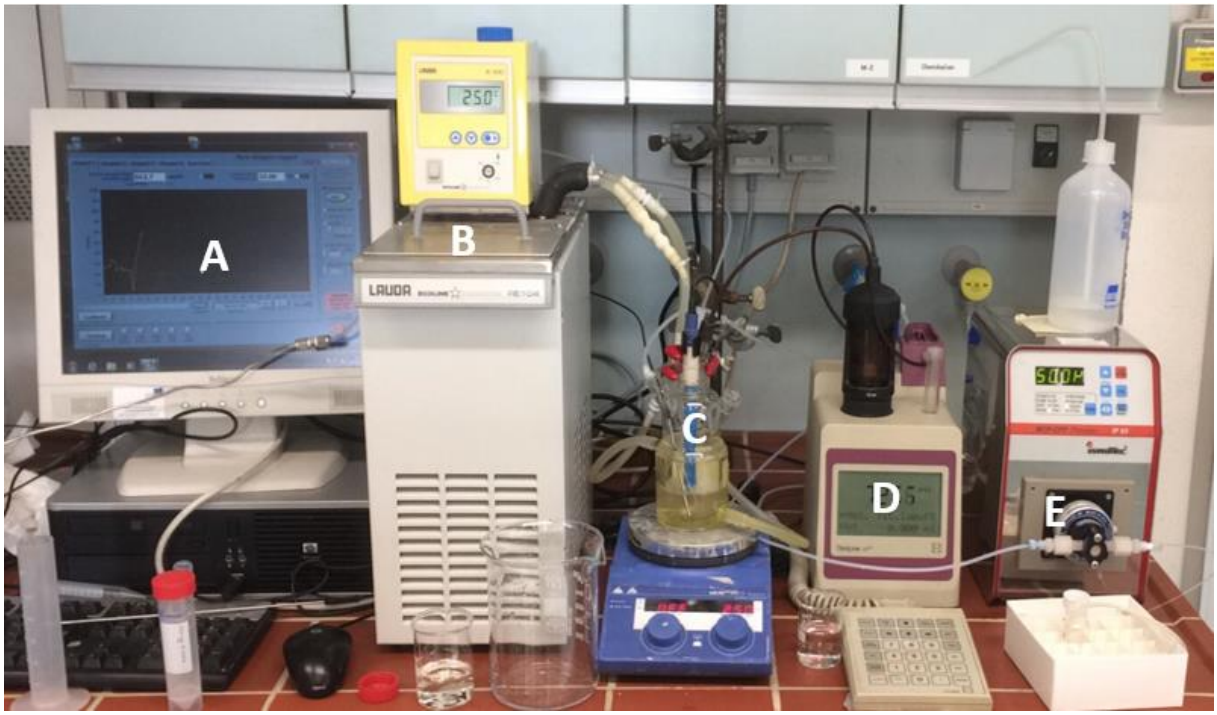

Figure 14: **General set-up for the preparative scale production of C12-OHs with the P450 BM3/GDH reaction system.** (A) PC monitoring O_2 concentration, (B) Brinkmann Lauda Ecoline RE104 Recirculating chiller for temperature control, (C) Double-walled reaction vessel (Wheaton) containing pH electrode and titration tip, O_2 sensor and O_2 inflow and standing on a magnetic stirrer plate, (D) TitroLine Alpha titration device for pH stabilization, (E) MCP-CPG piston pump used for fed-batch supplementation of C12:0.

2.7 Preparative isolation of C12:0-OHs

Two-phase solvent extraction of C12:0-OHs

Depending on whether the co-immobilizate was re-used or not, it was separated from the liquid reaction by centrifugation (2 minutes at 3220 x g) or included in the product extraction process. In general, reactions were acidified to a pH of 1.0 or lower using 37% HCl which leads to the formation of a white precipitate. Fatty acids and products were extracted into the organic phase by adding equal amounts of EtOAc. The solution was mixed vigorously to enhance the mass transfer. Afterwards, the water and organic phase were separated by centrifugation for 2 minutes at 3220 x g and room temperature. The supernatant was transferred into a beaker containing anhydrous Na_2SO_4. This extraction process was repeated for three times. Afterwards, the organic phase was transferred into a round bottom flask. Organic solvent was removed under vacuum in a rotavapor. For the 45 to 50 mL reactions, the oily residue was transferred into a 25 mL glass vessel. Residues were transferred by washing the round bottom flask with a few mL DMSO. For the 500 mL reaction the round bottom flask was directly used for removal of DMSO and EtOAc under a constant airflow for several hours. Before freezing the samples, dH_2O was added (roughly 2 mL dH_2O per mL sample) and mixed vigorously to form an emulsion that was finally lyophilized to remove organic solvents.

Product quantification and determination of purity via GC analysis

The extracted products were quantified and characterized for their specific mass and the isolated yield (%) was calculated. The isolated yield is defined as the ratio of the extracted mass and the theoretical maximal obtainable product mass. The maximal obtainable product mass was calculated based on the applied substrate and considering the insertion of the oxygen atom into the fatty acid backbone. Consequently, 100% conversion of 200 mg of C12:0 (molecular weight = 200 g mol^{-1}) should result in maximal 216 mg of C12:OHs (molecular weight = 216 g mol^{-1}). For purity analysis, about 10 mg of the solid material was dissolved in 1 mL EtOAc containing 20 mM 1-octanol. The samples were diluted 1:5 in EtOAc containing 20 mM 1-octanol and 120 µL were mixed with 60 µL MeOH and 10 µL trimethylsilyl-diazomethane. Derivatized samples were analysed by GC-MS or GC-FID. The GC chromatograms were checked for the corresponding peaks of product(s) and remaining substrate. In order to calculate the GC-purity of products the following equation was used:

$$\text{GC purity (\%)} = \frac{\text{GC peak area C12:0} - \text{OHs}}{\text{total GC peak area (excluding solvent peak)}} \times 100$$

2.8 Determination of kinetic key parameters of P450 BM3

Kinetic key parameters for Wt_P450 BM3 and free and immobilized Z_P450 BM3 were determined to obtain a deeper understanding of the reaction system in terms of oxygen consumption, substrate conversion and product overoxidations. Different methods, including photometrical measurements (NADPH oxidation), measurements of oxygen depletion, and determination of substrate consumption and product formation via GC-FID, were used to calculate key parameters such as maximal NADPH and O_2 consumption rates, K_m, k_{cat}, k_{eff} as well as the coupling efficiency for selected substrates.

Determination of the maximal O_2 consumption rate, K_m and k_{cat}

The reaction set-up for the determination of v_{max} and K_m based on the oxygen consumption of the respective monooxygenase catalyst is summarized in Table 11 and Table 12. In general, reactions were carried out at 22 °C in 2 mL Eppendorf tubes at reaction volumes of 1 mL. The reaction was mixed with a magnetic stirrer at 300 rpm. A 50 mM KPi buffer (pH 7.5) was used as reaction buffer and in total 10% DMSO (v/v) were applied. The reaction was started by adding NADPH. The decrease of oxygen concentration was measured and used to calculate the maximal O_2 depletion rate and K_m for different enzyme preparations and the substrates C12:0 and C12:0-OHs. For Z_P450 BM3 (CFE) solely the maximal O_2 consumption rate was determined (triplicates). The turnover number k_{cat} was calculated by multiplying the maximal O_2 consumption rate with the corresponding coupling efficiency, k_{eff} by dividing k_{cat} with k_m.

Table 11: **Reaction set-up for the determination of v_{max} and K_m for conversion of C12:0.**

Catalyst	P450 BM3 (µM)	C12:0 (mM)	NADPH (µM)
Wt_P450 BM3 (CFE)	0.15	0 – 2	500
Z_P450 BM3 (CFE)	0.14	1 [a]	
Wt_P450 BM3 (purified)	0.30	0 – 1.5	
Z_P450 BM3 (purified)	0.35	0 – 2	
Co-immobilizate	0.50	0 – 6	

[a] for Z_P450 BM3 (CFE) solely the maximal O_2 consumption rate was determined

Table 12: **Reaction set-up for the determination of v_{max} and K_m for conversion of C12:0-OHs.**

Catalyst	P450 BM3 (µM)	C12:0-OHs (mM)	NADPH (µM)
Wt_P450 BM3 (CFE)	0.15	0 – 5	500
Z_P450 BM3 (CFE)	0.14	3 [a]	
Wt_P450 BM3 (purified)	0.42	0 – 5	
Z_P450 BM3 (purified)	0.45	0 – 5	
Co-immobilizate	1.0	0 – 10	

[a] for Z_P450 BM3 (CFE) solely the maximal O_2 consumption rate was determined

Determination of maximal NADPH consumption rates

The maximal NADPH consumption rate was determined spectrophotometrically in 1 mL reactions in cuvettes. The reaction compositions for different enzyme loadings and C12:0 and C12:0-OH (stocks in DMSO) is summarized in Table 13 and Table 14, respectively. In general, a 50 mM KPi buffer (pH 7.5) was used and the reactions contained 10% DMSO (v/v). The reactions were mixed excluding NADPH, blanked at 340 nm and started by adding NADPH (50 mM stock). The change of absorption at 340 nm was recorded and used to calculate the change of NADPH concentration over time based on the Beer-Lambert law (ε_{340} = 6.22 mM^{-1} cm^{-1}). All reactions were measured in triplicates and reactions without enzymes were measured as blanks.

Table 13: **Reaction set-up for the determination of the maximal NADPH consumption rate with C12:0 as substrate.** The co-immobilizate was excluded from the experiment, as it is not feasible to perform reliable spectral analysis with solid compounds/particles with this technical setup.

Catalyst	P450 BM3 (µM)	C12:0 (mM)	NADPH (µM)
Wt_P450 BM3 (CFE)	0.32	1	250
Z_P450 BM3 (CFE)	0.20		
Wt_P450 BM3 (purified)	0.28		
Z_P450 BM3 (purified)	0.28		

Table 14: **Reaction set-up for the determination of the maximal NADPH consumption rate with C12:0-OHs as substrate.** The co-immobilizate was excluded from the experiment, as it is not feasible to perform reliable spectral analysis with solid compounds/particles with this technical setup.

Catalyst	P450 BM3 (µM)	C12:0-OHs (mM)	NADPH (µM)
Wt_P450 BM3 (CFE)	0.73	3	250
Z_P450 BM3 (CFE)	0.60		
Wt_P450 BM3 (purified)	0.84		
Z_P450 BM3 (purified)	0.50		

Determination of coupling efficiencies

The reaction set-up for the determination of the coupling efficiency for different enzyme loadings and C12:0 and C12:0-OHs (stocks in DMSO) is shown in Table 15 and Table 16. The reaction volume was 250 µL (50 mM KPi, pH 7.5) and in total 10% DMSO (v/v) was applied as final concentration. The reactions were incubated in a thermomixer at 25 °C and 400 rpm overnight. Afterwards, 25 µL HCl (37%) were added and the converted/depleted C12:0 and formed C12:0-OHs were quantified via GC-FID analysis. The reactions were carried out in triplicates and reactions without enzymes were prepared as controls (100% substrate). The coupling efficiency is defined as followed:

$$\text{coupling efficiency}\ (\%) = \frac{\text{mol NAD(P)H consumed}}{\text{mol product formed}} \times 100$$

Table 15: **Reaction set-up for the determination of the coupling efficiency for conversion of C12:0.** CFEs were excluded from the experiment, as significant background oxidation from NADPH was observed.

Catalyst	P450 BM3 (µM)	C12:0 (µM)	NADPH (µM)
Wt_P450 BM3 (purified)	1.1	300	250
Z_P450 BM3 (purified)	1.0		
Co-immobilizate	2.2		

Table 16: **Reaction set-up for the determination of the coupling efficiency for conversion of C12:0-OHs.** CFEs were excluded from the experiment, as background oxidation from NADPH was observed.

Catalyst	P450 BM3 (µM)	C12:0-OHs (µM)	NADPH (µM)
Wt_P450 BM3 (purified)	1.1	500	500
Z_P450 BM3 (purified)	1.0		
Co-immobilizate	2.2		

3 Results and discussion

3.1 Expression and immobilization of enzymes

Z_P450 BM3 expression was induced at OD_{600} between 1.8 and 2.0 and expressed for 48 h at 16 °C. The highest-achieved expression yield was 27.4 mg Z_P450 BM3 per g lyophilized CFE. In total, 5 g (dry weight) of lyophilized CFE were produced from 3 L culture, which corresponds to 45.6 mg Z_P450 BM3 (molecular weight = 127 kDa) per L of culture. In comparison, the highest-achieved expression yield for Wt_P450 BM3 was 75.6 mg per g of lyophilized CFE. From 1.5 L of culture, 2.5 g CFE were prepared, which corresponds to 126 mg of Wt_P450 BM3 (molecular weight = 120 kDa) per litre of culture. Wt_P450 BM3 is therefore faster and better expressible (three-fold higher protein yield) compared to the Z_P450 BM3. However, according to previously reported results no influence of the Z_{Basic2} module on the expression yield of *Tv*DAO and *Lm*SPASE was observed [47]. Probably, the dimeric structure of P450 BM3 and the folding of the large multidomain protein with the Z_{Basic2}-module could be reasons for a worse expression. Z_GDH expression was induced at OD_{600} between 0.8 and 1.0 and expressed for 20 h at 25 °C. In total, 2 g of lyophilized CFE from 2.6 L culture could be obtained. The activity of the CFE was determined to be 2.18 U mg^{-1} CFE (dry), which corresponds to 1677 U Z_GDH per L of culture.

3.1.1 Optimized immobilization process for Z_{Basic2}-tagged enzymes

Scaling up the immobilization from mg-scale to g-scale (based on applied carrier material) resulted in unsatisfactory immobilization yields for Z_P450 BM3. While average immobilization yields of 56% could be reached at the mg-scale (directly from the bacterial cell extract), the overall immobilization yield was only 20% at g-scale [31]. Therefore, crucial immobilization parameters like the pH and the NaCl concentration were investigated and the immobilization process itself was reviewed in more detail. For the first attempts of co-immobilizate preparation, the disrupted cell suspension of the Z_P450 BM3 was centrifuged for 10 min according the original protocol from Valihkani et al (2018) [31]. However, the supernatant remained viscous and not transparent indicating presence of insoluble particles that potentially interfere with the immobilization process. Enhancing the centrifugation time to 30 minutes resulted in a much clearer supernatant. It is very likely that for the first g-scale immobilization experiments, the poorly prepared cell free extract (CFE) might have led to a clogging of the ReliSorb^{Tm} SP400 and hence low immobilization efficiencies were obtained. To remove the majority of particles the CFEs were additionally filtered through a 0.45 µm filter. Enhancing the centrifugation time in combination with a subsequent filtration step increased the amount of loaded Z_P450 BM3 by a factor of two to three compared to initial immobilizations on g-scale. Next, the immobilization process was performed at different pH and NaCl concentrations applying 100 mg ReliSorb^{Tm} SP400 per sample. The ionic strength and the pH are important parameters as the immobilization is based on the ionic interaction between the negatively charged sulphonic groups of

ReliSorb^{Tm} SP400 and the positively charged and arginine rich (pKa >12) Z_{Basic2}-module [49]. To determine binding efficiencies, the overall nmol of loaded Z_P450 BM3 and U Z_GDH per g ReliSorb^{Tm} SP400 were calculated (Table 17). The immobilization efficiency for each condition and each loading step is shown in Figure 15 and Figure 16. The results indicate that a pH variation between 7.0 and 8.0 do not significantly influence on the immobilization yield. This could be expected as the chosen pH values were below the pKa of arginine. However, increasing the NaCl concentration to 500 mM drastically decreased the amount of immobilized Z_P450 BM3. Interestingly, the amount of loaded Z_GDH increased with elevated NaCl concentration. This might be explained by a higher stringency of the system and therefore less occupied spots by other proteins found in the CFE. The initial immobilizations conditions (pH 7.5, 250 mM NaCl, not optimized) were suitable to bind both proteins in sufficient quantity [31].

Table 17: **Loaded nmole Z_P450 BM3 and Units Z_GDH on ReliSorb ^{Tm} SP400 at different pH values and NaCl concentrations.**

	Varying pH (@250 mM NaCl)			Varying NaCl concentration (@pH 7.5)			
	pH 7.0	**pH 7.5**	**pH 8.0**	**0 mM**	**100 mM**	**250 mM**	**500 mM**
Z_P450 BM3 per g ReliSorb^{Tm} SP400 (nmol g^{-1})	42.6	47.3	48.3	48.7	56.3	58.6	33.6
Z_GDH per g ReliSorb^{Tm} SP400 (U g^{-1})	288	298	355	113	214	321	394

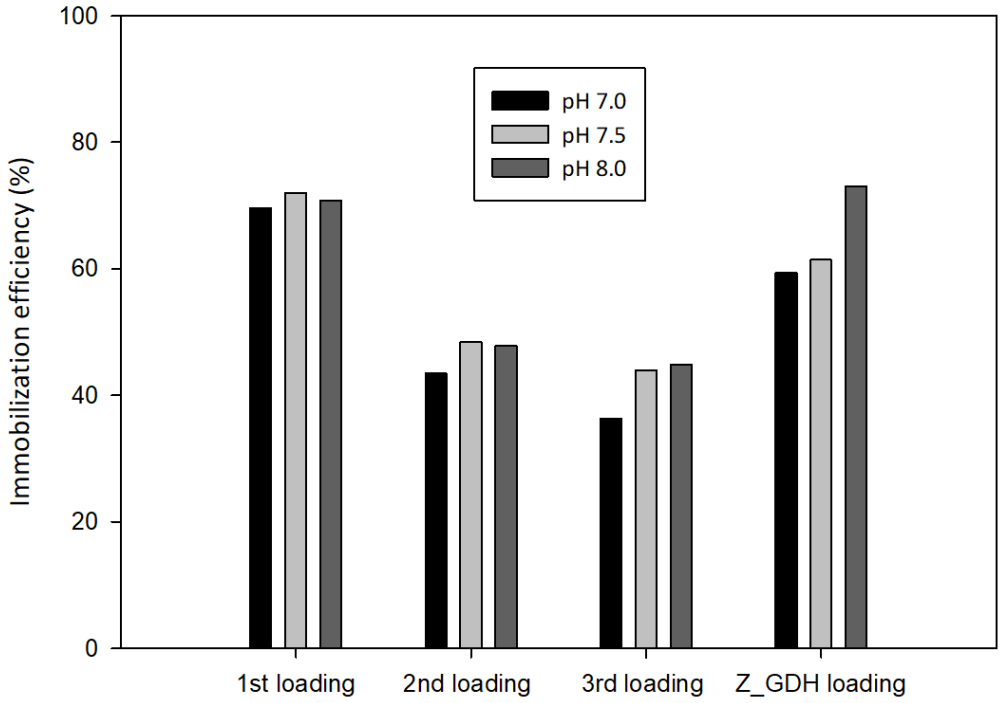

Figure 15: **Immobilization efficiency for Z_P450 BM3 (loaded in three steps) and Z_GDH (loaded in one step) at varying pH values.**

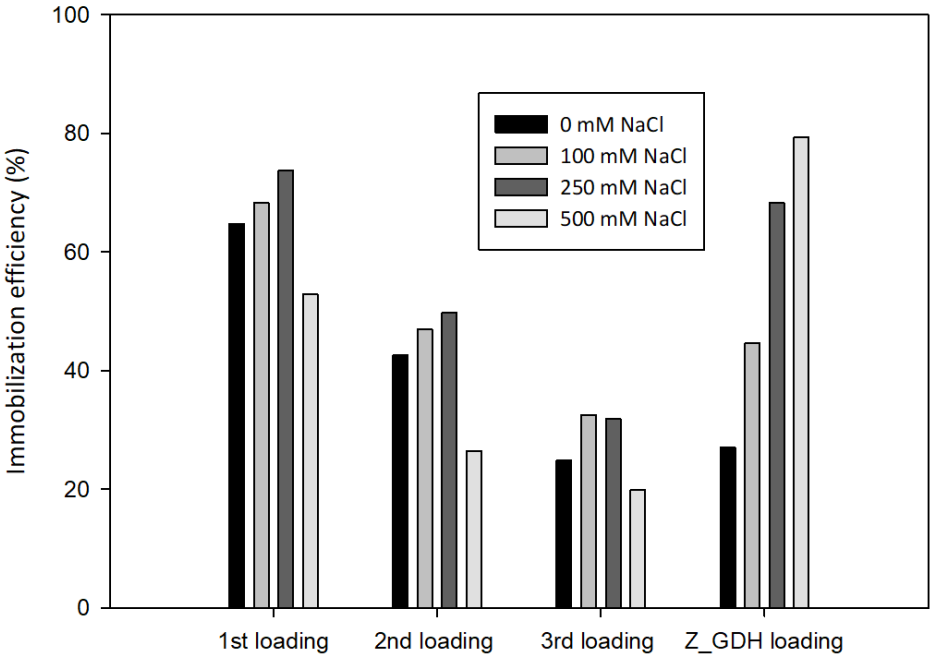

Figure 16: **Immobilization efficiency of Z_P450 BM3 (loaded in three steps) and Z_GDH (loaded in one step) at varying NaCl concentrations.**

3.1.2 Co-immobilization of Z_P450 BM3 and Z_GDH on g-scale

Using the adapted protocol including the enhanced centrifugation time for CFE preparation and the filtration of the enzyme solutions resulted in useful immobilization efficiencies at g-scale. The immobilization can be followed by the naked eye, as the white ReliSorb^{Tm} SP400 became reddish-brown colored mainly due to the heme group of the Z_P450 BM3 (Figure 17).

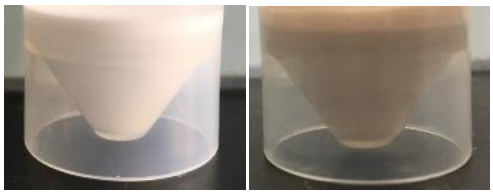

Figure 17: **ReliSorb^{Tm} SP400 before (left) and after the immobilization (right) of Z_P450 BM3 and Z_GDH.** The heme group of the Z_P450 BM3 led to a reddish-brown colour of the carrier.

Figure 18 shows the average immobilization efficiency for each loading step of Z_P450 BM3 and Z_GDH of three independent immobilization approaches. For the Z_P450 BM3 loading it decreases from 90.0% in the first loading step to 59.7% in the third loading step. The immobilization efficiency for the Z_GDH was 80.5%. Notably, less than 10% of Z_P450 BM3 eluted during the loading of the Z_GDH. In three repeated batches (N = 3) average immobilization efficiencies of 67.4% over three consecutive binding steps for Z_P450 BM3 could be achieved (including elution in step 4). Finally, an average of 83.0 nmol Z_P450 BM3 and 488 U Z_GDH were immobilized on 1 g of ReliSorb^{Tm} SP400. Calculating the U Z_P450 BM3 per g carrier via the kinetic parameters determined for purified Z_P450 BM3 (1.7 nmol O_2 per s

and nmol Z_P450 BM3, Table 31) results in 8.3 U Z_P450 BM3 per g ReliSorb^{Tm} SP400. Effectiveness factors η for immobilized Z_P450 BM3 (η=0.48) and Z_GDH (η =0.31) were reported [31], which results in active 4 U Z_P450 BM3 and 151 U Z_GDH per g ReliSorb^{Tm} SP400. One should consider that the kinetic parameters for Z_P450 BM3 were determined in presence of 10% DMSO, which was reported to have a significant influence on the P450 BM3 activity [50]. Therefore, calculated activities for immobilized Z_P450 BM3 might be under-evaluated. Nevertheless, Z_GDH was loaded in the desired excess to provide enough NADPH for the monooxygenase.

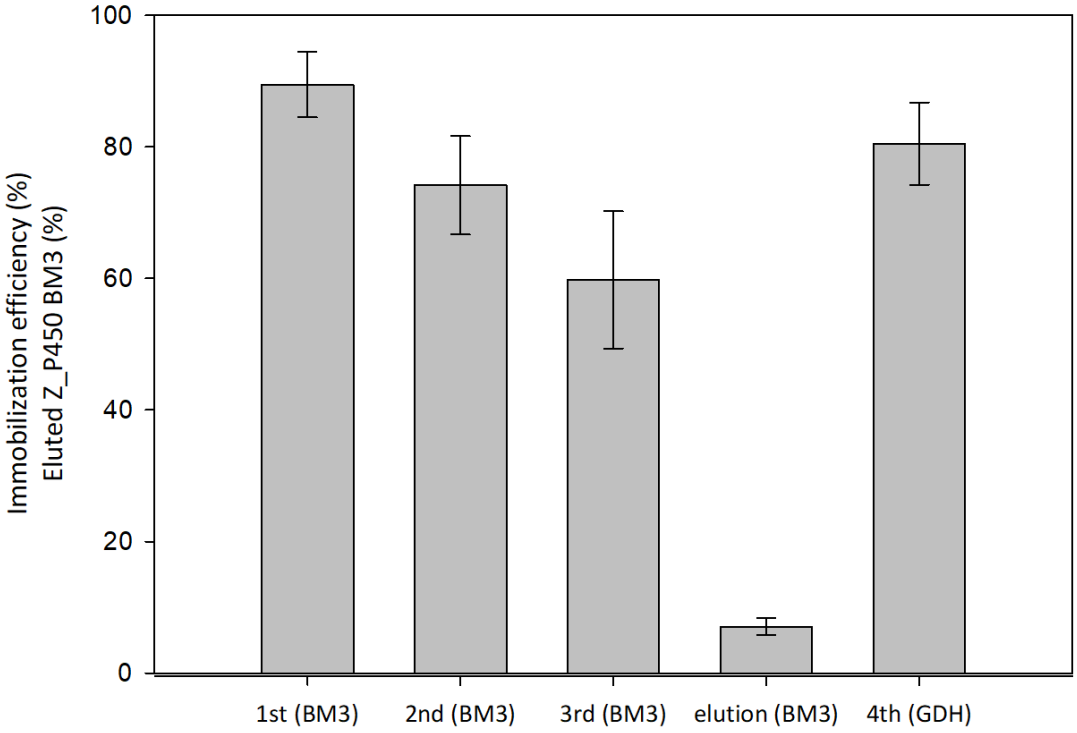

Figure 18: **Immobilization efficiencies for the preparation of the co-immobilizate on g-scale.** The average immobilization efficiency and standard deviation for three Z_P450 BM3 and one Z_GDH loading step of three independent immobilization processes (N=3) are depicted. Additionally, the percentage of eluted Z_P450 BM3 during the Z_GDH loading step in dependency of the total loaded Z_P450 BM3 is shown.

3.1.3 Single step immobilization of Z_P450 BM3

As the immobilization step is a time intensive process (incubation and washing steps; enzyme assays), the reduction of handling steps for the immobilization Z_BM3 P450 was tested. The application of lyophilized Z_P450 BM3 CFE enables the preparation of solutions of arbitrary enzyme concentrations. Therefore, loading three times 4 µM was compared to loading single step immobilization of 11 µM Z_P450 BM3. Considering the Z_P450 BM3 leakage in the Z_GDH loading step the immobilization efficiency for Z_P450 BM3 was 71% in the four-step loading and 75% in the two-step loading. For the Z_GDH 88% immobilization efficiency were reached in the four-step loading and 73% in the two-step loading. In comparison to the four-step loading approach (84 nmol BM3, 604 U GDH per g carrier),

80 nmol Z_P450 BM3 and 479 Units Z_GDH per g carrier were loaded in the shortened two-step loading approach. Influences on a possible effect on the catalytic characteristics of the co-immobilizate were not investigated. Both loading strategies led to a similar immobilization success for the Z_P450 BM3 and Z_GDH.

Table 18: **Comparison of loading three times 4 µM Z_P450 BM3 and one time 10.9 µM Z_P450 BM3.** The immobilization effieciency for each step was calculated by dividing the sum of supernatant fraction (S) and washing fraction (W) by the loading fraction (L).

Four step loading				Two step loading			
	Z_P450 BM3 (µM)	**Z_GDH (U mL^{-1})**	**Efficiency (%)**		**Z_P450 BM3 (µM)**	**Z_GDH (U mL^{-1})**	**Efficiency (%)**
L (P450)	3.96	-		L (P450)	10.9	-	
S1 (P450)	0.28	-	93	S (P450)	2.65	-	76
W1 (P450)	0.0	-		W (P450)	0.06	-	
S2 (P450)	0.79	-	78	L (GDH)	-	65.5	
W2 (P450)	0.08	-		S (GDH)	0.1	16.8	73
S3 (P450)	1.38	-	65	W (GDH)	0.02	0.8	
W3 (P450)	0.02	-					
L (GDH)	-	68.9					
S (GDH)	0.9	8.4	88				
W (GDH)	0.01	0.1					

L = loading fraction, S = supernatant after loading, W = wash fraction

3.1.4

3.1.5 Storage stability of immobilized enzymes

The liquid phase of a stored co-immobilizate became coloured over time indicating elution of P450 protein. Therefore, the storage stability of the co-immobilizate in liquid (50 mM KPi buffer, pH 7.5, 250 mM NaCl) was investigated. For this, 100 mg co-immobilizate were stored at 4 °C in 50 mM KPi (pH 7.5, 250 mM NaCl) and the enzyme content on the carrier after three days and seven days of immobilization was monitored via SDS-PAGE (Figure 19). The SDS-PAGE revealed a clear release of Z_P450 BM3 from the carrier, while Z_GDH remained in bound form to a large extend. The red supernatant found during longer storage time clearly supports that Z_P450 BM3 elutes from the carrier (Figure 19, B).

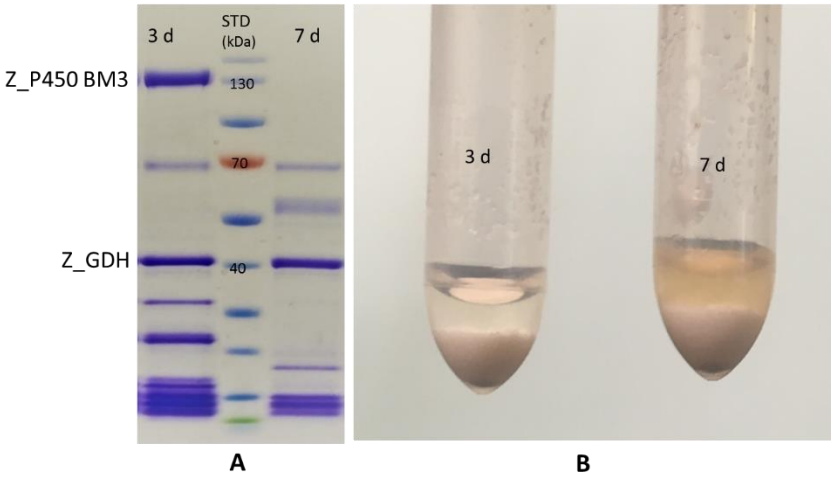

Figure 19: **SDS-PAGE to monitor the storage stability of the co-immobilizate in liquid (A) and the respective carriers in solution (B).** (A) The left lane shows the protein composition on the carrier after three days (d) of storage at 4 °C in 50 mM KPi (pH 7.5, 250 mM NaCl), the right lane after seven days. As standard (STD) serves the PageRuler™ Prestained Protein Ladder from Thermo Fisher. (B) The left eppendorf tube shows carrier stored for three days, the right Eppendorf tube contains carrier material stored for seven days.

In order to prevent elution during storage and to achieve high storage stability of enzymes, lyophilization of the carrier was conducted. To benchmark both treatments/storage strategies, liquid-stored and lyophilized carrier, both stored at 4 °C, were compared. The enzyme quantity and distribution on both carriers was investigated via SDS-PAGE directly after preparation (same day) and after one week of storage. Additionally, the enzyme binding stability on the lyophilized carrier at -20 °C was studied over several weeks (Figure 20). To remove unbound enzymes from the lyophilized carrier it was washed with 50 mM KPi (pH 7.5, 250 mM NaCl) before eluting bound proteins by the SDS-PAGE loading dye treatment. Lyophilization of the co-immobilizate drastically increased the binding stability of Z_P450 BM3 on ReliSorb^{Tm} SP400 during storage compared to the liquid stored co-immobilizate. Even after 52 days of storage at -20°C there is no elution of Z_P450 BM3 from the carrier observable. The removal of aqueous solution prevents elution of the enzyme from the carrier providing a simple formulation of the enzymes.

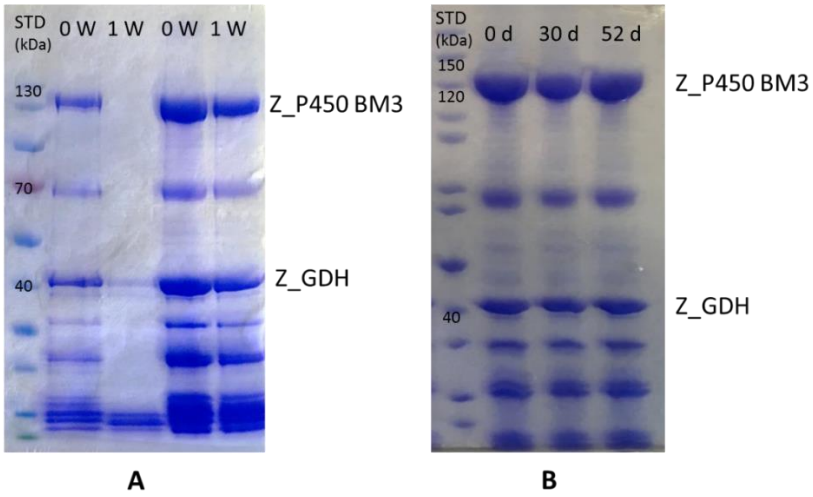

Figure 20: **Analysis of storage stability of BM3/GDH on ReliSorb^{Tm} SP400 via SDS-PAGE.** (A) The left lanes depict the protein composition of the liquid stored carrier after zero and one week (W) of storage. The right lanes depict the protein composition of lyophilized carrier after zero and one week of storage. As reference protein mass standard (STD) serves the PageRuler™ Prestained Protein Ladder from Thermo Fisher. (B) The lanes display the protein compostion of lyophilized carrier after zero, 30 and 52 days (d) of storage at 4°C. As standard (STD) serves the PageRuler™ Unstained Protein Ladder from Thermo Fischer.

In addition, conversion experiments were performed to test the activity of the stored carriers. Three mg lyophilized carrier or 10 mg liquid stored carrier were used in one mL reactions in 50 mM KPi (pH 7.5) containing 200 mM glucose, 2 mM C12:0, 200 µM $NADP^+$, 1 mg mL^{-1} catalase and 2% EtOH (v/v). GC-MS analysis showed full conversion for the liquid stored carrier after zero weeks of storage and for the lyophilized carrier after zero and one week of storage. For the liquid stored carrier 0% conversion was detectable after one week of storage (Figure 21, Figure 45). In summary, lyophilization increases the storage stability of the carrier.

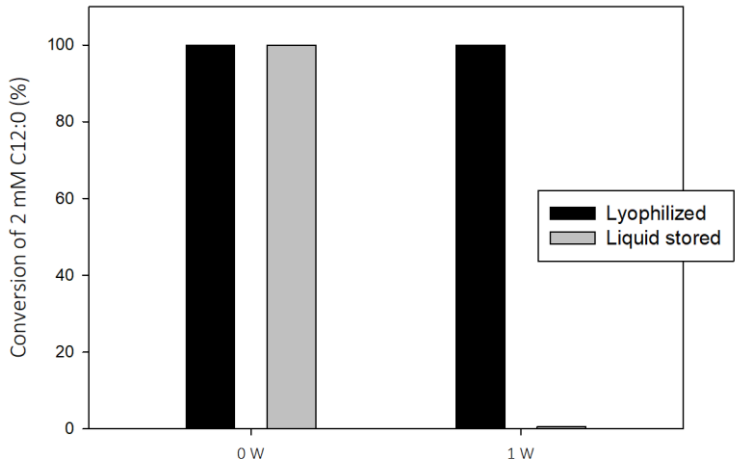

Figure 21: **Conversion of 2 mM C12:0 catalyzed by the co-immobilizate after zero weeks (0 W) and one week (1 W) storage at 4°C.** The lyophilized stored co-immobilizate reached full conversion after zero and one week of storage, the liquid stored carrier reached full conversion after zero weeks of storage. No conversion was detected after one week of storage in liquid.

Attempts to determine a possible activity loss during storage of the co-immobilizate at -20 °C were performed. However, investigation of kinetic parameters (see section 3.3.2) revealed that it is not possible to saturate the carrier with substrate (C12:0). Consequently, the maximal catalytic turnover of the co-immobilizate was measured at time points over several weeks. Co-immobilizate with one nmol of Z_P450 BM3 (finally 0.1 µM) and 4.4 U Z_GDH (finally 0.44 U mL^{-1}) was incubated in 10 mL reactions containing 4 mM C12:0, 200 mM glucose, 500 µM $NADP^+$, 1 mg mL^{-1} catalase and 5% (v/v) DMSO. The O_2 concentration was recorded and the reaction was stirred at 250 rpm. After 22 hours of reaction and no further O_2 consumption a sample was analysed by GC-FID. The percentage GC-area of the C12:0-OHs in relation to the total GC-area of C12:0-OHs and C12:0 was calculated. The calculation resulted in 98.5% GC-area C12:0-OHs after zero days of storage (39400 TTN). The percentage GC-area decreased to 21.9% after 28 days and 8.0% after 75 days of storage indicating a significant loss of catalytic activity of the lyophilized co-immobilizate over time (Figure 22). However, as the co-immobilizate was used for multiple purposes and hence was frozen and thawed frequently, the amount of H_2O was determined in the stored sample. Therefore, 200 mg co-immobilizate were analysed in a moisture analyser (105 °C, end of analysis was reached when less than 1% weight change per min, Satorius MA 100) after 76 days of storage. The analysis was finished after 9 min resulting in a final weight of 152 mg, what corresponds to 24% moisture. Despite lyophilization of the carrier (complete dry powder obtained) significant amount of H_2O was detected and potentially accumulated after 76 days storage time, which might contribute to the clear activity loss of the co-immobilizate.

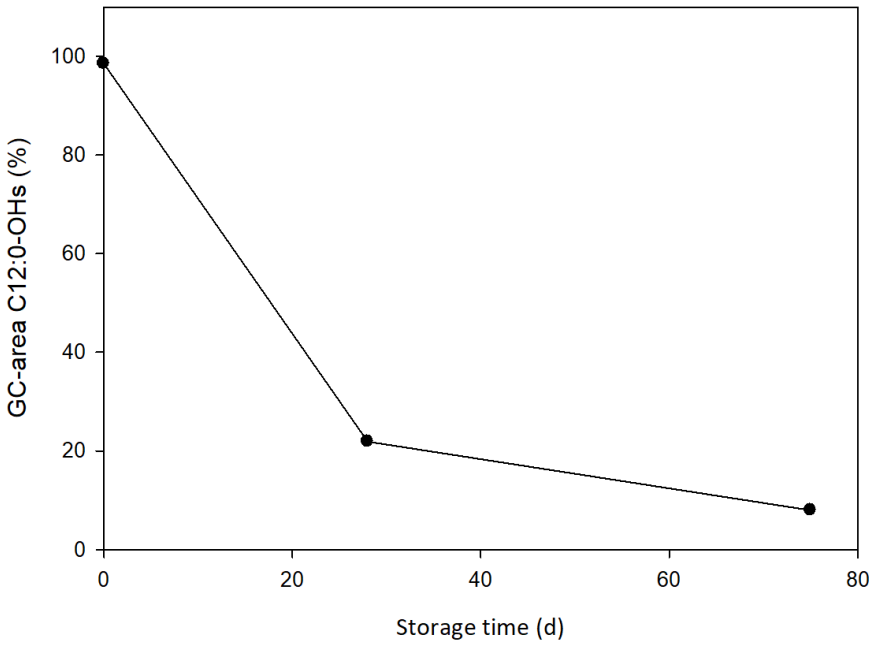

Figure 22: **Activity study for the co-immobilizate stored at -20°C.** A significant loss of activity from 98.5% GC-area C12:0-OHs after zero days of storage to 8.0% after 75 days of storage was observed.

3.2 Preparative scale reaction to convert dodecanoic acid

3.2.1 Relevance of pH stabilization and O_2 supply in the P450/GDH coupled reaction

The P450 BM3/GDH system should be used to convert C12:0 on preparative scale. Preliminary tests were conducted for investigation of crucial reaction parameters such as pH and the effect of O_2 supply into the reaction. The regeneration of NAD(P)H based on a GDH system and hence the formation of gluconic acid (pKa = 3.7) from glucose leads to a drop in pH (Figure 23) [38, 51]. This has severe influence in reactions with high loading of fatty acids, as multiple NAD(P)H regeneration cycles must occur. Additionally, uncoupling of the P450 reaction promotes further release of free protons in the bulk (Figure 1).

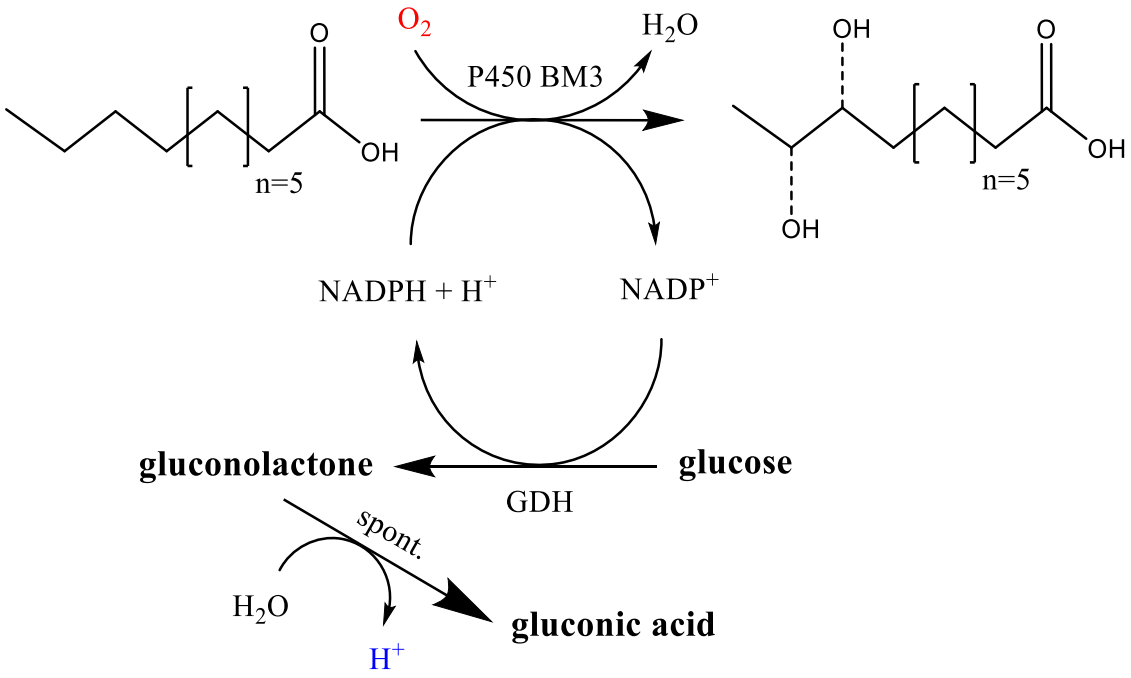

Figure 23: **Reaction scheme for the catalyzed reaction by the P450 BM3/GDH system to convert C12:0.** The consumption of O_2 (red), leads to a release of protons (blue) and hence the decrease of the pH.

A five mL reaction was set-up (2 µM Z_P450 BM3, 14 U mL^{-1} Z_GDH, 10 mM C12:0 (in EtOH; 2% (v/v)), 200 mM glucose, 200 µM NADP, 1 mg mL^{-1} catalase, 50 mM KPi buffer (pH 7.5 , 250 mM NaCl) to monitor the change in pH over longer reaction times. The reaction was mixed at 130 rpm with a magnetic stirrer bar and the pH was noted every 15 minutes. The pH decreased by 0.48 in the first three hours (0.15 h^{-1}). After 20 hours, the pH was close to 6.1 and compared to the reaction start the pH change per time was five times slower (0.035 h^{-1}). The pH was reset to 7.5 and 25 µL $NADP^+$ (50 mM stock) were added, which nearly led to the initial pH decrease rate (0.14 h^{-1}) (Figure 24). These results indicate a high stability of the enzymatic system for elevated reaction times (>20 h). After 43.5 hours reaction time 98% conversion was reached (GC-MS). This experiment clearly shows the necessity of pH stabilization for this system to reach high product titers even at high coupling rates. Additionally, it

reveals that at least one of both enzymes is highly limited by a lower pH. According to Liu et al (2017) a variant of P450 BM3 exhibits its pH optimum at pH 7 and a decrease of activity of more than 95% at pH 6 was measured [52]. Tamura et al (2012) reported the highest activity for the GDH (type IV) from *B. megaterium* at alkaline pH (>8) and a decrease in activity of 75% at pH 6 [53].

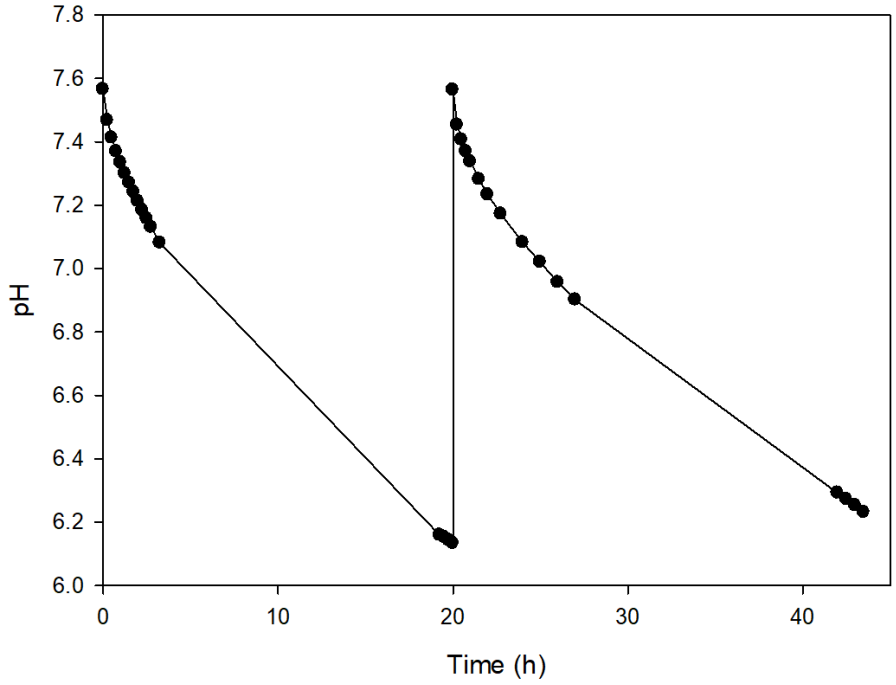

Figure 24: **Change in pH in the Z_P450 BM3/Z_GDH system overtime.** Due to the formation of gluconic acid to regenerate NADPH, the pH decreases over the reaction time. Initially, the decrease in pH per time is five times faster compared to the change after 20 hours of reaction. The initial pH change rate was restored by resetting the pH to 7.5 and adding of 25 µL $NADP^+$ (50 mM stock) after 20 h reaction time.

Consequently, the reaction was repeated on 10 mL scale (40 mM instead of 10 mM C12:0), but this time the pH was kept manually between 7.2 and 7.5 by adding 5 M KOH. Additionally, the influence of air supply into the reaction was investigated by setting-up a non-aerated reaction and an aerated reaction. O_2 was supplied by pumping air (21% O_2) into the liquid reaction phase at a rather undefined volumetric mass flow (strong bubbling occurred). As the aeration led to the formation of foam, Antifoam 204 was applied when necessary. The pH was noted and samples (250 µL) were drawn every hour and measured via GC-MS. The initial product formation rate (0 to 6 hours) was six to seven times faster for the aerated reaction compared to the non-aerated reaction (Figure 25). Additionally, a clear correlation between product formation and pH decrease was observed (Figure 26). This experiment shows that O_2 supply and defined pH control is crucial and requires precise control over the whole reaction time.

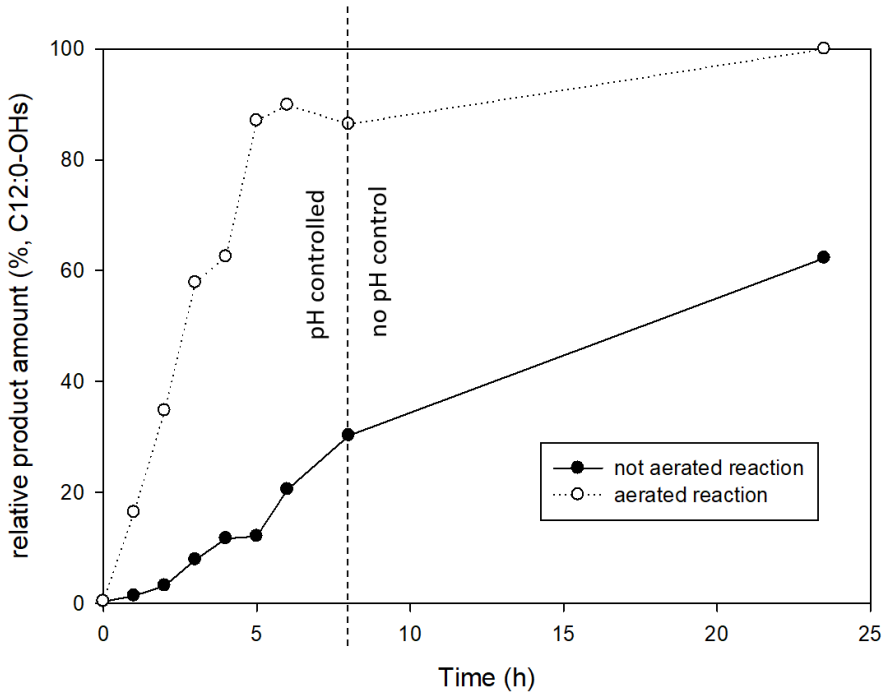

Figure 25: **Influence of aeration (21% O_2) on the formation of C12:0-OHs.** The initial product formation rate (0 to 6 hours) was six to seven times faster for the aerated reaction compared to the not aerated reaction. After 8 hours reaction time, the manual pH stabilization was stopped (dashed line).

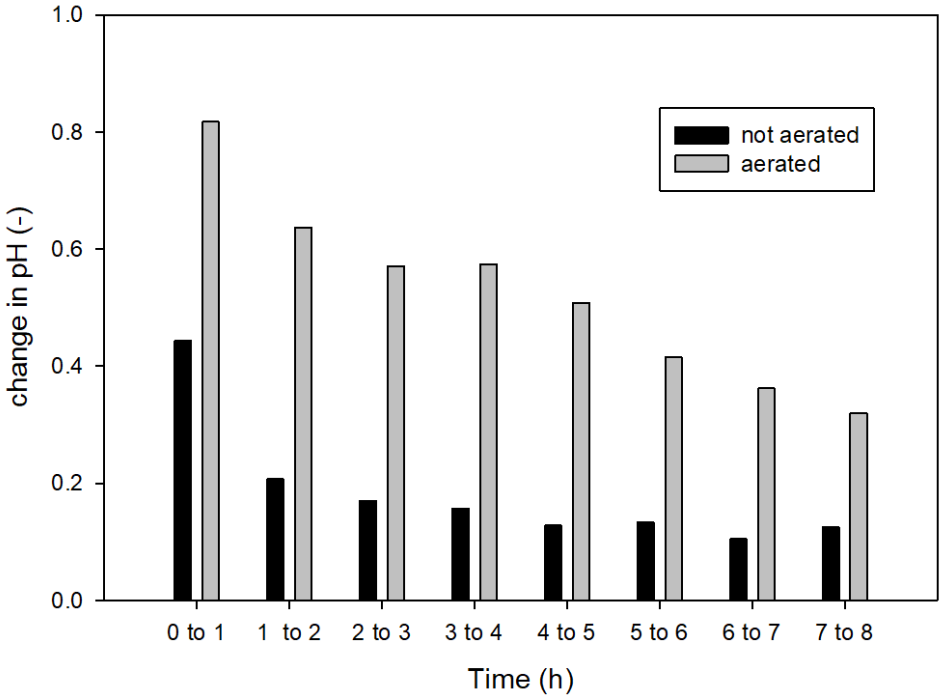

Figure 26: **Influence of aeration (21% O_2) on the change in pH in the Z_P450 BM3/Z_GDH system.** A clear correlation between the product formation (Figure 25) and the change in pH can be observed.

3.2.2 Establishing a robust reaction platform for oxyfunctionalization

Comparison of co-immobilizate and free enzymes in batch mode

First attempts to convert C12:0 on preparative scale were carried out at 45 mL scale in a double-walled reaction vessel (Wheaton) at 25 °C in a 50 mM KPi buffer (pH 7.5, 250 mM NaCl). The composition of the reactor components is summarized in Table 19. Pure oxygen (100%) was supplied at a volumetric mass flow rate of 20 mL min^{-1} and the reaction was stirred at 250 rpm. The oxygen concentration and KOH consumption were recorded over the whole reaction time. Co-immobilized Z_P450 BM3 and Z_GDH as well as free enzyme preparations (CFEs) were benchmarked against each other. As the aeration led to extensive foaming, approximately 600 µL Antifoam 204 were added to both reactors.

Table 19: **Composition of the 45 mL reactor to convert C12:0 on preparative scale**

	Concentration/volume
Z_P450 BM3 (CFE or immobilized)	2 µM
Z_GDH (CFE or immobilized)	6.8 U mL^{-1}
C12:0	40 mM dissolved in EtOH
Glucose	200 mM
$NADP^+$	200 µM
Bovine liver catalase	1 mg mL^{-1} (2000 - 5000 U mg^{-1})
EtOH	2% (v/v) final concentration
Buffer	50 mM KPi (pH 7.5, 250 mM NaCl)
Antifoam 204	~ 600 µL

Samples (250 µL, excluding carrier material) were drawn every hour and quantified by GC-MS. Figure 27 and Figure 28 display time studies for the oxygen concentration, the relative product amount, the concentration of substrate and the consumed KOH. Both reactors reached full conversion after 23 hours. Conversions were calculated based on the remaining substrate in the reactor as soon as ~2 mM (solubility limit in water) of C12:0 were reached. An initial product formation rate (0 to 1 hour) was calculated assuming the peak after full conversion corresponds to 40 mM product. The co-immobilizate reached product formation rates of 14.5 mM per h, their free counterparts 7.5 mM per h, respectively. Calculated values are summarized in Table 21. Results indicate that the co-immobilized enzymes outperformed the free enzymes under these reaction conditions. High conversions (>95%) were reached faster, and the initial reaction rate was two-fold higher. For both reactions the oxygen concentration increased as soon as the substrate was nearly depleted (arrow in Figure 27 and Figure 28). However, conversion data should be viewed with caution as following experiments (see page 46) indicated a substrate accumulation in the particles. Because of reusability attempts, the carrier was

not used for extraction experiments and GC-MS analysis (in this experiment). Both systems reached TTNs of 20000 for P450 BM3.

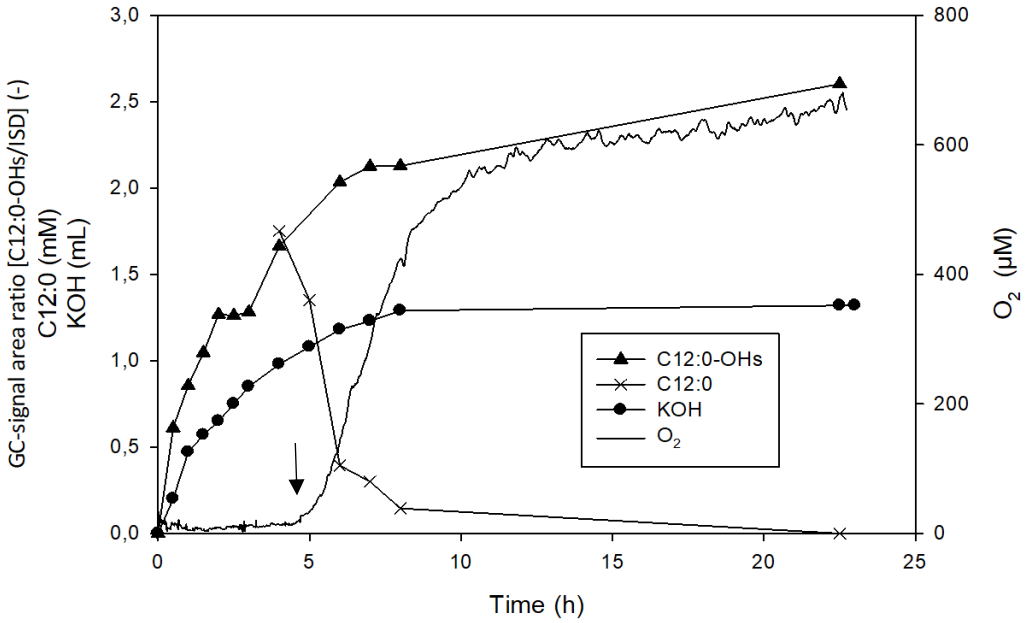

Figure 27: **Time courses for the products (C12:0-OHs), the substrate (C12:0), the consumed KOH and the O_2 concetration for a reaction with 2 µM Z_P450 BM3 and 6.8 U mL^{-1} Z_GDH (co-immobilizate).** Full substrate conversion (40 mM) could be achieved after 23 hours. The arrow indicates the increase of the O_2 concentration at nearly full depletion of C12:0.

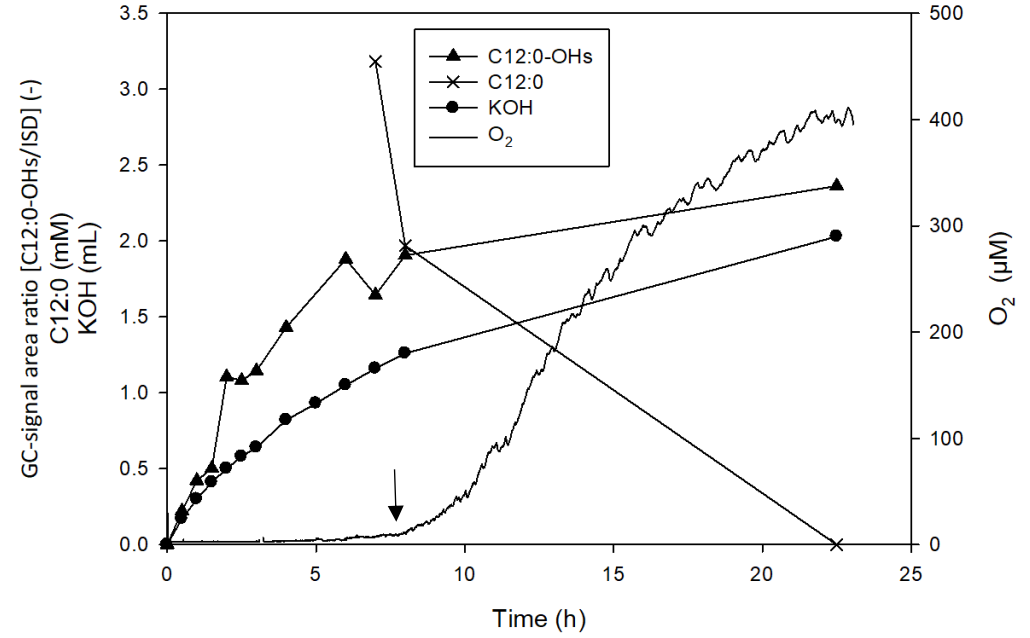

Figure 28: **Time courses for the products (C12:0-OHs), substrate (C12:0), consumed KOH and O_2 concetration for a reaction with 2 µM Z_P450 BM3 and 6.8 U mL^{-1} Z_GDH (free).** Full substrate conversion (40 mM) could be achieved after 23 hours. The arrow indicates the increase of the O_2 concentration at nearly full depletion of C12:0.

A key parameter for describing O_2 mass-transfer is the k_La value, which describes the volumetric mass transfer coefficient from the gas to the liquid phase. It is strongly dependent on the reactor geometry, the type of stirrer, the stirrer speed, the type of O_2 sparger unit, the O_2 mass flow rate and liquid properties, like viscosity or the surface tension [34, 35]. Due to O_2-limitation in the reaction system, the respective k_La values for the current reaction set-up were determined. Therefore, a 50 mL reaction containing 40 mM C12:0, 200 mM glucose and 1 mg mL^{-1} catalase were stirred at 250 rpm and 20 mL min^{-1} O_2 (100%) was pumped into the vessel (single 200 µL tip as gas outlet). The effect of Antifoam 204 (600 µL) and ReliSorb^{Tm} SP400 carrier material (3 g) was further investigated separately. Determined k_La values are summarized in Table 20. The k_La value are rather low to possible values reported in literature for stirred tank reactions (up to 180 h^{-1} with a Rusthon turbine (twin impeller) at 1000 rpm and 2 to 5 L min^{-1} air (21% O_2) flowrate) [34]. However, no optimisation of the process parameters (mass flow, stirring speed) were performed and rather basic lab-equipment was used (200 µL pipette tip as gassing unit placed above the magnetic stirrer bar). Antifoam 204 increased the k_La by 25% while subsequent addition of ReliSorb^{Tm} SP400 led to a decrease of the k_La by 8%.

Table 20: **Influence of Antifoam 204 and ReliSorb^{Tm} SP400 on the k_La.** The reaction was stirred at 250 rpm and O_2 was supplied at a volumetric mass flow rate of 20 mL min^{-1} O_2.

ReliSorb^{Tm} SP400 (g)	Antifoam 204 (µL)	k_La (h^{-1})	C* (O_2) (µM)	OTR (mM h^{-1})
0	0	17.6	1045	18.4
0	600	23.4	1030	24.0
3	600	21.6	1050	22.7

C* (O_2) = equilibrium concentration of O_2, OTR = maximal oxygen transfer rate

Based on the maximal oxygen transfer rate (OTR, mM h^{-1}) calculated from determined k_La values and the equilibrium O_2 concentration (C* (O_2)) it was possible to calculate coupling efficiencies of the P450/GDH reaction. Activation and cleavage of one molecule of O_2 requires oxidation of one molecule of NAD(P)H to NAD(P)$^+$. As the entire oxygen was consumed in the initial reaction phase of both reactors, the coupling efficiency was determined by the following equation:

$$\text{coupling efficiency (\%)} = \frac{\text{product formation rate (mM h}^{-1})}{\text{OTR (mM h}^{-1})} \times 100 \text{ or } \frac{\text{product formation rate (mM h}^{-1})}{\text{consumed NAD(P)H (mM h}^{-1})} \times 100$$

The free enzymes displayed a coupling efficiency of 31% while the co-immobilized enzymes reached 65%. Valikhani et al (2018) reported a coupling efficiency of 75% for free Z_P450 BM3 and C12:0. However, this value was determined with purified enzyme, indicating the presence of further NAD(P)H consuming enzymes in the used CFE. The coupling efficiency for the co-immobilizate (65%) is comparable to the coupling efficiency of the purified Z_P450 BM3 (75%). This shows the partial purification of the Z_P450 BM3 via the immobilization and removal of unwanted NAD(P)H consuming side reactions. For the co-immobilizate a coupling efficiency of 50% was determined with the substrate

anisole [31]. Based on the determined coupling efficiency the recycling number for NADPH was calculated with the following equation:

$$\text{NADPH regeneration cycles } (-) = \frac{\text{converted C12:0 (mM)}}{\text{applied NADP}^+ \text{ (mM)} \times \text{coupling efficiency (\%)}}$$

Overall, the reaction allowed recycling of NADPH for 660 times for the CFE and 313 for the co-immobilizate, respectively. The higher value for the free enzyme is also reflected in the higher KOH consumption for the free enzymes (2 mL) indicating increased formation of GlcA (Figure 23) as compared to the co-immobilizate (1.3 mL). Regeneration of the costly cofactor (when applied *in-vitro*) plays an essential role in the economy of a NAD(P)$^+$ depending enzymatic process. Depending on the product value, regeneration cycles of 10^3 to 10^6 are desired for industry. However, no optimization regarding this value were studied and decreasing the amount of applied NADP$^+$ without loss of process efficiency could benefit the economy of the process [54, 55].

Table 21: **Summary of determined key reaction paramters obtained for the initial reaction with free enzymes and the co-immobilizate.**

	Free enzymes	**Co-immobilized enzymes**
Conversion after 4 h (%)	61 [a]	95
Conversion after 8 h (%)	95	99.7
Conversion after 23 h (%)	>99	>99
Initial product formation rate (mM h^{-1}) [b]	7.5	14.5
STY (g L^{-1} h^{-1})	0.95	1.95
TTN_{P450}	20000	20000
Coupling efficiency based on OTR (%)	31	65
NADPH recycling (mol mol^{-1})	660	313
KOH consumption (mL)	2.0	1.3

[a] estimated based on the ratio of the GC-product area after 4 and 23 h (40 mM C12:0 converted) reaction time
[b] determined for 1 h reaction time

Substrate distribution between water phase and ReliSorb™ SP400

Fatty acids potentially accumulate in the pores of the ReliSorb™ SP400 carrier due to its chemical properties. Hydrophobic interactions between the polymethacrylate backbone of ReliSorb™ SP400 and aliphatic chains of fatty acids might lead to strong binding and clogging of carrier material providing a significant diffusion barrier. Defined amounts of ReliSorb™ SP400 (0, 10, 25 and 50 mg, no enzyme bound) were incubated in 500 µL buffer (50 mM Kpi, pH 7.5) containing 1 mM C12:0 and 10% DMSO (v/v) leading to a homogeneous liquid phase. After incubation for 20 h in the end-to-end rotator (20 rpm, RT), the carrier was separated from the liquid by centrifugation (2 min, 16100 x g, 21°C). The carrier and the water phase were acidified by adding 25 µL HCl (37%) and the substrate was extracted with EtOAc from both samples followed by quantification with GC-FID. The more carrier was applied in the reaction, the less substrate could be recovered from the water phase (Figure 29). Additionally, significant amounts of substrate were recovered after a second and third extraction step from 50 mg carrier. Therefore, calculated conversion rates for reactions, where carrier was excluded from the quantification, should be viewed carefully.

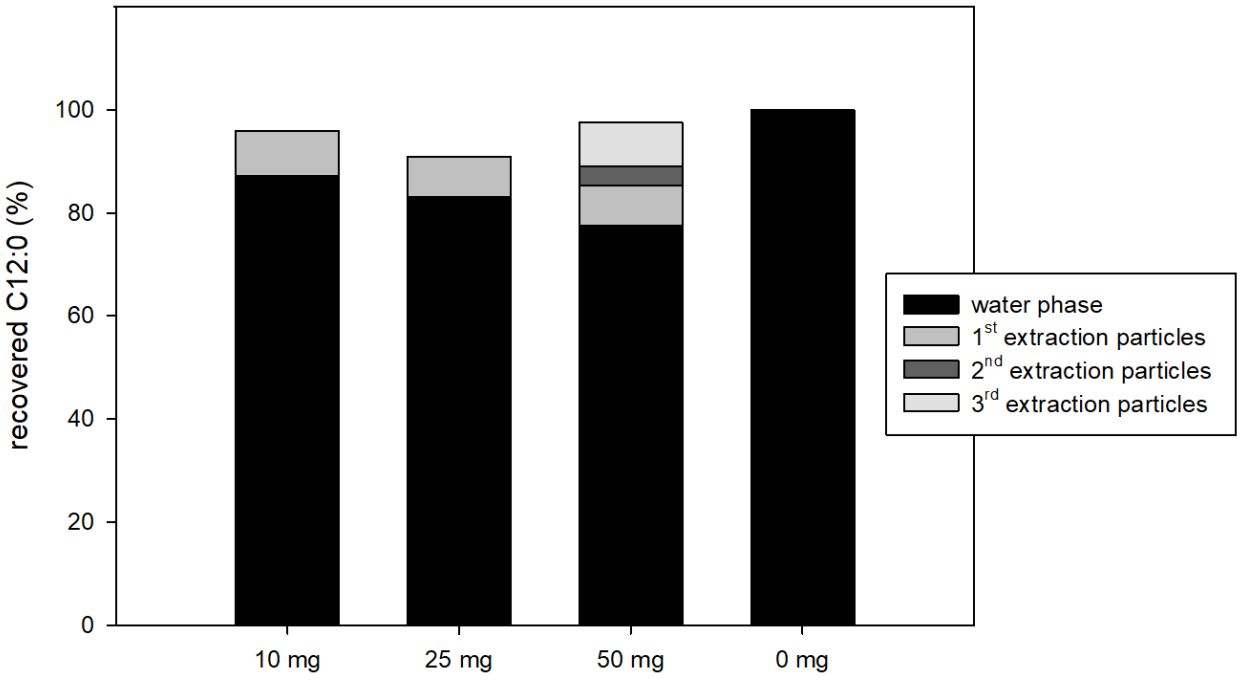

Figure 29: **C12:0 distributon between ReliSorb™ SP400 and the water phase.** Varying amounts of ReliSorb™ SP400 were incubated in 500 µL reactions containing 1 mM C12:0, 10% (v/v) DMSO and 50 mM KPi (pH 7.5). The reactions were gently inverted for 20 hours at room temperature and 20 rpm in an end-to-end rotator. Afterwards, the recovered C12:0 of the water phase and the carrier were quantified via GC-FID analysis. One reaction without carrier was prepared and served as a control (= 100% C12:0).

To show a possible clogging of the particles, 27 mg lyophilized co-immobilizate (0.185 nmole Z_P450 BM3 per mg) were incubated in 5 mL reactions containing 0 or 10 mM C12:0, 5% DMSO and 50 mM KPi (pH 7.5). The reactions tubes were turned at 20 rpm and 22°C for 5 h in an end-to-end rotator. Afterwards, the liquid reaction phase was removed by centrifugation (2 min, 3220 x g, 22°C) and the carrier was used for 5 mL reactions (200 mM glucose, 500 µM $NADP^+$ and 10 mM C12:0, 5% DMSO). Samples for GC-FID analysis were drawn over time and the clogged and not clogged particles were compared in terms of substrate consumption and product formation. Figure 30 shows a lower substrate consumption and hence lower product formation within the first reaction hours for the particles initially incubated in C12:0. Probably, the incubation in the fatty acid and a crystallization process in the particles led to a clogging of the nanoporous carrier structure and decreased mass transfer.

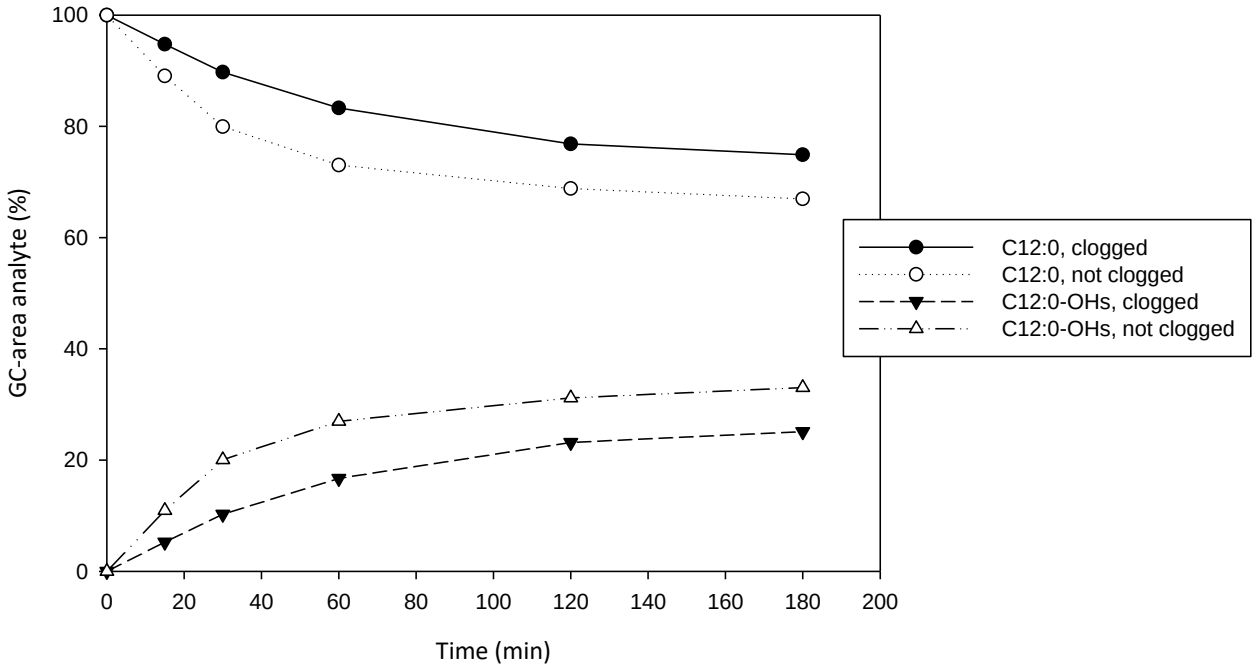

Figure 30: **Comparison of the product formation and substrate consumption for clogged and not clogged particles.** The experiment indicates a potential clogging of the nanoporous structure of the carrier because of crystallization of C12:0 in the particles.

Comparison of background NAD(P)H and oxygen consumption rates in absence of C12:0

Initial experiments led to the question why the immobilized enzymes performed better than free enzymes (two-fold higher activity, two-fold higher coupling efficiency). Typically, immobilized enzymes are less active due to steric hindrance, inaccessibility of the active site for the substrate or conformational changes of the enzymes during the immobilization [41]. As both reactions were strongly limited by oxygen supply, the background consumption of oxygen of the CFEs containing P450 BM3 and of the co-immobilizate was investigated (in absence of the substrate). Therefore, the oxygen depletion rate was measured in 1 mL reactions (500 µM NADPH, 10% (v/v) DMSO, 50 mM KPi, pH 7.5). Activity was measured and calculated as µM consumed O_2 per second and µM P450 BM3 (Table 22). The highest O_2 consumption rate could be measured for the Z_P450 BM3 CFE, the second highest for the Wt_P450 BM3 CFE and the lowest for the co-immobilizate. During the immobilization process O_2-consuming *E. coli* enzymes were removed resulting in a lower O_2 consumption per µM P450 BM3. As the expression yield of the Wt_P450 BM3 is higher compared to the Z_P450 BM3, less CFE was applied and hence less O_2-consuming *E. coli* enzymes were present in the reaction. The lower background consumption of O_2 of the immobilized enzymes provides more oxygen for the target hydroxylation reaction. As both 40 mM C12:0 conversions (Figure 27 and Figure 28) were limited by O_2 this provides a possible explanation for an enhanced product formation rate for the co-immobilizate compared to the Z_P450 BM3/Z_GDH CFEs.

To verify the results of the enhanced O_2 background consumption of the CFE compared to the immobilized enzymes, the NAD(P)H background consumption was investigated as well. In order to exclude consumption of NAD(P)H via potential uncoupling by the P450 BM3, Z_GDH CFE and immobilized Z_GDH were tested and compared. 3 mL reactions containing 5 U mL^{-1} Z_GDH (immobilized), 5 mM benzaldehyde (reported electron acceptor for *E. coli* alcohol dehydrogenases [56]) and 400 µM NADH or 300 µM NADPH were mixed at 250 rpm with a magnetic stirrer bar. Samples (100 µL) were taken and centrifuged (30 s) to separate the ReliSorb™ SP400 from the water phase. The water phase was diluted 1:10 followed by measuring NAD(P)H concentration at 340 nm. The absorbance signal remained stable for both cofactors over longer time range. Five U mL^{-1} (final activity in the mixture) free Z_GDH CFE (2.18 U mg^{-1}, dry) were spiked into the reaction and additional samples were measured. Figure 31 shows the course of the NAD(P)H concentration over the reaction time. The immobilized enzymes do not consume significant amount of NAD(P)H in contrast to the spiked CFE. The immobilized Z_GDH consumed 0.12 µM NADH per minute, while the Z_GDH CFE consumed 22 µM NADH per minute, which equals an 190-fold faster NADH consumption for the Z_GDH CFE. The values for the NADPH consumption are lower, which constitutes a reason to use NADPH over NADH. The immobilized Z_GDH consumed 0.075 µM NADPH per minute, while the Z_GDH CFE consumed 1.9 µM NADPH per minute, which equals a 25-fold faster NADH consumption for the Z_GDH CFE. It can be

concluded that the partial purification of the enzymes via immobilization led to a removal of unwanted NAD(P)H consuming enzymes of the CFE. Consequently, this results in a decrease of the necessary reaction time in O_2 limited preparative scale reactions and an enhanced coupling efficiency.

As the oxidation of one molecule NADPH must (in practice) result in the consumption of one molecule O_2, the U mg^{-1} applied CFE or particles were calculated for the P450 BM3 CFEs and the Z_GDH CFE and the co-immobilizate and immobilized Z_GDH, respectively (Table 22). The calculation revealed, that despite the exclusion of substrate (C12:0) for the monooxygenase, the CFEs containing P450 BM3 consumed about 50 to 70-fold more O_2/NADPH than the Z_GDH CFE. Probably, fatty acids found in the CFE could activate the monooxygenase cycle. Similar results were obtained for the immobilized enzymes. Although the carrier was washed to remove any fatty acids which potentially activate the monooxygenase cycle, the co-immobilizate still consumed about 200-fold more O_2/NADPH, than the single immobilized Z_GDH. Probably, fatty acids already present in the active centre of the Z_P450 BM3, which were not removed during the washing or the loading of more undesired background consuming enzymes during the preparation of the co-immobilizate could be the reason.

Table 22: **Comparison of the oxygen background consumption for different enzyme preparations.**

Catalyst/Enzyme formulation	**Catalyst (CFE or carrier in mg mL^{-1})**	**O_2 consumption rate (µM s^{-1} $µM^{-1}$ BM3)**	**U mg^{-1} CFE or carrier**
Wt_P450 BM3 CFE (0.63 nmole mg^{-1})	0.24	1.5	5.7×10^{-2}
Z_P450 BM3 CFE (0.23 nmole mg^{-1})	0.6	2.9	4.0×10^{-2}
Co-immobilizate (0.185 nmole Z_P450 BM3 and 0.82 U Z_GDH mg^{-1} carrier)	2.7	0.48	4.0×10^{-3}
		NADPH consumption rate (µM min^{-1})	
Z_GDH CFE (2.18 U mg^{-1})	2.3	1.9	8.0×10^{-4}
Immobilized Z_GDH (1.4 U mg^{-1} carrier)	3.6	0.075	2.1×10^{-5}

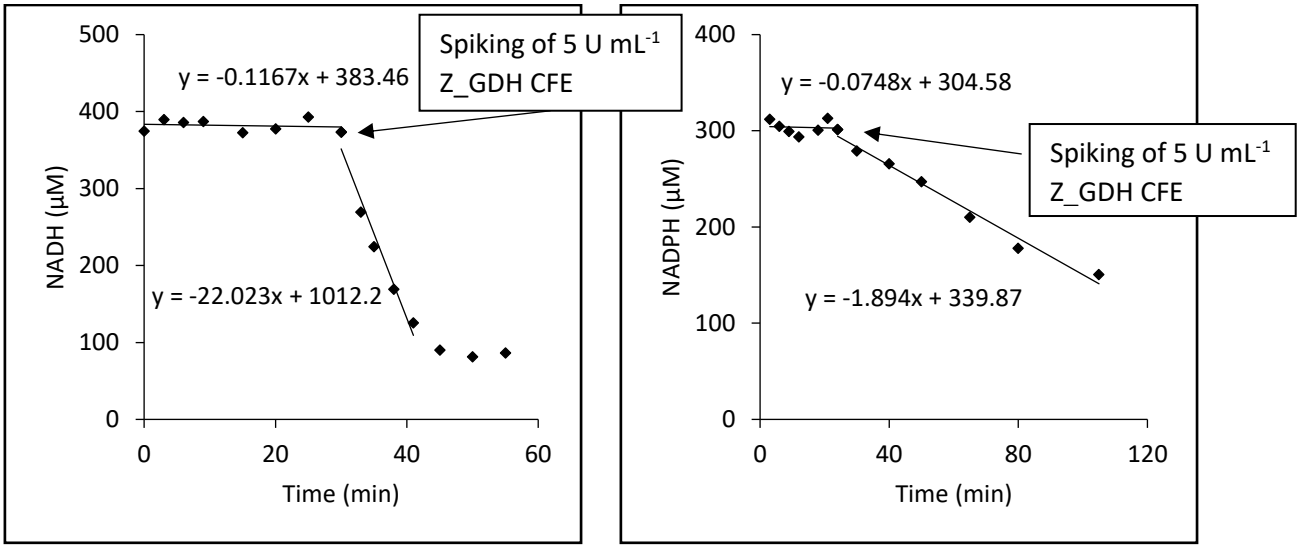

Figure 31: **NADH (left) and NADPH (right) consumption of immobilized Z_GDH and spiked free Z_GDH.** After 30 minutes (left) and 20 minutes (right) 5 U mL^{-1} free Z_GDH (CFE) was added to the reaction. The immobilized Z_GDH consumed hardly any NAD(P)H, while the CFE did.

It was assumed, that mainly alcohol dehydrogenases (ADHs) from *E. coli* contribute to the unwanted NAD(P)H oxidation [56]. However, comparing reactions with free Z_GDH CFE that contain 5 mM or 0 mM benzaldehyde show hardly any difference in the decrease of absorption at 340 nm (Figure 47 and Figure 48). Additionally, one mL reactions (5 U mL^{-1} Z_GDH CFE, 100 mM glucose, 400 µM NADH or NADPH) containing 5 mM acetophenone or 5 mM benzaldehyde were conducted. The reactions were extracted in 500 µL EtOAc containing 20 mM 1-octanol. After centrifugation (16100 x g, 2 min, RT), 180 µL of the organic phase were transferred into GC-vials and analyzed via GC-MS. Neither 1-phenylethanol nor benzyl alcohol could be detected (Figure 49 and Figure 50). The substrates were identified by comparing the MS-spectrum with the provided NIST database. From this we conclude that *E. coli* ADHs either are inactivated during the preparation of the CFE or are mostly membrane-associated enzymes and therefore removed during centrifugation. The adapted GC- temperature program for this experiment is shown in Table 32.

Reusability and *in-operando* stability of the co-immobilizate

The reusability of immobilized enzymes was tested by repeating the first reaction (page 42, Figure 27) with the already used co-immobilizate (40 mM C12:0 fully converted). The reactor was emptied, refilled and the reaction was only run for 5.5 hours as the oxygen concentration stayed stable at 1000 µM and no change in pH was detectable. GC-MS analysis of drawn samples revealed no product formation over the whole reaction time (Figure 46). Notably, the reused ReliSorb^{Tm} SP400 carrier material changed structure (white slurry instead of powder-like compound) potentially due to mixing and constant grinding for 24 h between the magnetic stirrer bar and the bottom of the glass vessel. It was assumed that this might lead to a separation/elution of enzymes from the carrier. To investigate this in more detail, the *in-operando* stability of particles was tested by comparing a magnetic bar stirred system and a top stirred system with a Rushton turbine (no grinding of particles possible). ReliSorb^{Tm} SP400 at 0 and 6 hours of the reaction and samples of the water phase were analysed by SDS-PAGE. Figure 32 shows that mainly Z_P450 BM3 is released from the carrier under both applied agitation conditions. Therefore, the destruction of the particles has no or only minor influence on retaining binding and potentially activity of immobilized Z_P450 BM3. For both stirring systems a significant amount of Z_P450 BM3 was released from the carrier (80%). In contrast, Z_GDH remained bound to the carrier material over longer incubation times. Potentially, the multimeric structure of P450 BM3 or its surface charge might contribute to a decreased binding stability. The release of Z_P450 BM3 is time-dependent as can be seen by an increasing band on the SDS-PAGE for the Z_P450 BM3 in the water phase (127 kDa, Figure 32). Valikhani et al (2017) showed the release of a double Z_{Basic2}-tagged (C-and N-terminus) homodimeric sucrose phosphorylase from *Bifidobacterium longum* (Z_*BlS*Pase) in a continuous microchannel reactor (negatively charged silica surface). Wall-immobilized protein amount was visualized via labelling with fluorescein isothiocyanate (FITC) and CLSM image recording. The visual washing out of the enzyme was also reflected in the determined apparent activities (E_{app}). Consequently, they concluded that mainly the washing out of the enzyme than enzyme inactivation is responsible for a decrease of E_{app}.

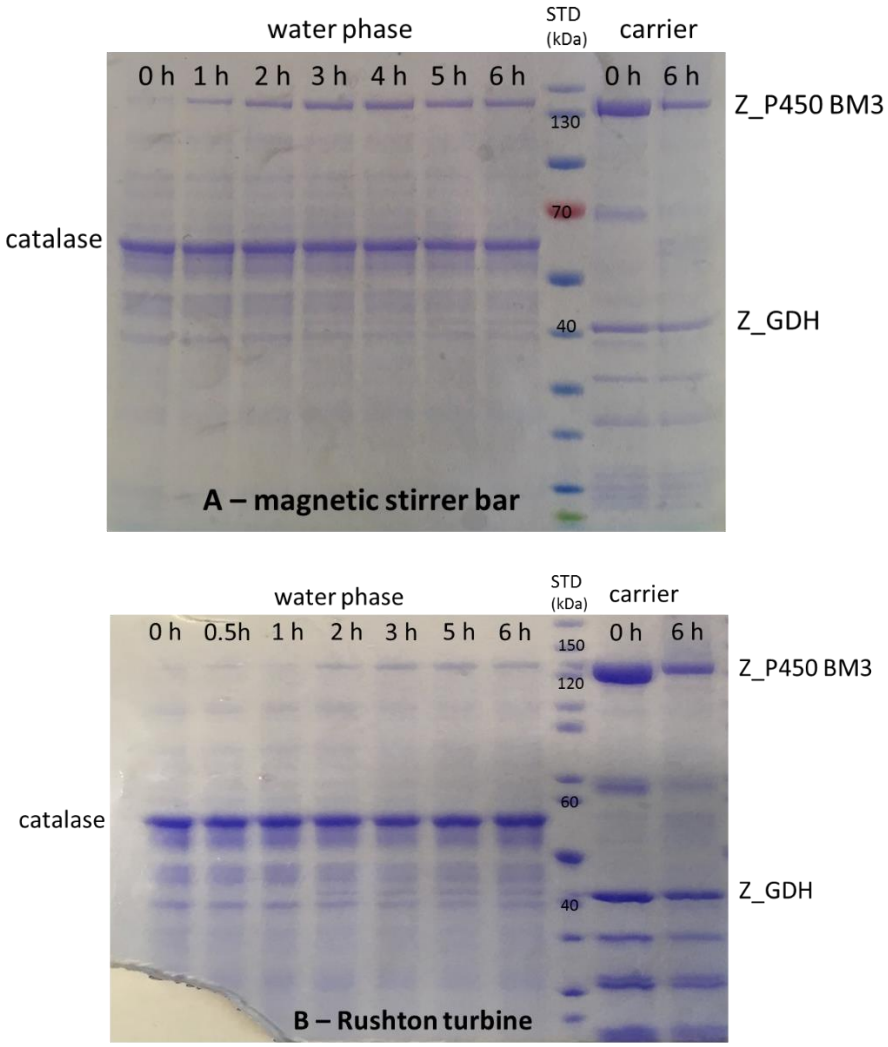

Figure 32: **SDS-PAGE for analysis of the *in-operando* binding stability of Z_P450 BM3 and Z_GDH on ReliSorb™ SP400.** Reactions were either mixed with a magnetic stirrer bar (A) or from the top with a Rushton turbine (B). The analysis of the water phase and the carrier revealed time-dependent elution of Z_P450 BM3 from the carrier independent on the stirring system. As protein reference standard (STD) serves the PageRuler™ Prestained Protein Ladder from Thermo Fisher (top) or PageRuler™ Unstained Protein Ladder from Thermo Fischer (bottom).

As the principle of the immobilization is based on ionic interaction of the positve charge of the Z_{Basic2}-module and the negativly charged sulphonic groups of ReliSorb™ SP400, it is likley, that further charged components in the system potentially influence the binding stability of enzyme(s)/proteins on the carrier. In order to investigate this in more detail, one mL samples (200 mM glucose, 200 µM $NADP^+$, 1 mg mL^{-1} catalase, 50 mM KPi with pH 7.5) containing immobilized Z_BM3 (14.3 mg co-immobilizate ≙ 2 µM Z_P450 BM3) and Z_GDH were incubated for 6 h at 250 rpm (magnetic stirring bar). Incubations with and without C12:0 and NaCl in 50 mM KPi (ph 7.5) were conducted. Additonally, the influence of stirring and different buffer systems was investigated. In the latter case, 14.3 mg co-immobilizate (2 µM Z_P450 BM3 and Z_GDH) were incubated in 1 mL 50 mM KPi (pH 7.5), 1 mL 50 mM Tris-HCl buffer (pH 7.5) or 1 mL ddH_2O. For systems with varying bulk phase a stirred reaction (250

rpm, magnetic stirrer bar) as well as a non-agitated reaction was prepared and incubated over the weekend (68 h). The enzyme composition on the carrier was monitored via SDS-PAGE. Figure 33 shows the result of the binding stability study. Charged compounds such as C12:0 or NaCl seem to have a negligible influence on the binding stability, as in all cases similar amounts of Z_P450 BM3 were removed from the carrier. However, stirring has influence on the binding stability. Altough, the entire Z_P450 BM3 was released for the stirred and not stirred reaction, Z_GDH stayed bound in the not stirred reaction, but was released in the stirred reaction. Interesstingly, a significant amount of both enzymes could be found bound to the carrier in the stirred and not stirred reactions in ddH_2O.

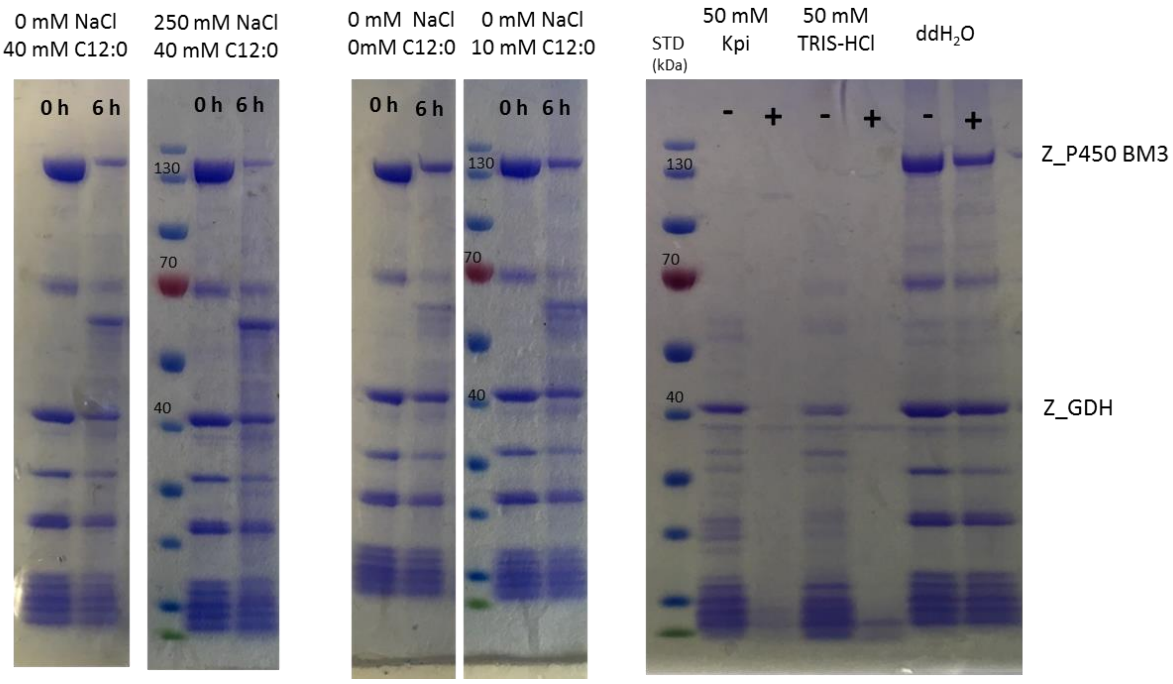

Figure 33: **Influence of reaction components (NaCl, C12:0), stirring and different buffer systems/bulk phases on the binding stability of Z_P450 BM3 and Z_GDH on ReliSorb ™ SP400.** As standard (STD) serves the PageRuler™ Prestained Protein Ladder from Thermo Fisher - = not stirred, + = stirred

The preparative isolation of C12:0-OHs

Isolation of reaction products from initial conversions of 40 mM C12:0 resulted in too high isolated yields (229 and 197%). The maximum theoretical isolated product yield was 388.8 mg (40 mM C12:0-OHs in 45 mL, molecular weight (C12-OHs) = 216 g mol^{-1}). However after lyophilisation of extracted material, 891 mg were obtained for the reaction with free enzymes (Figure 28) and 766 mg for the co-immobilized enzymes (Figure 27), respectively. Additionally, the isolated material had an oily appearance (hydroxy acids are typical obtained as solids at RT[1]). A test extraction/solubilisation of Antifoam 204 showed that this additive (mixture of organic non-silicone polypropylene-based polyether dispersions) is highly soluble in EtOAc, which makes it unsuitable for the envisioned process and product down-stream.

Development of an Antifoam 204 free reaction system in fed-batch mode

Taking a closer look at the previously described top-stirred reaction set-up (Rushton turbine) showed that less foam was accumulated compared to reactions, which were stirred via a magnetic stirrer plate (the impeller stirred above the surface of the reaction partially destroyed the foam mechanically). A batch reaction (40 mM C12:0 dissolved in EtOH) with co-immobilizate and the identical composition of the first reactions (see page 42) was conducted, but Antifoam 204 was excluded this time. Hardly any foaming was observable, but GC-MS analysis revealed that only very little product was formed (>10% conversion). Additionally, white rigid solids were formed in the reactor indicating a crystallization of the substrate. The reaction was repeated, but the substrate was grinded (white emulsion formed) beforehand in 10 mL 50 mM KPi (pH 7.5) to achieve a better initial substrate accessibility before starting the reaction. This led to an increased conversion (95% GC-area product, solid substrate particles were present at the end of the reaction). Despite stirring from the top, heavy foaming was observable. The foam and white solids accumulating on top parts of the stirrer and reaction vessel (flushed upwards by O_2-stream) were identified mainly as substrate (>82% peak area, Figure 51) by GC-MS. To overcome high substrate loading, contemporaneous foaming and crystallization of the fatty acid a fed-batch strategy for substrate delivery was conducted. In this case free Z_P450 BM3 (2 µM) and Z_GDH (6.8 U mL^{-1}) were used and 2 mM C12:0 in EtOH (final concentration) were manually pulsed 18 times into the reaction. The vanish of solid particles in the liquid reaction bulk was used as measure for defining substrate pulsing intervals (50 µL substrate solution per feed, 2 M C12:0 stock in EtOH). The continuous addition of EtOH (co-solvent for substrate) led to a partial and immediate defoaming effect. After 17 h reaction time 98% conversion could be reached, and 316 mg product (GC-purity: 66%, Figure 56) was isolated which corresponds to an isolated

[1] National Center for Biotechnology Information. PubChem Database. 12-Hydroxydodecanoic acid, CID=79034, https://pubchem.ncbi.nlm.nih.gov/compound/12-Hydroxydodecanoic-acid (accessed on Nov. 18, 2019)

yield of 80%. The same reaction was repeated and tested with the respective co-immobilizate (2 µM Z_P450 BM3 and 9.85 U mL^{-1} Z_GDH). Twelve times 3 mM C12:0 in 75 µL EtOH and one time 4 mM C12:0 in 100 µL EtOH were manually pulsed into the reaction. After 7 h reaction time, 79% product (GC-area) could be reached but rigid solids were formed at the end of the reaction indicating a too fast pulsing or too low enzyme activity to convert supplemented C12:0. Although EtOH is a good co-solvent it was not sufficient to keep the substrate entirely in solution or to prevent the formation of rigid white solids. Typically, crystallization requires a nucleation point, which is dependent on the solubility and concentration of a compound. If the concentration exceeds the solubility (supersaturated state), nucleation starts [57]. Due to the general resemblance of the fatty acids and the carrier material (polymethacrylate, nanoporous structure), local high C12:0 concentrations in the particles are likely, which could finally result in crystal formation and particle clogging. The product isolation resulted in 397.9 mg (GC-purity: 76%, Figure 57) which corresponds to an excellent isolated yield of 92% and lies within the range of reported extractions from similar reactions [58].

Following intermediate conclusions were drawn from the experiments:

1.) Dissolved substrate leads to strong foaming and substrate loss under continuous gassing. If substrate is not dissolved and white solid crystals appear no foaming is observable, but the substrate is not accessible for the enzyme for catalysis.

2) Running reactions without Antifoam 204 results in reasonable isolated product yields. Better antifoaming agents need to be identified that do not interfere with product downstreaming.

3.) EtOH is not a suitable co-solvent for higher substrate concentrations, but rapidly quenches formation of foam for a short period.

4.) Fed-batch strategies are useful to prevent early and fast crystallization of the substrate and minimize the formation of foam due to low substrate concentrations in the reactor and the partial defoaming effect of EtOH.

Investigation of alternative co-solvents

Although EtOH was a good and reasonable co-solvent (renewable/easy to remove) for the initial reactions (Figure 27 Figure 28) substrate precipitation/crystallization occurred, when excluding Antifoam 204 from the reaction. Especially, solids that did not re-dissolve caused problems, as they were not accessible for the catalysts. Therefore, DMSO was tested as an alternative co-solvent. Reactions were conducted using EtOH, DMSO or a combination of both. Instead of the co-immobilizate or the free Z_P450 BM3, the easier and better expressible Wt_P450 BM3 was used for the initial experiments. In general, the reactions (50 mL scale) contained: 2 µM Wt_P450 BM3, 7 U mL^{-1} Z_GDH, 200 mM glucose, 200 µM $NADP^+$, 1 mg mL^{-1} catalase and 50 mM KPi (pH 7.5). The substrate (dissolved

in EtOH, DMSO or a combination of both) was supplemented automatically by using a MCP-CPG piston pump from Ismatec®. Table 33 depicts an overview of the feeding strategies and substrate pulsing rates. The reactions were started with 20 mL min^{-1} O_2 and stirred at 250 rpm. The experiment was evaluated by extracting the whole reactor volume when the oxygen measurement indicated that the reaction was finished (no further O_2 consumption). The reaction bulk was acidified with HCl (37%) to pH 1 and the equal volume of EtOAc (1x) was used to extract the substrate and products. The conversion (% GC-area product) was calculated and compared for each reactor (Table 23, Figure 52). The reaction with EtOH as sole co-solvent reached 49% conversion. Chromatograms of samples taken in the first 1.5 hours of the reaction with EtOH indicate a high reaction rate at the beginning (0 to 1 hour). The formation of rigid solids and the increase of oxygen after 1 hour suggests a limitation of substrate accessible to the catalysts. However, due to EtOH supply no foam was formed during the feed. When using DMSO as co-solvent an excellent 98% conversion of 40 mM C12:0 could be achieved. Additionally, solid substrate particles re-dissolved in the aqueous reaction bulk, which was not entirely observable in the reaction with EtOH as co-solvent. Unfortunately, the strong foaming made problems with this reactor setting. After 3 h reaction time, the O_2 mass flow was reduced to 10 mL min^{-1} and ~250 µL EtOH were pulsed manually and stepwise to destroy foam. The combination of DMSO and EtOH (1:1) as co-solvent in the substrate feed resulted in full conversion to product (>99%) and no foam was detectable during the conversion. However, as soon as EtOH was not supplied regularly into the reactor foaming started. In case of foaming, the addition of silicone-based antifoam in the low mg range (<10 mg) destroyed the foam immediately and prevented a new formation over longer reaction times.

Table 23: **Influence of different co-solvents on the conversion and defoaming.**

Co-solvent	**% DMSO (v/v)**[a]	**% EtOH (v/v)**[a]	**Conversion (% GC-area)** [b]	**Foaming** [c]	**Solids/crystals**	**Re-dissolving of substrate particles**
EtOH	4	--	49	No	Yes	No
DMSO	4	0.5	98	Yes	Yes	Yes
DMSO/EtOH	2	2	>99	No	Yes	Yes

[a] final concentration in the reaction, [b] GC-area percentage of products/whole reactor extracted, [c]no foaming only during feed

The used silicone antifoam was hardly soluble in 50 mM KPi buffer (pH 7.5) or EtOAc. In a test extraction the brownish silicone antifoam accumulated at the interphase between the buffer and the organic EtOAc phase. Consequently, silicone antifoam outperforms Antifoam 204 in terms of practicality for the extraction process and to prevent foaming in the reactor.

3.2.3 Oxygen concentration dependent substrate feed

Based on the initial observation that full depletion of substrate led to a rapid increase of the O_2 concentration in the reaction vessel and the usability of a fed-batch strategy, an oxygen dependent substrate feed was established. For a 50 mL reaction, 10 mL dH_2O and 0.5 mL DMSO were mixed and stirred with 80 mg C12:0 pre-solubilized in 1.25 mL DMSO for 15 minutes at 350 rpm to generate an emulsion (finally 8 mM C12:0). Rest of the volume was made up to 50 mL with 50 mM KPi buffer (pH 7.5) and adding catalysts (2 µM Wt_P450 BM3 and 1.9 U mL^{-1} GDH (DSM)), 1 mg mL^{-1} catalase and 200 mM glucose. The pH was re-adjusted to 7.2 and 500 µM $NADP^+$ was added to start the reaction. The reaction was stirred at 350 rpm and 25 mL min^{-1} O_2 were supplied. Silicone antifoam (<10 mg) was used to prevent foaming. As soon as the oxygen increased, a sample for GC-FID analysis was drawn and 80 mg C12:0 in 1.25 mL DMSO were added to the reaction which led to a rapid drop in O_2 concentration (Figure 34). The feed was repeated four times to reach a final substrate amount of 400 mg which equals 40 mM C12:0 in 50 mL reaction volume. Figure 34 displays the progression of the oxygen concentration. GC-FID analysis showed conversions higher >95% before each feeding step. Finally, >99% conversion of 400 mg C12:0 at 50 mL scale could be reached within 5 h. This corresponds to 8 mM h^{-1} or 1.6 g L^{-1} h^{-1}. Kaluzna et al (2016) reported a STY of 1.5 g L^{-1} h^{-1} for the batch conversion of α-isophorone to 4-hydroxy-α-isophorone based on a P450 BM3/GDH system [39]. Kuehnel et al (2007) reached a STY of 0.14 g L^{-1} h^{-1} for the conversion of C12:0 with a P450 BM3/FDH system over 48 h reaction time [29].

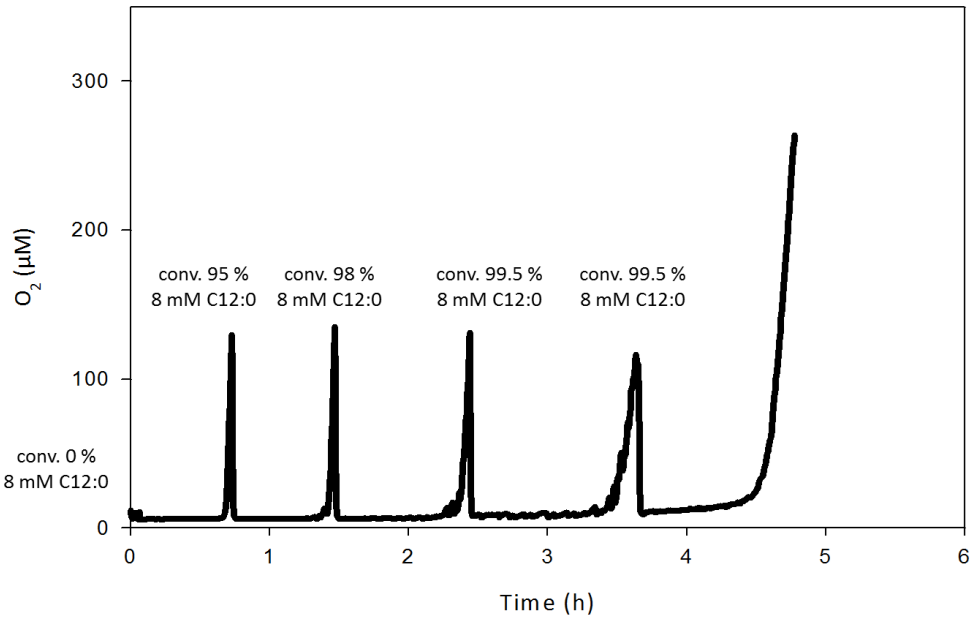

Figure 34: **Initial experiment for oxygen dependent substrate feed to convert C12:0 on preparative scale.** Every time the oxygen concentration increased 80 mg C12:0 (8 mM; in 1.25 mL DMSO) were added to the reaction. GC-FID analysis revealed conversions (conv.) higher than 95% for samples drawn as soon as the oxygen increased. Finally, >99% conversion of 40 mM C12:0 could be reached within only 5 h reaction time.

Influence of silicone antifoam on the k_La

As the initial reaction with the oxygen dependent substrate feed was very promising, k_La values for this reaction system were determined. Especially, the influence of the silicone antifoam was unknown and therefore investigated. Reaction conditions were mimicked excluding P450 BM3, GDH and $NADP^+$. The reaction was composed of 10 mL dH_2O, 8 mM C12:0, 200 mM glucose, 1 mg mL^{-1} catalase, 1.5 mL DMSO and finally made up to 50 mL with 50 mM KPi (pH 7.5). The suspension was stirred at 350 rpm and 25 mL min^{-1} O_2 were supplied. Table 24 depicts the results of the study. Independent on the amount of silicone antifoam applied it has a severe influence on the k_La and the O_2 equilibrium concentration (C* (O_2)). In general, the k_La is three-fold lower for reactions containing silicon antifoam. Additionally, it was not possible to reach the same equilibrium concentrations for O_2 compared to reaction without silicone antifoam. In general, the application of silicone antifoams results in a decrease of surface tension and hence lower average bubble diameter and a higher value for a. However, the impact of a reduced gas-liquid phase mobility leads to a comparable higher decrease of the k_L, resulting in an overall lower k_La [59]. Notably, ReliSorb™ SP400 shows only a minor influence on the k_La.

Table 24: **Influence of ReliSorb™ SP400 and silicone antifoam on the k_La value.** The reactions were performed at 350 rpm and 25 mL min^{-1} O_2 supply**.**

Silicone antifoam (mg)	ReliSorb™ SP400 (g)	k_La (h^{-1})	C* (O_2) (µM)	OTR (mM h^{-1})
0	0	30.6	990	29.7
1	0	10.4	700	7.3
3	0	10.1	720	7.3
10	0	10.4	690	7.2
0	1	33.3	990	33.0
10	1	10.0	700	7.0

C* (O_2) = equilibrium concentration of O_2, OTR = maximal oxygen transfer rate

Comparison of free Z_P450 BM3 and the co-immobilizate in fed-batch mode (O_2 dependent feed)

Based on the success of the preparative scale conversion of 400 mg C12:0 with the Wt_P450 BM3, the co-immobilizate and free Z_P450 BM3 were compared. Reaction set-ups were identical with the exception that only 0.92 mL DMSO containing 80 mg C12:0 were added during each feeding step (80 mg C12:0 corresponds to ~80 µL C12:0). Consequently, for each feeding step 1 mL substrate solution was added. Additionally, 10.8 U mL^{-1} Z_GDH were used for NADPH regeneration instead of the commercial GDH (DSM). Five times 8 mM C12:0 were supplied to the reaction with free Z_P450 BM3. The reaction with co-immobilizate was performed in duplicates with total substrate loadings of 40 and 48 mM C12:0. In contrast to the first reactors, ReliSorb™ SP400 was included in the extraction for GC-

FID analysis. Table 34, Table 35 and Table 36 give an overview of applied process parameters to characterize the reaction system in more detail. Time courses for the O_2 concentration, the product formation and the substrate concentrations before each substrate feeding step are shown in Figure 53, Figure 54 and Figure 55. The reaction with free enzymes reached >99% conversion after 22.2 hours, while the co-immobilizate reactions reached 96.5% conversion after 23 hours (40 mM substrate loading) and 75% GC-area product after 23.5 hours (48 mM substrate loading), respectively. However, the feed intervals were 2- to 1.5-fold longer for the free z_{Basic2} enzymes compared the co-immobilizate and thus indicating a higher reaction rate for the co-immobilizate. This confirms the removal of unwanted side reactions consuming O_2 or NADPH (as shown and discussed in section 3.2.2 page 48) which results in a faster and more efficient reaction. As compared to the Wt_P450 BM3, the Z_P450 BM3 based systems had longer/larger feed intervals (Table 25). This can be explained by the higher expression yield of Wt_P450 BM3 per g CFE and therefore less background activity and/or the general lower activity of immobilized enzymes. The difference in interval times for both co-immobilizate reactions might be related to a microbial contamination (strong uncommon smell detectable after 24 h conversion) of the CFE for the preparation of one co-immobilizate (reaction with 40 mM C12:0). Additionally, GC-FID analysis of the free Z_P450 BM3 CFE reaction (Figure 53) resulted in lower peak area ratios for the product (C12:0-OHs/ISD) compared to the reactions with free Wt_P450 BM3 CFE (Figure 35) and co-immobilizate (Figure 54). As the entire substrate was consumed, probably less than 8 mM C12:0 were added per feeding step indicating an even worse performance of the free Z_P450 BM3. The possible lower product concentration is also reflected in the product isolation, as a comparable low isolated yield (66%) could be achieved in comparison to other reactions (>80%) (Table 30).

Table 25: **Comparison of feed intervals for free Wt_P450 BM3, free Z_P450 BM3 and co-immobilizate.** The conversion (conv.) was calculated based on the remaining substrate in the reaction and the so far total supplied substrate.

	1st pulse of C12:0		2nd pulse of C12:0		3rd pulse of C12:0	
Catalyst	**Time (min)**	**Conv. (%)**	**Time (min)**	**Conv. (%)**	**Time (min)**	**Conv. (%)**
Wt_P450 BM3 CFE (in total 40 mM C12:0)	43	95.0	88	98.0	144	99.5
Z_P450 BM3 CFE (in total 40 mM C12:0)	105	99.0	200	98.0	280	98.5
Co-immobilizate (in total 40 mM C12:0) (contaminated CFE used)	66	98.3	168	99.9	264	98.3
Co-immobilizate (in total 48 mM C12:0)	43	94.5	99	96.8	184	98.7

Conv. = conversion of 8 (1st feed), 16 (2nd feed) and 24 mM C12:0 (3rd feed), respectively

Increasing substrate loading in fed-batch conversion of C12:0

As the reaction with 2 µM Wt_P450 BM3 and 1.9 U mL^{-1} GDH (DSM) and O_2-controlled substrate supplementation reached full conversion of 40 mM C12:0, the number of feeding steps was increased to boost product titers (80 mM final; 800 mg in 50 mL). The catalyst loading, the assembly of the reaction and the reaction conditions were kept identical to the 40 mM C12:0 conversion with Wt_P450 BM3 (Figure 34). The glucose concentration was enhanced from 200 to 300 mM to prevent a potential limitation for NADPH regeneration. The feeding steps were adapted to avoid the addition of too much DMSO into the reaction. Five times 80 mg C12:0 in 0.92 mL DMSO (1 mL substrate solution per feeding step) and four times 100 mg C12:0 in 0.5 mL DMSO (0.6 mL substrate solution per feeding step) were supplied (finally 12.4% DMSO). Table 37 gives an overview of different process parameters over time. Figure 35 displays the time course for the O_2 concentration and the product formation. Additionally, the determined substrate concentration at each feeding step is shown. After 28 hours of reaction, 99.8% conversion and a TTN of 39920 for the Wt_P450 BM3 could be achieved. The correct time for the first five feeding steps was identified easily based on the oxygen concentration. However, after the conversion of 40 to 60 mM C12:0 the O_2 concentration increased and it was not possible anymore to identify a suitable pulse time based on the O_2 concentration. Nevertheless, the substrate flocs slowly disappeared over time in the reaction indicating suitable selection of feeding intervals.

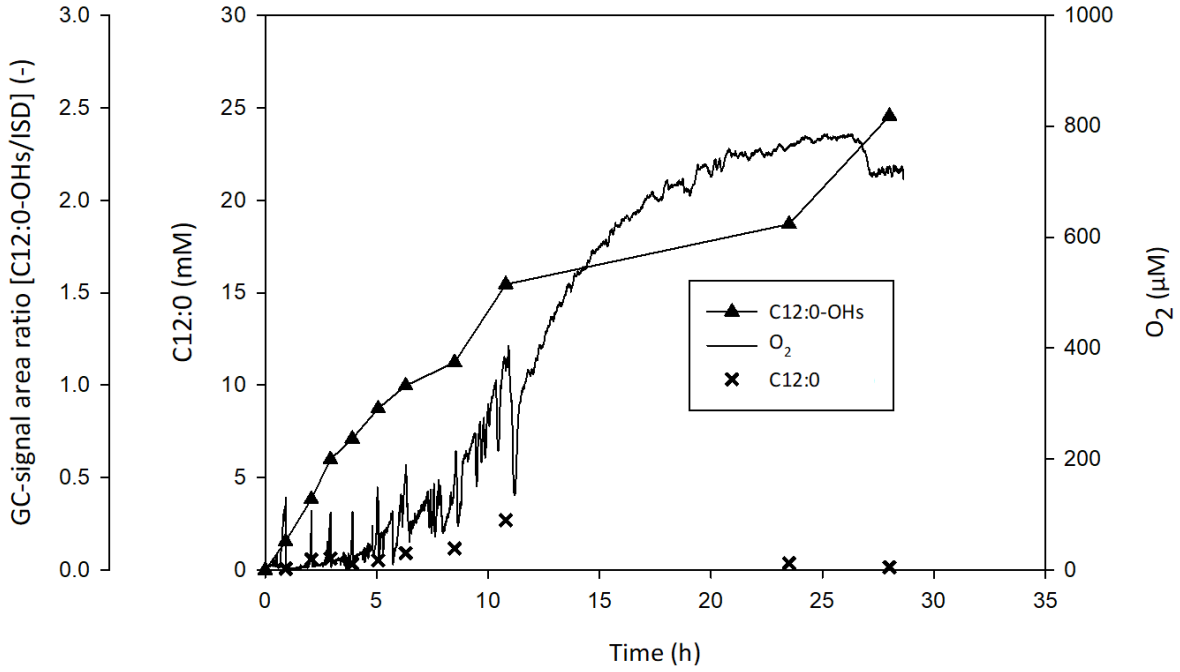

Figure 35: **Time course for the O_2 concentration and C12:0 and C12:0-OHs concentration during conversion of 80 mM C12:0 with 2 µM Wt_P450 BM3 and 1.9 U mL^{-1} GDH (DSM).** As soon as the O_2 concentration increased, the remaining substrate concentration in the reaction was determined via GC-FID and additional substrate was supplied. Overall, 99.8% conversion of 80 mM (800 mg) C12:0 could be achieved within 28 h. Time points of substrate pulsing are indicated by crosses between 0 and 9 hours of reaction time ISD = internal standard (1-octanol).

Influence of silicone antifoam on the product formation rate

Silicone antifoam has significant impact on the k_La and hence O_2-transfer into the liquid bulk (see page 58) which potentially further impacts the product formation rate under O_2-limited reaction conditions. Therefore, the above described 80 mM C12:0 conversion with Wt_P450 BM3 (2 µM) and GDH (DSM, 1.9 U mL^{-1}) was repeated excluding silicone antifoam. To prevent strong foaming the O_2 mass flow rate was decreased from 25 to 10 mL min^{-1}. Overall 100 mM C12:0 were supplied in the reaction (five times 80 mg C12:0 in 0.92 mL DMSO and six times 100 mg C12:0 in 0.5 mL DMSO). The foam was partially destroyed by pipetting EtOH (a few drops) onto the reaction surface whenever needed. Figure 36 shows a comparison of the initial product formation for the reactor with and without silicone antifoam added. In the reaction without antifoam the product was formed 2.4 times faster, which correlates very well with the determined k_La values (30.6 vs 10.4 h^{-1}) that are three-fold higher in the reaction without antifoam (Table 24). Space-time-yields (STYs) of 2.9 (no antifoam) and 1.2 g L^{-1} h^{-1} (with antifoam) for the first 2.5 h reaction time were calculated, an excellent value for a P450 catalysed hydroxylation reaction. Kaluzna et al (2016) reported a STY of 1.5 g L^{-1} h^{-1} for the batch conversion of α-isophorone to 4-hydroxy-α-isophorone based on a P450 BM3/GDH system [39]. Kuehnel et al (2007) reached a STY of 0.14 g L^{-1} h^{-1} for the conversion of C12:0 with a P450 BM3/FDH

system over 48 h reaction time [29]. Noteworthy, the reaction without silicone antifoam reach good but lower conversion (67% GC-area product), likely because the substrate was partially and constantly removed out of the vessel due to stronger foaming overnight. Although, silicone antifoam has a significant influence on the product formation rate, it is not practicable to exclude it entirely from the reaction with the present set-up and equipment. Further, it is a common observation that strong foaming can lead to a decrease of the enzyme stability at gas-liquid interphases [60] .

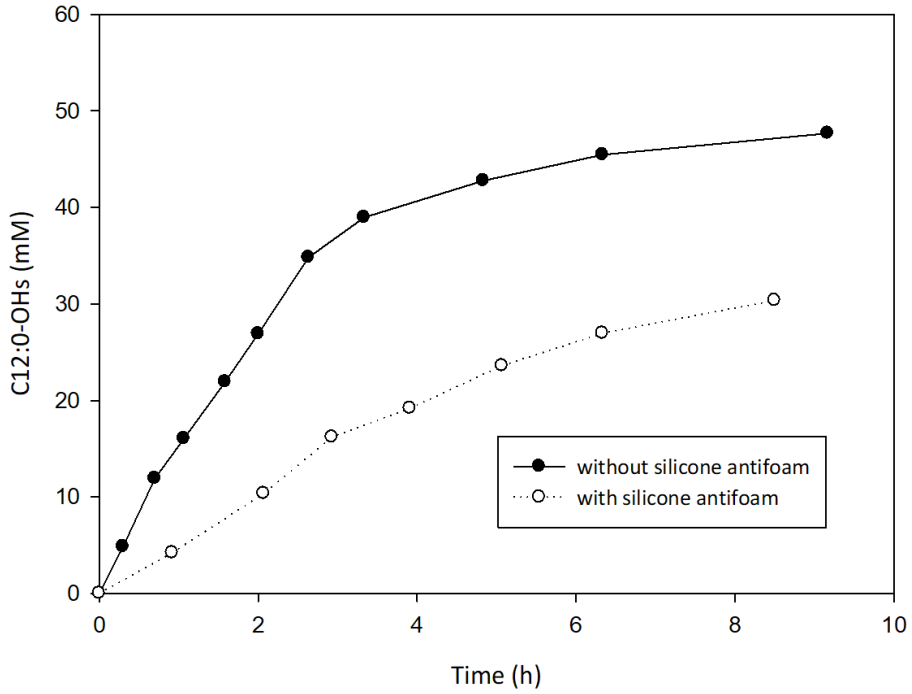

Figure 36: **Influence of silicone antifoam on the initial product formation rate.** The effect of the silicone antifoam on the k_La is reflected in the formation of product. For the reactions STYs of 2.9 and 1.2 g L^{-1} h^{-1} were calculated for the reaction without and with silicone antifoam, respectively. The STY was calculated based on the total loaded and remaining substrate after 2.5 hours of reaction.

Catalyst titration experiment to determine the minimal amount of needed Wt_P450 BM3

The supply of O_2 under the used reaction conditions is critical but proofed to be an excellent tool to monitor conditions in the reactor. So far moderate catalyst loading was applied (0.005%), which can be a key cost factor in designing bioprocesses. Therefore, a titration experiment was performed to explore how much catalyst loading is required without comprising productivity. A reaction supported by oxygen dependent substrate feed was set up (350 rpm, 25 mL min^{-1} O_2, with silicone antifoam) excluding the Wt_P450 BM3 enzyme. A Wt_P450 BM3 stock was prepared (29.7 µM) and titrated stepwise into the reaction to increase the Wt_P450 BM3 concentrations by 0.1 µM per step. New enzyme was supplied as soon as the O_2 concentration stabilized for a few seconds. Overall, 1.1 µM of Wt_P450 BM3 were titrated into the reaction to fully consume the constantly supplied O_2 (Figure 37). In order to proof that the reaction is catalyst and not substrate limited, additional 80 mg of C12:0 in

0.92 mL DMSO were supplied after 33 minutes. The results indicate that in previous experiments P450 BM3 was supplemented in excess under these conditions. Remarkably and despite the already increased supply of O_2 and still very low catalyst concentration and loading (0.005%), the monooxygenase (2 µM) is not saturated by the oxidant leaving significant space for reaction optimization.

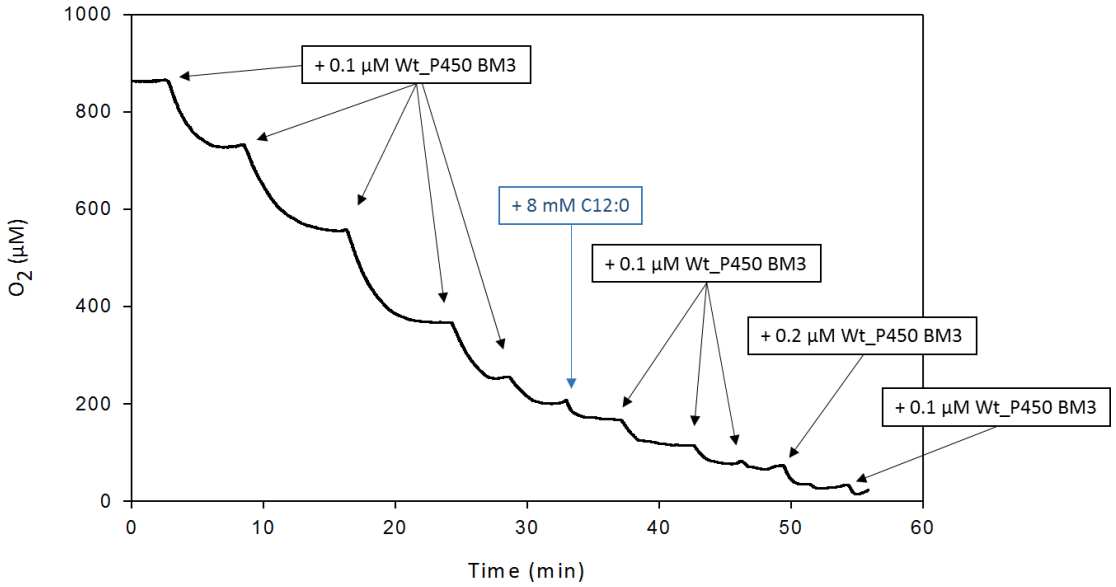

Figure 37: **Wt_P450 BM3 titration experiment.** Wt_P450 BM3 was titrated stepwise into the reaction to determine the minimal amount of Wt_P450 BM3 for complete depletion of supplied oxygen (350 rpm, 25 mL min^{-1} O_2). Overall, 1.1 µM Wt_P450 BM3 were added to the reaction to reach O_2 concentrations close to 0 µM. Silicone antifoam was supplemented in this experiment.

Scale-up to g-scale conversion of fatty acids

The best working reaction set-up (>99% conversion of 80 mM C12:0 with Wt_P450 BM3) was scaled up from 50 mL to 500 mL. Scaling reaction to larger volumes typically involves determination of key parameters that are impacted by the geometry of the reactor. The attempt to determine a k_La value with the initial gassing unit resulted in a low increase of the O_2 concentration at 500 mL scale and an equilibrium concentration was not reached in a useful time span (30 min). Therefore, an adapted gassing unit for the 500 mL reaction was assembled. Instead of one O_2 inlet (200 µL pipette tip), three inlets consisting of metal tubes were used. The stirring speed was increased to 500 rpm and 50 mL O_2 per minute were supplied. Determined k_La values (in presence of silicon antifoam) for the 50 mL and the 500 mL reaction are summarized in Table 26. The adapted O_2-supply allows comparable transfer values for O_2, a prerequisite to continue with bioconversions.

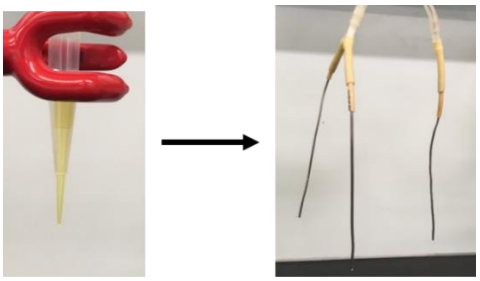

Figure 38: **Adaption of the self-assembled gassing unit for the 500 mL reaction.** The gassing unit of the 50 mL reactor (A) was exchanged, as no useful k_La values could be determined with the pipette tip for the 500 mL reaction (O_2 equilibrium concentration was not reached within a useful time span). The gassing unit for the 500 L reaction consisted of three metal tubes (B).

Table 26: **Comparison of k_La values for the 50 and 500 mL reaction, respectively.** The adaption of the gassing unit for the 500 mL reactor led to a reasonable O_2 mass transfer comparable to the k_La values for the 50 mL reaction. Both reactions contained silicone antifoam.

Scale	Stirring speed (rpm)	O_2 supply (mL min^{-1})	k_La (h^{-1})	C* (O_2) (µM)	OTR (mM h^{-1})
50 mL	350	25	10.4	700	7.3
500 mL	500	50	14.5	1075	15.6

C* (O_2) = equilibrium concentration of O_2, OTR = maximal oxygen transfer rate

Instead of the commercial GDH (DSM) 6 U mL^{-1} Z_GDH were used for NADPH regeneration. The starting concentration for the Wt_P450 BM3 was 1 µM. Additional Wt_P450 BM3 was stepwise added to final 2 µM when, despite the presence of visible substrate particles, the O_2 concentration increased. Substrate was supplied in following feeding steps: five times 800 mg C12:0 in 9.2 mL DMSO and four times 1 g of C12:0 in 5 mL DMSO totaling 8 g fatty acid. The initial O_2 mass flow rate was set to 50 mL min^{-1} and the reaction was stirred at 500 rpm. Figure 39 displays the time course for the O_2 concentration, the product formation and the KOH consumption. Additionally, the determined substrate concentration at each feeding step is shown. Table 38 gives an overview of various process and reaction parameters recorded over the whole reaction time course. After 24.2 hours the conversion was not satisfying, as still large amounts of solid substrate particles were visible. Investigation of the remaining enzyme activity revealed that 0.87 µM Wt_P450 BM3 were present but no activity could be determined for Z_GDH. The addition of 1400 U Z_GDH after 25.2 h instantly led to an O_2 concentration decrease and the KOH consumption restarted. After 47.5 hours around 90% conversion of 80 mM C12:0 could be achieved. The remaining active Wt_P450 BM3 was 0.40 µM (20% of the total loading) and the remaining GDH activity was 21.95 U (0.47% of the total loading). Unexpectedly, this result reveals higher enzyme operational stability for Wt_P450 BM3 than Z_GDH. Possibly, the commercial GDH (DSM) is significantly more stable than the in-house Z_GDH preparation.

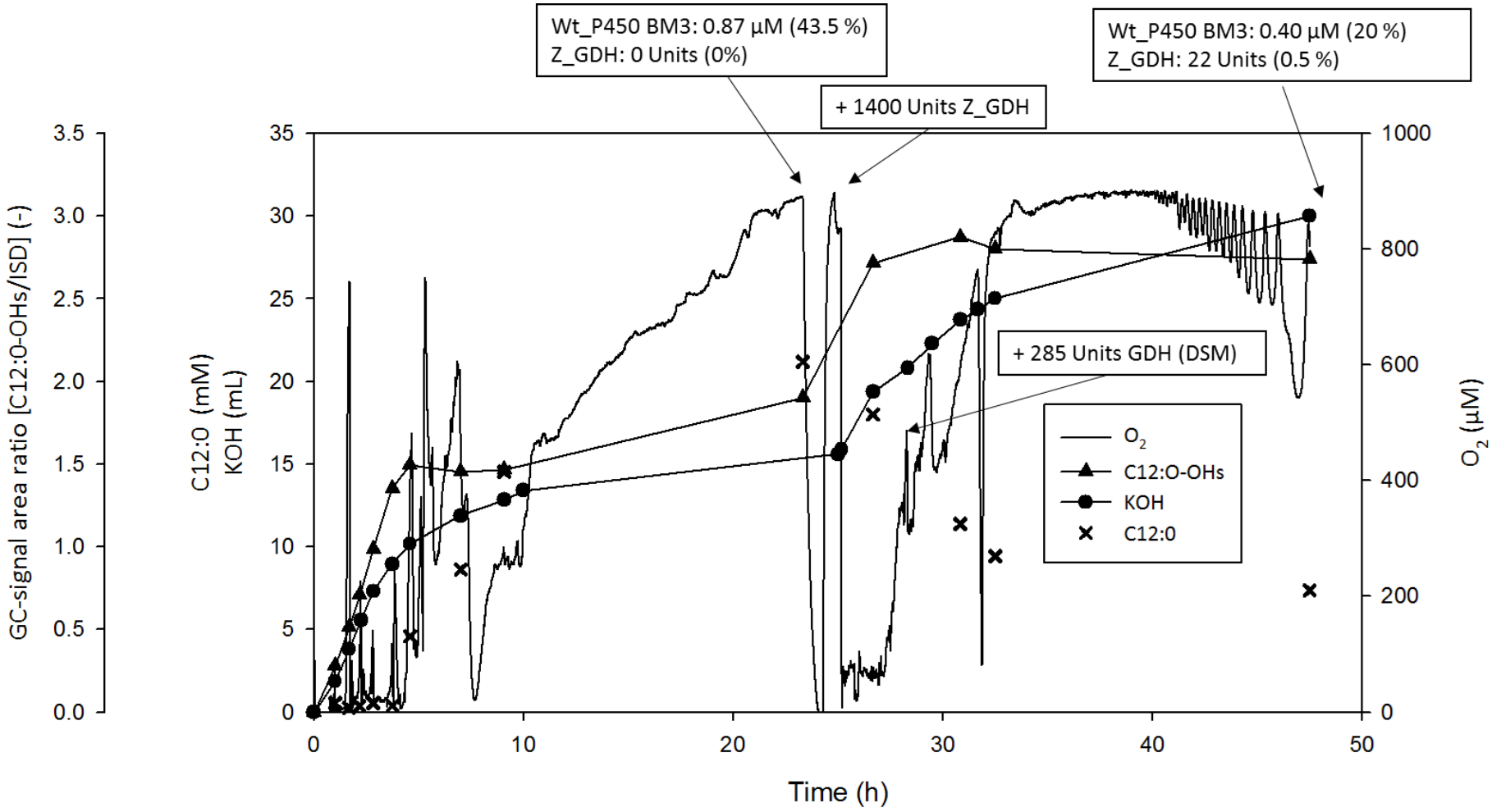

Figure 39: **Time course for the O_2 concentration, the product formation and the KOH consumption for an 80 mM C12:0 conversion at 500 mL scale.** As soon as the O_2 concentration increased, the remaining substrate concentration in the reaction was determined via GC-FID and additional substrate was supplied. Overall, 90% conversion of 80 mM (8 g) C12:0 could be achieved. As the conversion after 24 hours was far away from 100%, the remaining active Wt_P450 BM3 (43.5%) and the activity of Z_GDH (0%) were determined. The addition of 1400 Units Z_GDH after 25.2 hours led to an instant decrease of the O_2 concentration and consumption of additional KOH. ISD = internal standard (1-octanol).

In-operando coupling efficiency determination based on the formation of gluconic acid

Coupling efficiency is conventionally determined via the amount of consumed substrate/formed product (determined e.g. via GC) in relation to the applied NAD(P)H. This method is highly dependent on the correct photometric determination of the NAD(P)H stock concentration and adjusting the exact substrate concentration. Additionally, this method is not suitable to determine the coupling over a longer reaction time. An alternative is the determination of the produced GlcA in relation to the consumed substrate/formed product (if glucose in combination with GDH is used). For the preparative scale reactions with O_2 dependent substrate feed the regeneration of NADPH and hence the coupling efficiency was determined by comparing the produced GlcA to the consumed C12:0 at each feeding step. The GlcA concentration was measured via HPLC and the remaining C12:0 concentration via GC-FID analysis. In perspective of the coupling efficiency, the calculated values do not reflect a real uncoupling of the P450 BM3 but more an uncoupling of the entire reaction system. Previous preparative scale P450 BM3 reactions did not attempt deeper investigations on this important reaction parameter [29, 39, 39]. It has already been shown, that the CFE without available fatty acids consumes significant amounts of NAD(P)H and O_2 due to possible background reactions (Table 22 and Figure 31). Consequently, this value is of significant importance to describe the economy as well as overall efficiency of the production system. The *in-operando* coupling efficiency was calculated for different time points with the following equation:

$$\text{coupling efficiency (\%)} = \frac{\text{converted C12:0 (mM)}}{\text{formed GlcA (mM)}} \times 100$$

As expected, the free Z_P450 BM3 shows the highest uncoupling, while the free Wt_P450 BM3 and the co-immobilizate reach similar coupling efficiencies at the 50 mL scale (Table 27 and Table 28). These results can explain the slower reaction rate for Z_P450 BM3 compared to the Wt_P450 BM3 and the co-immobilizate as electrons and O_2 are channelled into undesired reactions. Beside the calculation of the coupling efficiency based on the GlcA formation, the coupling efficiency of the 500 mL reaction was also calculated based on the OTR (15.6 mM h^{-1}, Table 26, equation on page 44) when an O_2 limitation was present. The calculation for the 50 mL reaction is not feasible and would result in not reasonable coupling efficiencies (>100%), as OTRs of 7.0 to 7.3 mM h^{-1} were determined (Table 24). Probably, the decreasing effect on the k_La diminishes over time (silicone antifoam also lost its defoaming effect over time and had to be applied now and then into the reaction) resulting in underestimated *in-operando* k_La values and OTRs for the 50 mL reactions. Nevertheless, for the 500 mL reaction the calculation of the coupling efficiency based on the ORT results in meaningful values. In

general, the values are slightly higher than for the GlcA based coupling efficiencies, but the trend over time is comparable.

Table 27: **Determination of *in-operando* coupling efficiencies via GlcA concentration (50 mL and 500 mL reaction) and oxygen transfer rate (OTR, 15.6 mM h^{-1} for 500 mL reaction) for Wt_P450 BM3.**

Wt_P450 BM3, GDH (DSM) 80 mM C12:0, 50 mL

Time (min)	Converted C12:0 (mM)	GlcA (mM)	Coupling (%)
124	15.4	19.5	79.1
176	23.4	34.3	68.1
235	31.7	46.7	67.9
304	39.5	63.1	62.5
380	49.1	83.6	58.7
510	58.8	103.6	56.8
650	67.3	124.1	54.2
1410	79.6	155.5	51.2
1680	79.8	171.5	46.5

Wt_P450 BM3, Z_GDH, 80 mM C12:0, 500 mL reaction

Time (min)	Converted C12:0 (mM)	GlcA (mM)	Coupling based on GlcA (%)	Coupling based on OTR (%)
60	7.5	17.6	42.3	47.4
100	15.8	35.0	45.1	60.0
135	23.6	47.4	49.9	66.4
170	31.5	57.6	54.7	70.4
225	39.6	69.5	57.0	66.8
275	45.4	80.7	56.3	62.7
420	51.4	93.1	55.2	n.o.
545	55.5	98.4	56.4	n.o.
1400	58.8	111.8	52.6	n.o.
1680	62.0	152.9	40.5	n.o.
1850	68.6	210.6	32.6	n.o.
1950	70.6	199.7	35.3	n.o.
2850	72.6	227.9	31.9	n.o.

n.o. = no oxygen limitation in reaction

Table 28: **Determination of *in-operando* coupling efficiencies via GlcA concentration measurements in reaction with free Z_P450 BM3 and the co-immobilizate.**

Z_P450 BM3, Z_GDH, 40 mM C12:0, 50 mL

Time (min)	Converted C12:0 (mM)	GlcA (mM)	Coupling (%)
105	7.9	42	18.8
200	15.7	68	22.9
280	23.6	106	22.3
390	31.8	116	27.4
580	40.0	156	25.6
1330	40.0	162	24.7

Co-immobilizate, 48 mM C12:0, 50 mL

Time (min)	Converted C12:0 (mM)	GlcA (mM)	Coupling (%)
99	15.5	20.3	76.4
184	23.7	30.4	77.9
300	31.1	41.1	75.6
389	35.9	50.3	71.3
1410	42.1	57.9	72.7

In the preparative scale reactions for the conversion of C12:0 a time dependent formation of an additional peak was monitored, which was presumably assigned as overoxidation. Further investigation of this observation is described elsewhere (page 73). Figure 40 shows the dependency between the formation of overoxidation product and the coupling efficiency. The relative amount of overoxidation product (peak area) to the total amount of product (peak area) is compared to the coupling efficiency over time. For the reactions with Wt_P450 BM3 (50 and 500 mL) a general correlation between the formation of the overoxidation product and the coupling efficiency can be observed. While the relative amount of overoxidation product increases, the coupling efficiency decreases. This is not true for the Z_P450 BM3 reactions (free and immobilized). However, for both Z_P450 BM3 reactions the coupling efficiency was significant more stable over time than for the Wt_P450 BM3 reactions. Compared to the free enzyme preparations, the relative amount of final overoxidation product was three to five folds lower for the co-immobilizate reaction.

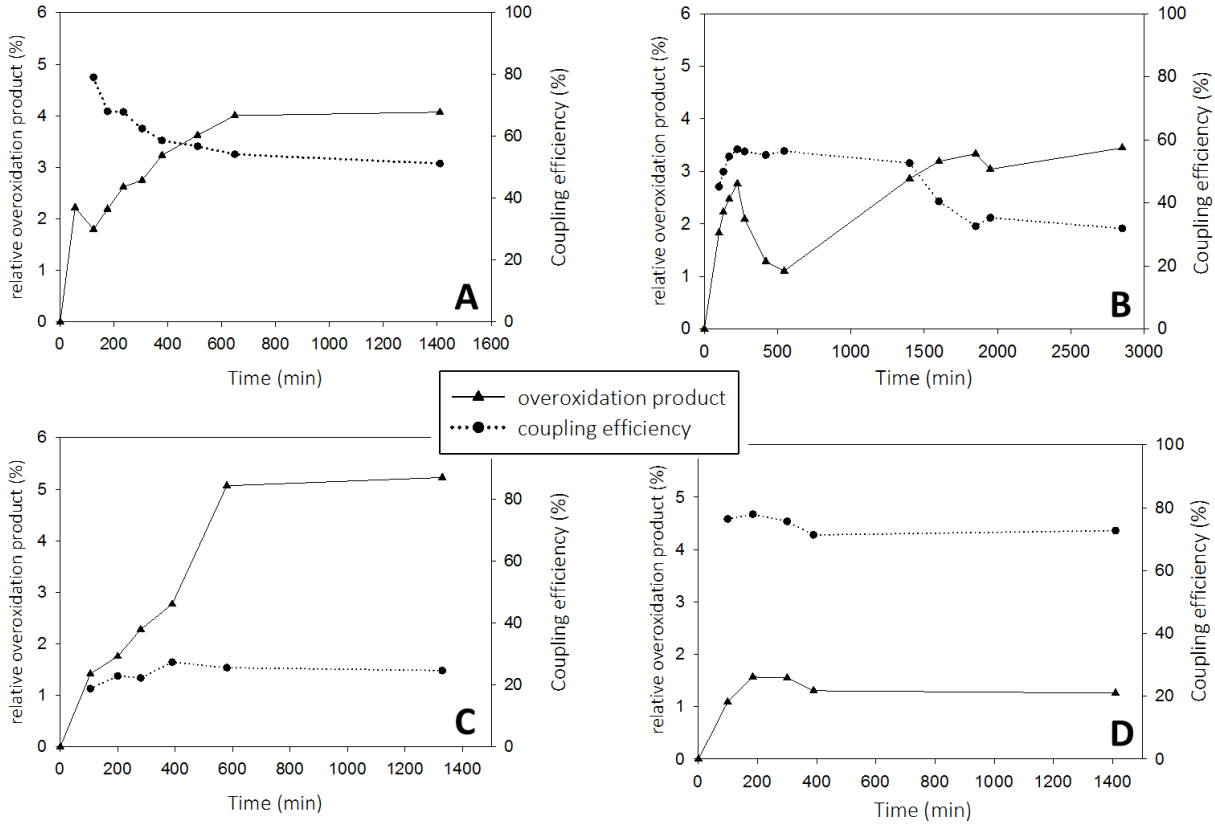

Figure 40: **Comparison of the relative overoxidation product (%) to the coupling efficiency (%).** Comparisons are shown for (A) the 50 mL Wt_P450 BM3, (B) the 500 mL Wt_P450 BM3, (C) the 50 mL free Z_P450 BM3 and (D) the co-immobilizate reaction.

Summary of key reaction parameters for reactions with O_2 dependent substrate feed

Key reaction parameters for the reactions with O_2 dependent substrate feed and different catalyst loadings/formulations were estimated and calculated and compared to already published results. Table 29 gives an overview of all calculated parameters. The highest product titre (99.8% conversion of 80 mM C12:0, 16 g L^{-1}) was achieved with Wt_P450 BM3 at 50 mL scale, followed by the 500 mL reaction with Wt_P450 BM3 (90% conversion of 80 mM C12:0). Although the initial product formation rates were comparable between the reactions with co-immobilizate and Wt_P450 BM3 for the co-immobilizate, the co-immobilizate never reached full conversion of the substrate (40 and 48 mM). Probably, clogging of the particles and hence mass transfer limitations are the reason. The reaction rate for the free Z_P450 BM3 was roughly two-fold lower compared to reactions with the co-immobilizate and the Wt_P450 BM3. These findings are mainly explained by the enormous O_2 and NADPH background consumption of the CFE (Table 22). The highest reaction rate (20.7 mM C12:0-OHs per h) could be achieved with Wt_P450 BM3 and excluding of silicone antifoam. However, the exclusion of antifoaming agents was not practicable as it resulted in foam formation and a removal of the substrate out of the reaction. Consequently, only 67% conversion (GC-area) of 100 mM C12:0 could be reached. TTNs close to 40000 were calculated for the 80 mM C12:0 conversions with Wt_P450 BM3 (50 and 500 mL) which are comparable to already reported P450 BM3 reactions containing DMSO (42000) [29]. The higher reaction rate of the Wt_P450 BM3 and co-immobilizate reaction compared to the free Z_P450 BM3 reaction is also reflected in the *in-operando* coupling efficiency. The free Z_P450 BM3 reaction produced the most GlcA and comparably low amount of C12:0-OHs hence providing the lowest coupling efficiency (23.6%). Consequently, the NADPH had to be regenerated more often to generate the same amount of product as compared to other catalytic systems.

The highest percentage of overoxidized product was measured in the 50 mL Wt_P450 BM3 and Z_P450 BM3 reactions (5.1 and 5.2%), followed by the 500 mL Wt_P450 BM3 reaction (3.4%) and the co-immobilizate reactions (2.4 and 1.3%). Interestingly, the reaction without silicone antifoam resulted in comparable low overoxidation product (1.0%). The highest overoxidation (up to 18%) was measured in the reaction with extended reaction time (110 h). Compared to already reported C12:0 conversions with P450 BM3 the product titre could be enhanced by more than two-fold from 33.5 to 79.4 mM. The highest achieved STY was eleven-fold higher (1.6 g L^{-1} h^{-1}) than for the previously published C12:0 conversion (0.14 g L^{-1} h^{-1}) [29].

Table 29: **Summary of determined key reaction parameters for reactions with oxygen dependent substrate feed.** Previously reported parameters of a P450 BM3 catalyzed C12:0 conversion from Kuehnel et al (2007) are shown for comparison [29].

	Kuehnel et al (2007) CYP102A1 3mDS/FDH [29]		**Wt_P450 BM3**	**Wt_P450 BM3**	**Wt_P450 BM3 (no antifoam)**	**Z_P450 BM3**	**Co-immobilizate**		**Wt_P450 BM3**
P450 BM3 (µM)	0.5	0.5	2	2	2	2	2	2	2
GDH (DSM or Z_{Basic2}) or FDH (U mL^{-1})	7 (FDH)	7 (FDH)	1.9 (DSM)	1.9 (DSM)	1.9 (DSM)	10.8 (Z_{Basic2})	10.8 (Z_{Basic2})	8.8 (Z_{Basic2})	8.8 (Z_{Basic2}) 0.57 (DSM)
Scale (mL)	20	20	50	50	50	50	50	50	500
Total substrate (mM)	50	50	40	80	100	40	40	48	80
Co-solvent/additive	CAVASOL W7 M (20 mM)	2% DMSO	11.9% DMSO [g]	12.4% DMSO [g]	14.8% DMSO [g]	9.3% DMSO [g]	9.9% DMSO [g]	9.9% DMSO [g]	12.4% DMSO [g]
Conversion (conv.) or GC-area product (%)[a]	67.7	42	99.5 (conv.)	99.8 (conv.)	67 (GC-area) [h]	99.9 (conv.)	96.5 (conv.)	75 (GC-area)	90 (conv.)
KOH consumption (mL)	--	--	---	2.9	2.1	2.3	1.4	0.63	30.0
Initial product formation rate (mM h^{-1}) [b]	n.r.	n.r.	10.4	8.6	20.7	4.5	7.2	10.6	7.5
Total reaction time (h)	48	48	5 (110)	28	21.6	23.5	23	22.2	47.5
STY (g L^{-1} h^{-1})	0.14	0.09	1.6	0.57	0.62	0.34	0.34	0.32	0.30
TTN (P450) [c]	66700	42000	19980	39920	---	19980	19300	---	36000
Coupling based on GlcA formation (%) [d]	---	---	---	79.1	---	22.9	---	76.4	45.1
Average coupling (%)	n.r.	n.r.	---	60.6	---	23.6	---	74.8	46.9
Regeneration of NADPH (cycles) [e]	n.r.	n.r.	---	343	---	324	---	116	454
Overoxidation product (%) [f]	n.r.	n.r.	(18)	5.1	1.0	5.2	2.4	1.3	3.5

[a]conversions (conv.) were calculated based on the final remaining substrate and total applied substrate, GC-area product was calculated by dividing the final product peak area with the sum of the final product peak area and the final remaining substrate peak area, [b]the initial substrate concentration (8 mM) and the remaining substrate concentration at the 1st feed were divided by the time point of the 1st feed, [c]calculated based on the conversion, the total substrate loading and the applied P450 BM3 concentration, [d]determined from the first two feed intervals (16 mM C12:0), [e]calculated by dividing the entire formed GlcA (mM, Table 27 and Table 28) with the applied $NADP^+$ (0.5 mM), [f]GC-area of overoxidation products in relation to GC-area of all detected products, [g]concentration after the final feed, [h]substrate was driven out of the reaction by gassing leading to strong foaming, n.r. = not reported

3.2.4 Preparative isolation of C12:0-OHs

The products and remaining substrate of all reactions conducted with oxygen dependent substrate feed were extracted in a two-phase solvent extraction. The weight of the isolated and dried products was determined, and the isolated yield was calculated based on weighed mass. All extractions resulted in good to excellent isolated yields ranging between 78 and 90% except for the reaction with free Z_P450 BM3 (66%). A possible explanation for the lower isolated yield for the reaction with free Z_P450 BM3 could be a lower substrate loading than intended. GC-FID analysis of the free Z_P450 BM3 CFE reaction (Figure 53) resulted in lower peak area ratios for the product (C12:0-OHs/ISD) compared to the reactions with free Wt_P450 BM3 CFE (Figure 35) and co-immobilizate (Figure 54), which supports this theory. For extraction of the reaction with 48 mM C12:0 (76% conversion) and co-immobilizate (Table 30, entry 5) the carrier was separated from the liquid phase by centrifugation (3220 x g, 5 minutes, 20 °C). After acidification, three times 50 mL EtOAc were used for extraction of the carrier and the liquid phase, respectively. The centrifugation step removed nearly the entire remaining substrate from the liquid reaction bulk (3.5% GC-area substrate remained, Figure 62). Ahead of the acidification and extraction of the 500 mL reaction (Table 30, entry 6) the remaining solid substrate in the reaction was removed by centrifugation (3220 x g, 5 minutes, 20 °C), while the dissolved C12:0-OHs stayed in the liquid bulk. GC-FID analysis was conducted to show that the solids were composed mainly of C12:0 (93.3%) and only traces of C12:0-OHs (6.7%) were removed during the additional centrifugation step (Figure 65). Figure 41 depicts a flow schema for the performed product downstream.

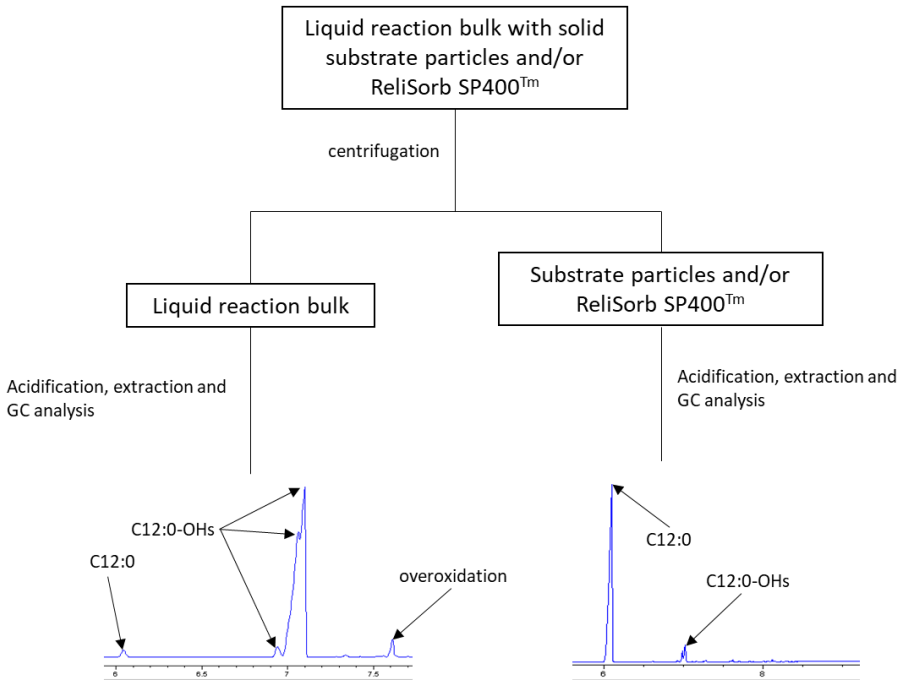

Figure 41: **Flow scheme for the separation of solid particles from the reaction bulk and subsequent extraction and GC-FID analysis.**

The purity of products was determined via GC-FID analysis. The peak area of the C12:0-OHs was divided by the entire integrable peak area (including the peak for the remaining substrate and the peak for the assigned overoxidation products). Respective chromatograms are shown in Figure 58 to Figure 64. Determined purities of extracted products range between 79 to 92%. The comparatively low purity (79.1%) for the Wt_P450 BM3 reaction with 40 mM C12:0 (Table 30, entry 1) is mainly related to an extended reaction time (110 h) resulting in higher overoxidation. The removal of the remaining substrate from the 500 mL reaction led to a comparable purity (92%) to the 50 mL reactions (88%) as the 10% remaining substrate were almost entirely removed via centrifugation from the non-acidified reaction bulk.

Table 30: **Summary of the preparative isolation of C12:0-OHs of various conducted reactions.**

Entry	Enzyme preparation	Reaction volume (mL)	Conversion (%)	Substrate (mg)	Theoretical product yield (mg)	Product (mg)	Isolated yield (%)	Purity GC-FID (%)
1	Free (Wt_BM3)	50	>99	400	432	352	82	80
2	Free (Wt_BM3)	50	>99	800	864	743	86	88
3	Free (Z_BM3)	50	>99	400	432	286	66	85
4	Co - immobilizate	50	96.5	400	432	386	90	91
5 (W) 5 (P)	Co - immobilizate	50	75% GC-area	480	518.4	294 (W) 115 (P)	79	--
6	**Free (Wt_BM3)**	**500**	**90**	**8000**	**8640**	**7074**	**82**	**92**

W = water phase, P = particles, ReliSorb^{Tm} SP400

3.2.5 Relevance of product overoxidation for the whole process

Based on the successful conversion of 80 mM C12:0 at 50 mL scale with Wt_P450 BM3 the question arose why the system is limited to efficient conversions of more than 80 mM substrate and why the O_2 concentration increases after 40 to 60 mM conversion of C12:0. The harsh reaction conditions, including interfacial phase boundaries (solid substrate material and the presence of gas bubbles), uncoupling and reactive oxygen species formation, the constant mechanical stress (stirring) and the addition of a concentrated base (5 M KOH), might have a negative influence on the catalyst stability. However, P450 BM3 was quite stable in the 500 mL reaction (20% active enzyme recovered after 47.5 hours of reaction time). Closer investigation of the obtained chromatograms in the GC-FID analysis shows the time-dependent formation of an additional peak at 7.6 minutes retention time (e.g.

Figure 58). First assumptions were that a further oxidation of the C12:0-OHs by the P450 BM3 catalyst could occur which has been reported previously for C14:0-OHs conversions [61]. Overoxidation of products has been rarely reported or investigated in P450 catalysis [9, 61, 62]. Figure 42 displays the proposed overoxidation reaction catalysed by P450 BM3 applying ω-2 hydroxy dodecanoic acids as substrate.

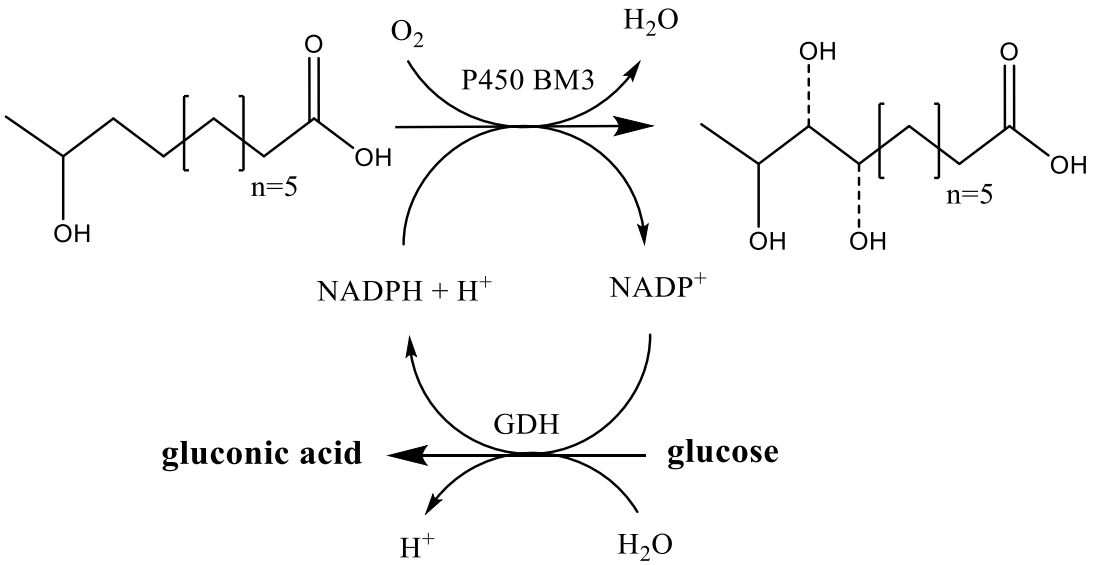

Figure 42: **Reaction scheme for overoxidation reaction catalysed by P450 BM3 and GDH yielding dihydroxylated fatty acids (other routes potentially forming ketones are not shown here) [61].**

The competition between the C12:0 and C12:0-OHs for the active centre of the P450 BM3 might be the reason for a certain limitation to reach higher fatty acid conversions. Previous reactions showed, that the C12:0-OHs were soluble up to 80 mM in the liquid reaction bulk, which is 40-fold higher compared to the solubility limit of C12:0 in water (~ 2 mM). The further the reaction proceeds, the further the ratio of dissolved fatty- to hydroxy fatty acid shifts towards the hydroxy fatty acid. If both compounds would exhibit comparable K_m values, the C12:0-OHs would compete with C12:0 in the active site of P450 BM3. Potentially, this could result in undesired side products, activation of the catalytic cycle and consequently uncoupling and a more difficult product downstream to yield solely mono-hydroxylated fatty acids. To proof overoxidation of C12:0-OHs by P450 BM3 a reaction with extracted C12:0-OHs (Table 30, entry 1 and Figure 58, ~80% purity (GC-FID)) was conducted. The reaction (10 mL) was composed of 10 µM Wt_P450 BM3, 9.5 U mL^{-1} GDH (DSM), 20 mM C12:0-OHs (41.6 mg), 5% (v/v) DMSO, 200 mM glucose, 500 µM $NADP^+$, 5 mg/mL catalase and 50 mM KPi buffer (pH 7.5). The pH was stabilized at 7.2 under continuous stirring at 250 rpm and supplementation of 5 mL min^{-1} O_2 (100%). Compared to C12:0, there were no solubility problems with C12:0-OHs and no foam formation was observed. The reaction ran for 17 hours and the product isolation of the entire reactor yielded 31.5 mg oily material. GC-FID analysis confirmed the conversion of C12:0-OHs. Beside the potential overoxidation-peak found in the C12:0 conversions (P1, Figure 58), additional peaks (P2

and P3) could be detected during conversion of C12:0-OHs (Figure 43). Products with longer retention time typically correspond to hydroxylations, which would be in agreement with previous reports from a C14:0-OHs conversion [61].

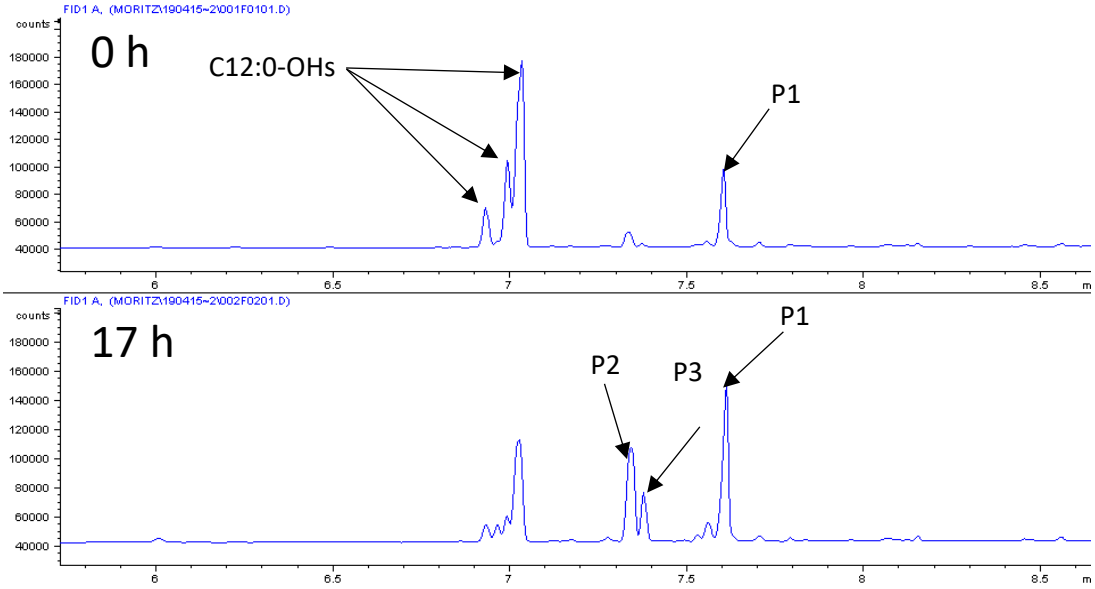

Figure 43: **Conversion of C12:0-OHs by the Wt_P450 BM3/GDH (DSM) system.** Isolated products (C12:0-OHs) were used to show the ability of the Wt_P450 BM3 to convert hydroxy fatty acids produced from C12:0. Beside the peak found in the C12:0 conversions (P1) additional peaks (P2, P3) could be found after 17 hours reaction time.

3.3 Determination of kinetic parameters of varying P450 formulations

Kinetic parameters for the conversion of C12:0 by P450 BM3 have been reported extensively in literature [19]. However, although the further conversion of primary P450 BM3 products has been shown [58, 61, 62], there are no information regarding the kinetic properties of the conversion of C12:0-OHs available. From the results shown here, the determination of key kinetic parameters (k_{cat}, K_m, k_{eff}, coupling efficiency) for the conversion of C12:0-OHs by P450 BM3 and comparison to parameters for C12:0 is a crucial factor to gain a deeper understanding for the design and operation of P450 monooxygenases for preparative scale conversions.

3.3.1 Purification of enzymes

P450 BM3 variants were purified via affinity chromatography (Wt_P450 BM3) with a $NiSO_4$-His-Trap or ion exchange chromatography (Z_P450 BM3) with pre-packed HiTrap SPFF columns, respectively. The chromatograms obtained during the purification are displayed in Figure 66. Figure 44 shows the SDS-PAGE to verify the successful purification and to check the fractions for any impurities. Fraction 28, 29, 30, 31 and 32 of the Wt_P450 BM3 purification were combined, dialysed and the molarity of Wt_P450 BM3 was determined via CO-titration. In total, 23 mL enzyme solution with estimated 90% purity and 2.7 mg mL^{-1} (22.4 µM) purified Wt_P450 BM3 were obtained and finally lyophilized. The CO-titration after combining and dialysis of fraction 34, 35, 36, 37 and 38 of the Z_P450 BM3 purification resulted

in 2.3 mg mL^{-1} (17.9 µM) purified Z_P450 BM3 in a total volume of 17 mL. The purity was estimated to be 90%. Both purifications yielded enzyme in sufficient amount and purity for the determination of the maximal NADPH and O_2 consumption rate, k_{cat}, K_m and the coupling efficiency for the conversion of C12:0 and C12:0-OH.

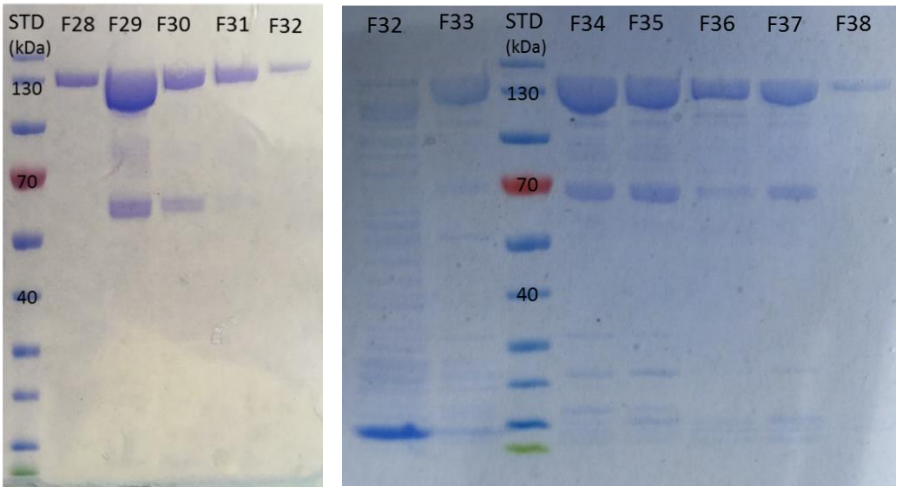

Figure 44: **SDS-PAGE for collected fractions during purification of Wt_P450 BM3 (left) and Z_P450 BM3 (right).** The bands around 130 kDa represents the Wt_P450 BM3 and the Z_P450 BM3, respectively. As standard (STD) serves the PageRuler™ Prestained Protein Ladder from Thermo Fisher. F = fraction collected during the elution of the P450 BM3.

3.3.2 Overview of determined kinetic parameters

Kinetic key parameters were determined and calculated for conversion of C12:0 and C12:0-OHs and various enzyme preparations. The maximal O_2 consumption rates and the K_m values for the purified Wt_P450 BM3 and Z_P450 BM3, the co-immobilizate and the Wt_P450 BM3 (CFE) were fitted using a hyperbolic function provided by Origin 9.0 or SigmaPlot 10.0 software (Figure 67 to Figure 70). For Z_P450 BM3 (CFE) solely the maximal O_2 consumption rate was determined, because the background O_2 consumption caused too much trouble and no feasible saturation curve could be calculated. An overview of the determined and calculated parameters is given in Table 31. In general, the maximal NADPH oxidation rates match the determined maximal O_2 consumption rates (except for the CFE of the Wt_P450 BM3). The determined maximal NADPH and O_2 consumption rates were two to four-fold lower for C12:0-OHs as substrate compared to C12:0 as substrate. Considering the coupling efficiencies for C12:0 (>77%) and C12:0-OHs (<12%) this results in comparatively low k_{cat} values for the conversion of C12:0-OHs (37 to 18-folds lower than for the conversion of C12:0). This is also reflected in the preparative scale reaction, as in general the amount of side product was low in comparison to the total product (~5%). Nevertheless, the reactions with C12:0-OHs as substrate showed a significant O_2 consumption, indicating a competition between C12:0 and C12:0-OHs for the P450 BM3 active centre during the preparative scale reactions. The two to three-fold higher K_m value for C12:0-OHs compared to C12:0, results in k_{eff} values 50-fold lower for C12:0-OHs than C12:0. The low coupling efficiency for

C12:0-OHs, which results in potential catalyst inactivation, and the competition of C12:0 and C12:OHs, might be a possible explanation for the increase of the O_2 concentration after conversion of 40 to 60 mM C12:0. Even additional pulsing of C12:0 did not decrease the O_2 concentration indicating a strong competition of substrate and product oxidation. The determined k_{cat} values for purified Wt_P450 BM3 and C12:0 as substrate are comparable low to values found in literature (values of 20 to 80 s^{-1} have been reported) [19]. However, significant amounts of DMSO (10%) were added to the reactions. Previous studies showed a decrease of catalytic activity when DMSO is added to reactions with P450 BM3 [50]. Additionally, crystallization of the haem domain (Thr1–Leu455) of the variant F87A in presence of elevated DMSO concentrations revealed a coordination of one DMSO molecule to the haem iron, indicating a competition between the water ligand (6^{th} heme ligand) and DMSO in the active centre [63].

Table 31: **Determined key kinetic parameters for different monooxygenase catalysts and C12:0 and C12:0-OHs as substrate.**

Substrate	**Catalyst (P450 BM3)**	**Max. NADPH oxidation rate (s^{-1})**	**Max. O_2-consumption rate (s^{-1})**	**K_m (µM)**	**k_{cat} (s^{-1})**	**k_{eff} (s^{-1} mM^{-1})**	**Coupling (%)**
C12:0	CFE (Wt)	3.1	8.0 ± 0.4	417 ± 54	6.3	15.8	79[a]
C12:0-OH	CFE (Wt)	0.7	2.3 ± 0.2	1126 ± 329	---	---	---
C12:0	CFE (z_{Basic2})	5.3	6.8 ± 0.9	---	1.6	---	23[a]
C12:0-OH	CFE (z_{Basic2})	0.9	2.1 ± 0.2	---	---	---	---
C12:0	Purified (Wt)	2.3	2.9 ± 0.2	340 ± 63	2.5	7.4	92
C12:0-OH	Purified (Wt)	0.7	1.0 ± 0.1	799 ± 197	0.1	0.13	6
C12:0	Purified (z_{Basic2})	3.4	4.6 ± 0.4	376 ± 85	3.7	9.8	79
C12:0-OH	Purified (z_{Basic2})	1.4	2.1 ± 0.1	1321 ± 176	0.1	0.08	5
C12:0	Co-immobilizate	---[b]	3.9 ± 0.6	3147 ± 851	3.0	1.0	77
C12:0-OH	Co-immobilizate	---[b]	0.7 ± 0.1	3829 ± 932	0.1	0.03	12

[a] values are based on the determination of GlcA (see page 66); [b]technical setup not suitable.

4 Summary and conclusion

The immobilization of Z_P450 BM3 and Z_GDH on ReliSorb^{Tm} SP400 was successfully implemented at g-scale by adapting the original protocol developed for mg-scale. Additionally, the time required for preparation was decreased by reducing the loading steps from four to two without comprising the loading of particles with sufficient catalyst. A key development for this purpose was the preparation and formulation of lyophilized CFEs for Z_P450 BM3 and Z_GDH and hence the possibility to prepare enzyme solutions of arbitrary concentrations. Useful immobilization yields could be achieved for the Z_P450 BM3 (83 nmole per g carrier, 67.4% immobilization efficiency) and Z_GDH (488 U per g carrier, 79% immobilization efficiency). However, investigation of the *in-operando* stability revealed a dissociation (~80%) of the P450 BM3 from the carrier within 6 h of reaction time, independent of the mechanical stress for the carriers in solution. The application of immobilized P450 BM3 "in flow" would require a stable immobilizate. Therefore, different immobilization strategies or adjusting of the reaction conditions should be considered. The instable binding of the Z_P450 BM3 was also reflected in the storage stability of the co-immobilizate in liquid buffer. Conversion experiments and SDS-PAGE analysis revealed a full dissociation of the Z_P450 BM3 from the carrier within a week of storage at 4°C in liquid form. However, lyophilization of the carrier drastically increased the binding stability of the Z_P450 BM3 on the carrier and no dissociation within 52 days of storage at -20 °C was observable via SDS-PAGE. Nevertheless, the catalytic activity decreased over time. After zero days of storage 98.5% conversion (GC-area) of 4 mM C12:0 could be achieved, while after 75 days only 8% conversion were measured. The frequent thawing and re-freezing of the co-immobilizate might have resulted in an increase of the moisture content from air/humidity that might contribute to the activity loss. Moisture analysis revealed 24% moisture in the lyophilized co-immobilizate after 76 days of storage at -20°. Microbial contamination might be a further challenge that has not been investigated here.

Initial preparative scale conversion with the co-immobilizate and free Z_P450 BM3 and Z_GDH resulted in promising full conversion of 40 mM C12:0 (8 g L^{-1}) within 23 hours of reaction time. Noteworthy, the co-immobilizate outperformed the free enzyme preparation in terms of initial product formation (14 vs. 7.5 mM h^{-1}), the time to reach high conversions (>95%, 4 vs. 8 h) and the coupling efficiency (65 vs. 31%). Closer investigation of the enzyme preparations revealed a significant higher O_2 and NADPH background consumption by the CFEs than by the co-immobilizate in absence of fatty acids. As the 40 mM C12:0 conversion ran under O_2 limited conditions, this is a reasonable explanation for the better performance of the co-immobilizate. However, the co-immobilizate could not be re-used (zero conversion, no O_2 consumption), mainly due to the previous mentioned dissociation of Z_P450 BM3 from the carrier into the liquid. Additionally, the accumulation of fatty acids on/into the particles and a possible clogging resulting from this might lead to mass transfer limitations over longer reaction times.

Efficient pH control and constant supplementation of O_2 are key to fast and high conversions of substrates in P450-catalyzed reactions, however poorly addressed in most studies. Bubbling of O_2 into a liquid solution of C12:0 resulted in strong foaming which makes preparative scale conversions of heterogeneous fatty acids without adding suitable defoaming agents cumbersome (substrate loss/enzyme inactivation at gas-liquid-interphases). However, the initial used Antifoam 204 is highly soluble in the extraction solution (EtOAc) providing an additional challenge in particular for product downstream. The latter used silicone antifoam did not interfere the downstream process. Nevertheless, it drastically decreased the k_La (29.7 to 10.3 h^{-1}) in the reaction resulting in a decreased product formation rate (from 2.9 to 1.2 g L^{-1} h^{-1}, 2.5 h of reaction time). Identification of better antifoaming agents and/or adaption of the general O_2 supply (here basic lab equipment was used) into the reaction will boost productivity and might decrease reaction times. Despite being problematic for the envisioned downstream process, Antifoam 204 seemed to support the dissolving of the substrate (C12:0) in the liquid reaction bulk in a positive way leading to high conversions (>99% conversion in batch with 40 mM C12:0). Reactions without Antifoam 204 and EtOH as co-solvent, resulted in lower conversions (49% of 40 mM C12:0) and rigid solid particles or crystals (identified as C12:0) were formed in the reaction bulk making the substrate practically inaccessible for P450 BM3. Consequently, a fed-batch conversion (on average lower substrate concentration in the reaction) with DMSO as alternative co-solvent was tested. Full conversion of 40 mM C12:0 could be achieved in a fed-batch, where C12:0 was dissolved in EtOH and DSMO (1:1, v/v). Silicone antifoam was added in the low mg range (<10 mg) whenever necessary.

Based on the initial observation that a depletion of substrate correlates perfectly with a rapid increase of the O_2 concentration an O_2 concentration dependent substrate feed was tested, optimized and established for preparative scale syntheses. The rapid increase of the O_2 concentration can easily be used as quantitative measure for nearly or full depletion of substrate. The addition of new substrate instantly led to a re-decrease of the O_2 concentration. Different enzyme preparations were tested. The co-immobilizate outperformed the free Z_P450 BM3/Z_GDH system in terms of feed intervals (and hence reaction time) but did not reach full conversion (96.5% of 40 mM C12:0 and 75% of 48 mM C12:0). However, the free Wt_P450 BM3/GDH (DSM) outperformed both Z_{Basic2}-based systems (immobilized and free) in terms of total substrate loading and product titers (99.8% conversion of 80 mM C12:0, 16 g L^{-1}). The higher reaction rate for the Wt_P450 BM3 compared to the free Z_P450 BM3 can be explained by the higher expression yield of the Wt_P450 BM3 and hence lower background of unwanted side reactions consuming O_2 and NADPH. Although the background consumption of O_2/NADPH was lower for the co-immobilized enzymes than for the Wt_P450 BM3 the reaction rates were comparable. This might be explained by the general lower activity of immobilized enzymes and mass transport limitations in the nanoporous carrier. The reaction rates were also reflected in the

formed GlcA. While the Wt_P450 BM3 and the co-immobilizate reached similar average coupling efficiencies (60.6 and 74.8%), the free Z_P450 BM3 reached only 23.6%. For the reactions with Wt_P450 BM3 (50 and 500 mL) a general correlation between the formation of the overoxidation product and the coupling efficiency over time could be observed. While the relative amount of overoxidation product constantly increased, the coupling efficiency decreased. For both Z_P450 BM3 reactions (free and immobilized) the coupling efficiency was significantly more stable over time than for the Wt_P450 BM3 reactions and the trend for both parameters is not observable.

Although the right time for the substrate addition based on the O_2 concentration was identified easily after conversion of 0 to 40 mM C12:0, it became more challenging in the later reaction. Despite the presence and addition of substrate, the O_2 concentration slowly increased. From this we assumed that a competition between C12:0 and C12:0-OHs and/or a catalyst inactivation could be the reason. Product overoxidation by P450 BM3 and the competition between C12:0 and C12:0-OHs for the active centre was studied by performing a reaction with produced and isolated C12:0-OHs and Wt_P450 BM3. This strategy allowed to confirm the origin of a product peak found in the C12:0 conversion likely related to overoxidation of C12:0-OH. However, further peaks were identified indicating formation of additional oxidation products that can be obtained in reactions with C12:0-OHs. Based on this findings, key kinetic parameters for C12:0-OHs (mixture of hydroxy acids produced by P450 BM3 from C12:0) as substrate were measured for the first time and compared to parameters for C12:0. Kinetic parameters for the conversion of C12:0 by P450 BM3 have been reported extensively in literature [19], but there are no information regarding the kinetic properties of the further conversion of the primary products (C12:0-OHs) available. This determination can be a key factor to gain a better and deeper understanding of the preparative scale conversions and the impact of product(s) in bioprocesses with P450s. The P450 BM3 consumed a 2- to 4-fold lower but still significant amount of O_2 and NADPH if C12:0-OHs was applied as substrate. Additionally, low coupling efficiencies (<12%) were measured resulting in 18 to 37-fold lower calculated k_{cat} values with C12:0-OHs as substrate compared to C12:0. This explains the low amount of side product (~5%) in the preparative scale reactions. The lower consumption of O_2 if C12:0-OHs are provided as substrate and a potential catalyst inactivation are a reasonable explanation for the increase of the O_2 concentration after conversion of 40 to 60 mM C12:0.

Scaling the reaction by ten-fold to 500 mL (80 mM C12:0) required an adaption of the gassing unit to reach comparable k_La values (> 10 h^{-1}). Finally, 90% conversion of 80 mM C12:0 (16 g L^{-1}) at 500 mL scale could be achieved with minimal changes in the overall technical reaction setup. This shows easy scalability of the process solely based on the oxygen transfer capability (k_La) and activity of P450 BM3. The product isolation of the 500 mL reaction resulted in excellent isolated yields of 82% and a GC-FID purity of 92% for the C12:0-OHs was measured.

Concluded, the O_2 and NADPH background consumption of the CFEs displayed a significant factor for the reaction under oxygen limited conditions. Although, the co-immobilized enzymes outperform their free counterparts (up to 40 mM C12:0), the low binding stability of Z_P450 BM3 requires further developments (entrapment or covalent binding) with focus on the applied reaction conditions, for example in a flow system. Compared to the Z_P450 BM3 the Z_GDH exhibits sufficient binding stability. A key factor for efficient usage of Z_{Basic2} based immobilizates could be a deeper understanding of the influences of certain enzyme characteristics on the binding (e.g. surface charge of the enzyme, influence of multimeric structures). Monitoring and precise control of the of O_2 concentration provides an excellent tool for fast design of the reaction process, namely by establishing a substrate feed strategy that overcomes challenges in substrate loading such as crystallization, inhomogeneity and inaccessibility. The characterisation of the kinetic parameters for C12:0 and C12:0-OHs and the overoxidation reaction showed, that an *in-situ* conversion of C12:0-OHs or *in-situ* removal might contribute to enhanced total substrate loadings and productivity of the system. A previously described P450 BM3 catalysed C12:0 hydroxylation reached a product titre of 33.5 mM C12:0-OHs (TTN_{P450}: 66700, STY: 0.14 g L^{-1} h^{-1}, 67% conversion) [29]. The established O_2 concentration dependent substrate feed allowed 99.8% conversion of 80 mM C12:0 (16 g L^{-1}, TTN_{P450}: 39920, STY: 0.57 g L^{-1} h^{-1}) for g-scale synthesis of hydroxy fatty acids. This is a remarkable improvement and an excellent starting point for further process intensification

5 Appendix

5.1 Storage stability of co-immobilizate

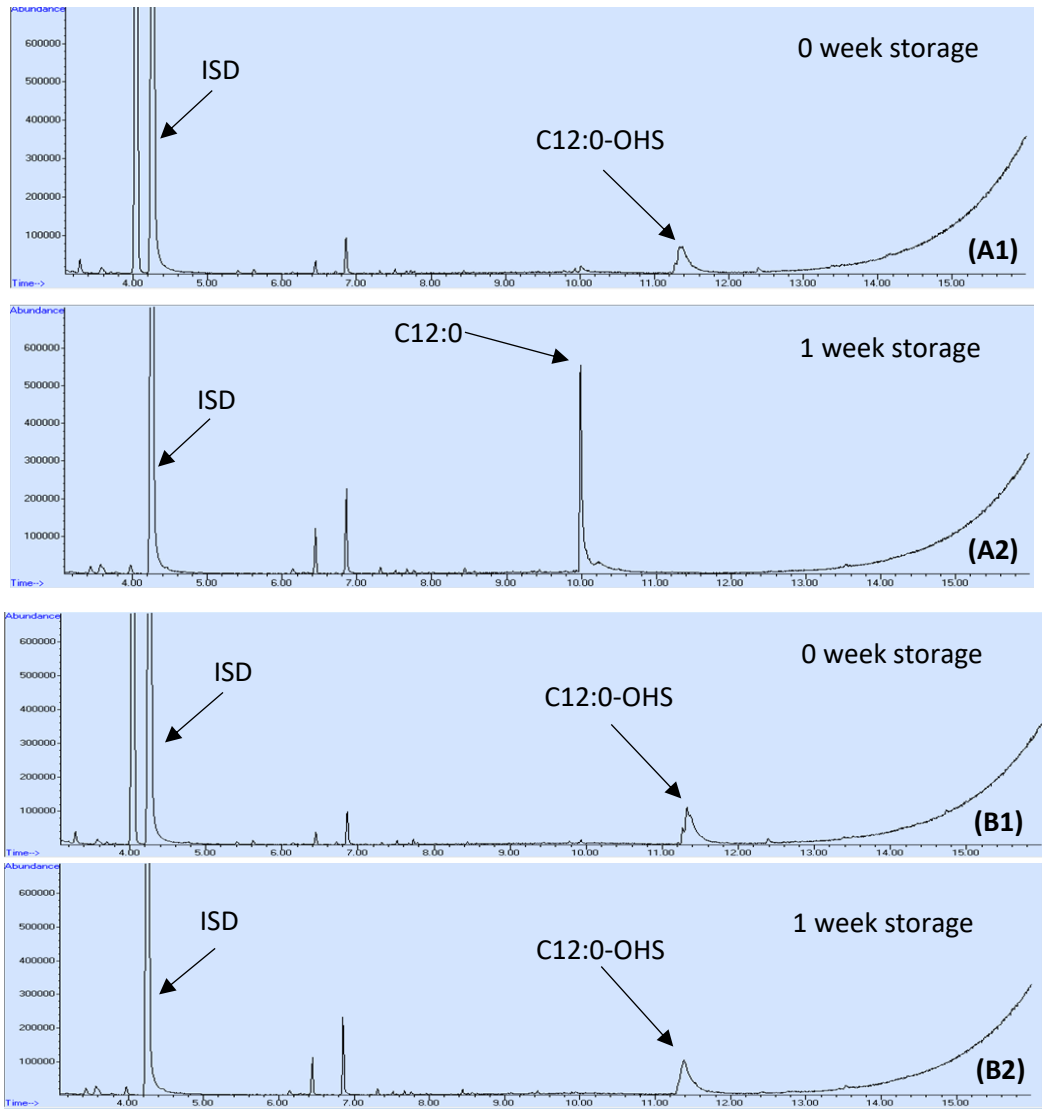

Figure 45: **Conversion experiments for the liquid stored carrier (A1 and A2) and the lyophilized carrier (B1 and B2) after zero and one week (W) of storage at 4°C.** The peaks at retention times of 6.45 at 6.85 minutes were identified as silane compounds (derived from derivatization agent) via the NIST database. ISD = internal standard (1-octanol)

5.2 Testing of carrier reusability

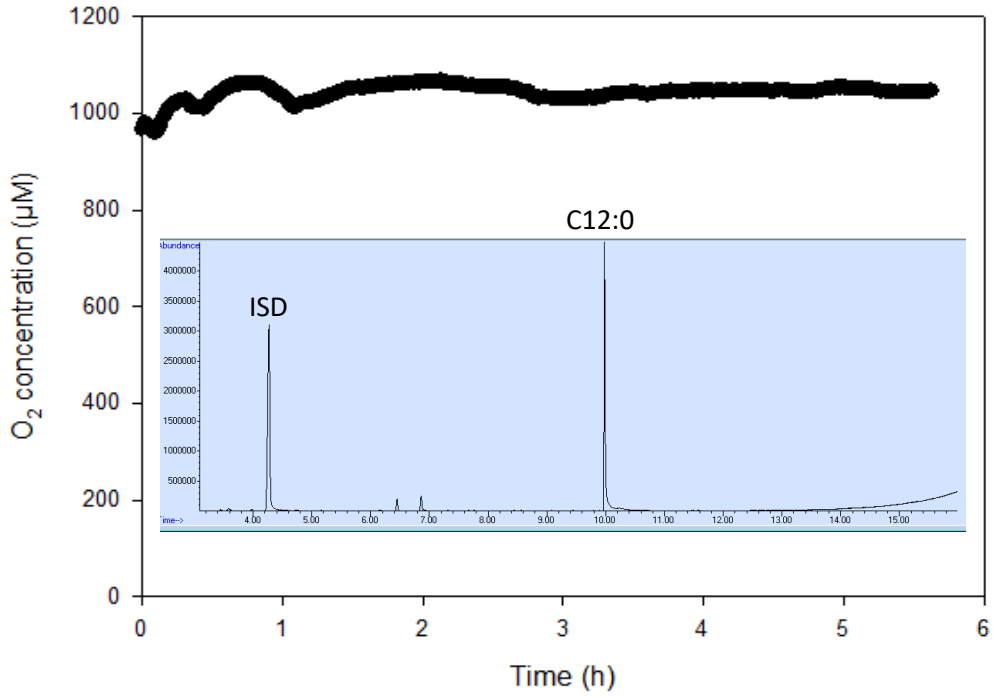

Figure 46: **Course of oxygen concentration and the GC-MS chromatogram after 5.5 h reaction time for a reaction with reused co-immobilizate (previous reaction ran for 23 h reaction, 20000 TTN_{P450}).** ISD = internal standard (1-octanol)

5.3 NAD(P)H oxidation reactions with CFE

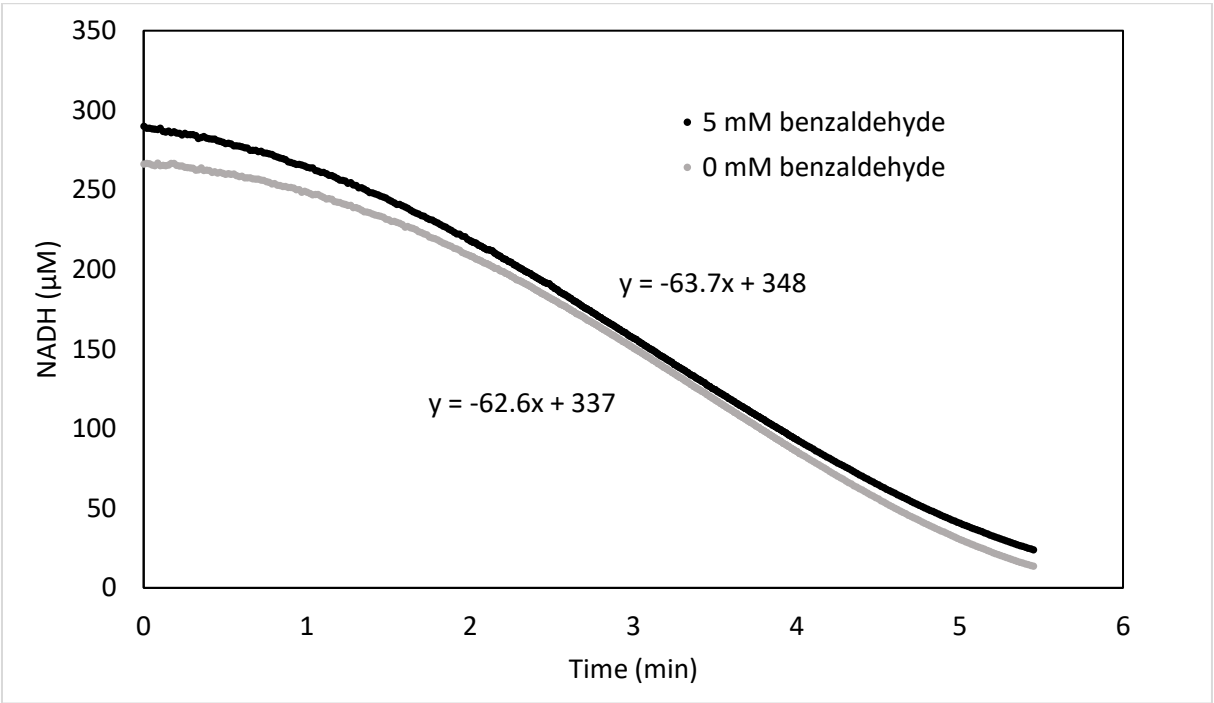

Figure 47: **Consumption of NADH in 1 mL reactions containing 10 U mL^{-1} Z_GDH CFE, 300 µM NADH, 50 mM KPi (pH 7.5) and 0 or 5 mM benzaldehyde.** An NADH oxidation rate of 63.7 and 62.6 µM min^{-1} was calculated (in the linear range) for reactions containing 5 and 0 mM benzaldehyde, respectively.

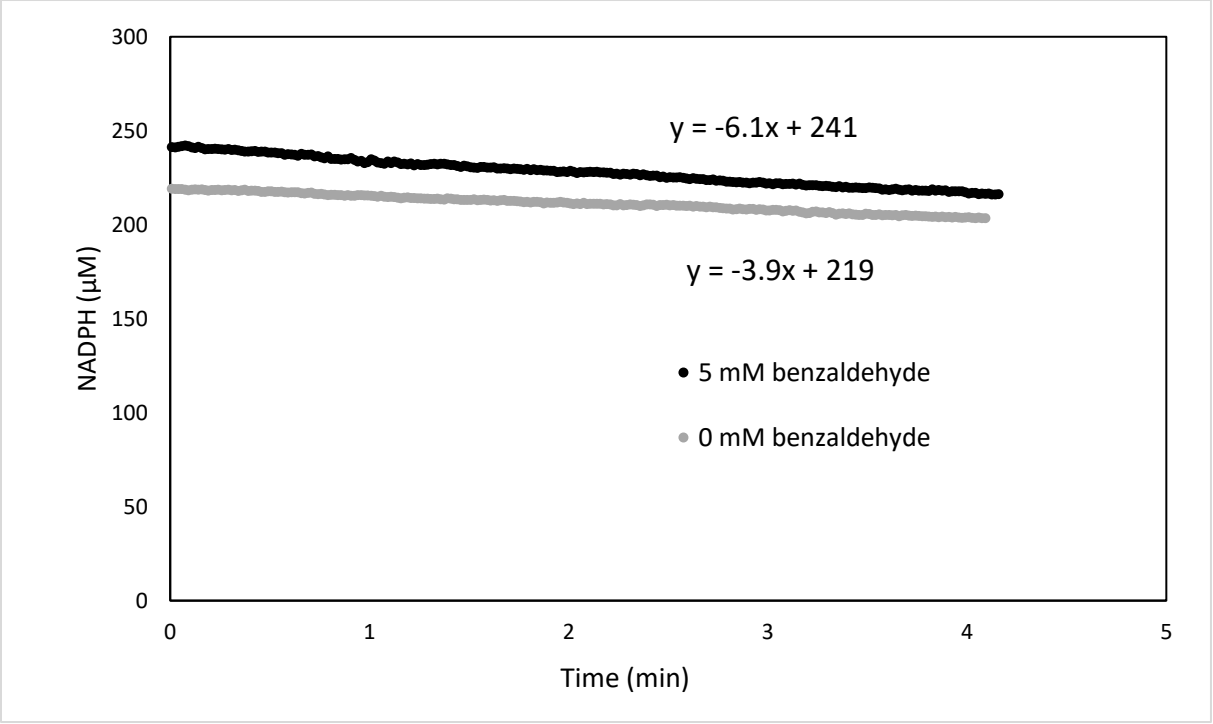

Figure 48: **Consumption of NADPH in 1 mL reactions containing 10 U mL^{-1} Z_GDH CFE, 300 µM NADPH, 50 mM KPi (pH 7.5) and 0 or 5 mM benzaldehyde.** An NADPH oxidation rate of 6.1 and 3.9 µM min^{-1} was calculated for reactions containing 5 and 0 mM benzaldehyde, respectively.

Table 32: **GC-MS temperature program for evaluation of the ADH background reactions in the Z_GDH CFE.**

	GC-MS
Start	50 °C
Hold	50 °C for 10 min
Rise	10 °C per min until 320 °C
End	320 °C for 0 min

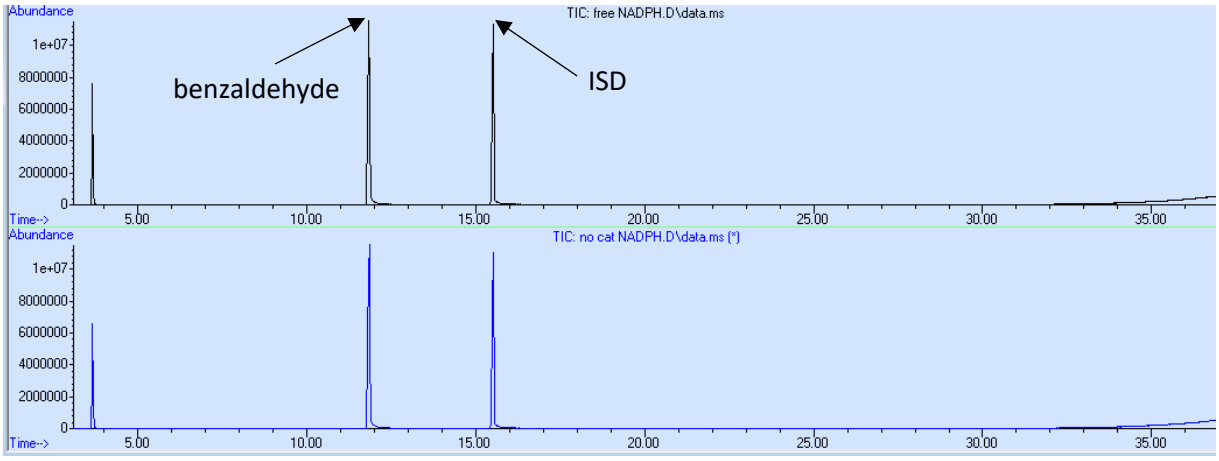

Figure 49: **Conversion of 5 mM benzaldehyde by 5 U mL^{-1} Z_GDH CFE to detect ADH background activity from *E. coli* enzymes.** The top chromatogram shows the reaction with free Z_GDH CFE, the bottom the reaction without catalyst (16 h reaction time). Formation of the corresponding benzyl alcohol was not detected. ISD = internal standard, 1-octanol. Co-factor = 400 µM NADPH.

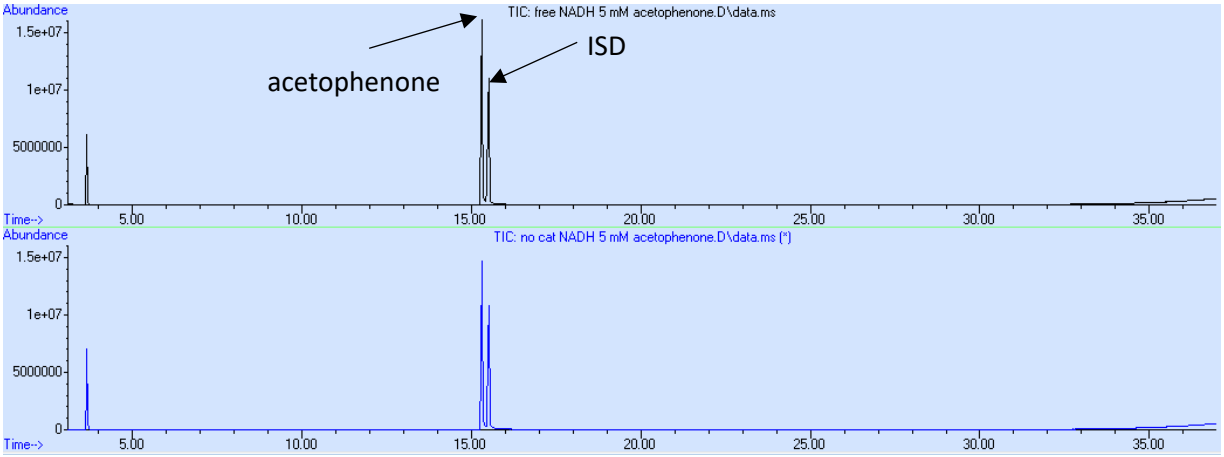

Figure 50: **Conversion of 5 mM acetophenone by 5 U mL^{-1} Z_GDH CFE to detect ADH background activity from *E. coli* enzymes.** The top chromatogram shows the reaction with free Z_GDH CFE, the bottom the reaction without catalyst (16 h reaction time). Formation of 1-phenylethanol was not detected. ISD = internal standard, 1-octanol. Co-factor = 400 µM NADH.

5.4 Foam composition analysis

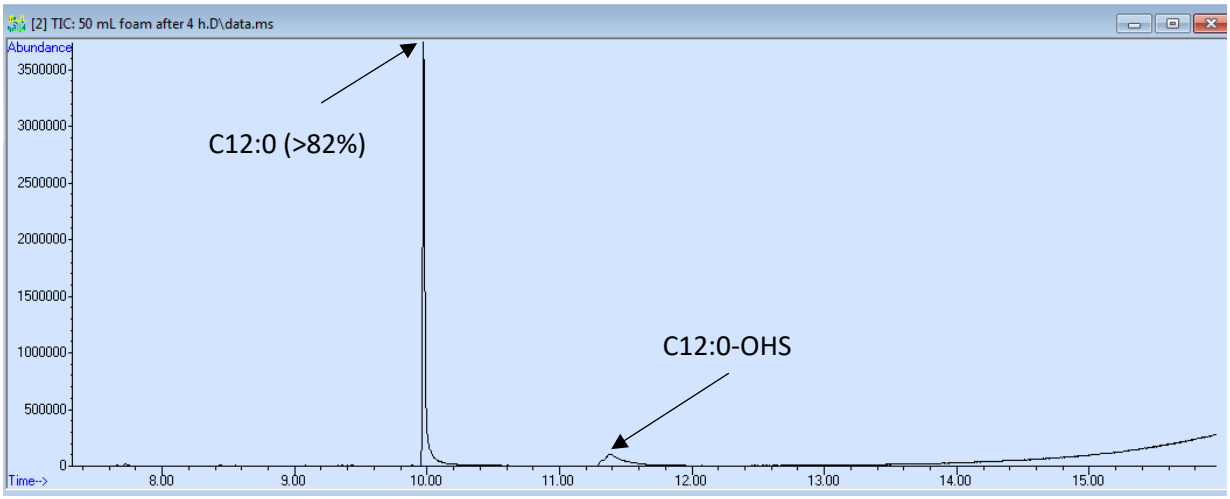

Figure 51: **Composition of the foam flushed upwards by the O_2-stream after 4 h of gassing (>82% C12:0).** No antifoam was applied in this reaction.

5.5 Influence of DMSO and EtOH on the conversion of C12:0

Table 33: **Fed-strategies for the substrate pulsing experiments for investigation of the co-solvent influence.**

Substrate stock and Co-solvent	**Fed-strategy and pulse intervals**	**Total pulsing time (min)**	**Total substrate added (mM)**	**Conversion (% GC-area)**	**Total reaction time (h)**[a]	**STY (g L^{-1} h^{-1})**
1 M C12:0 in EtOH	40 x 1 mM C12:0 1 x 5 min, 5 x 3 min, 34 x 2 min	88	40	49	5.3	0.80
1 M C12:0 in DMSO	250 x 0.16 mM C12:0 20 x 2 min, 45 x 1 min, 185 x 40 s	208	40	98	17.6	0.48
1 M C12:0 in DMSO/EtOH (1:1)	100 x 0.4 mM C12:0 3 x 100 s, 4 x 70 s, 53 x 60 s , 40 x 80 s	116	40	>99	20.2	0.43

[a] reaction was stopped as soon as no further O_2 was consumed (or in case of over night reaction at the next day)

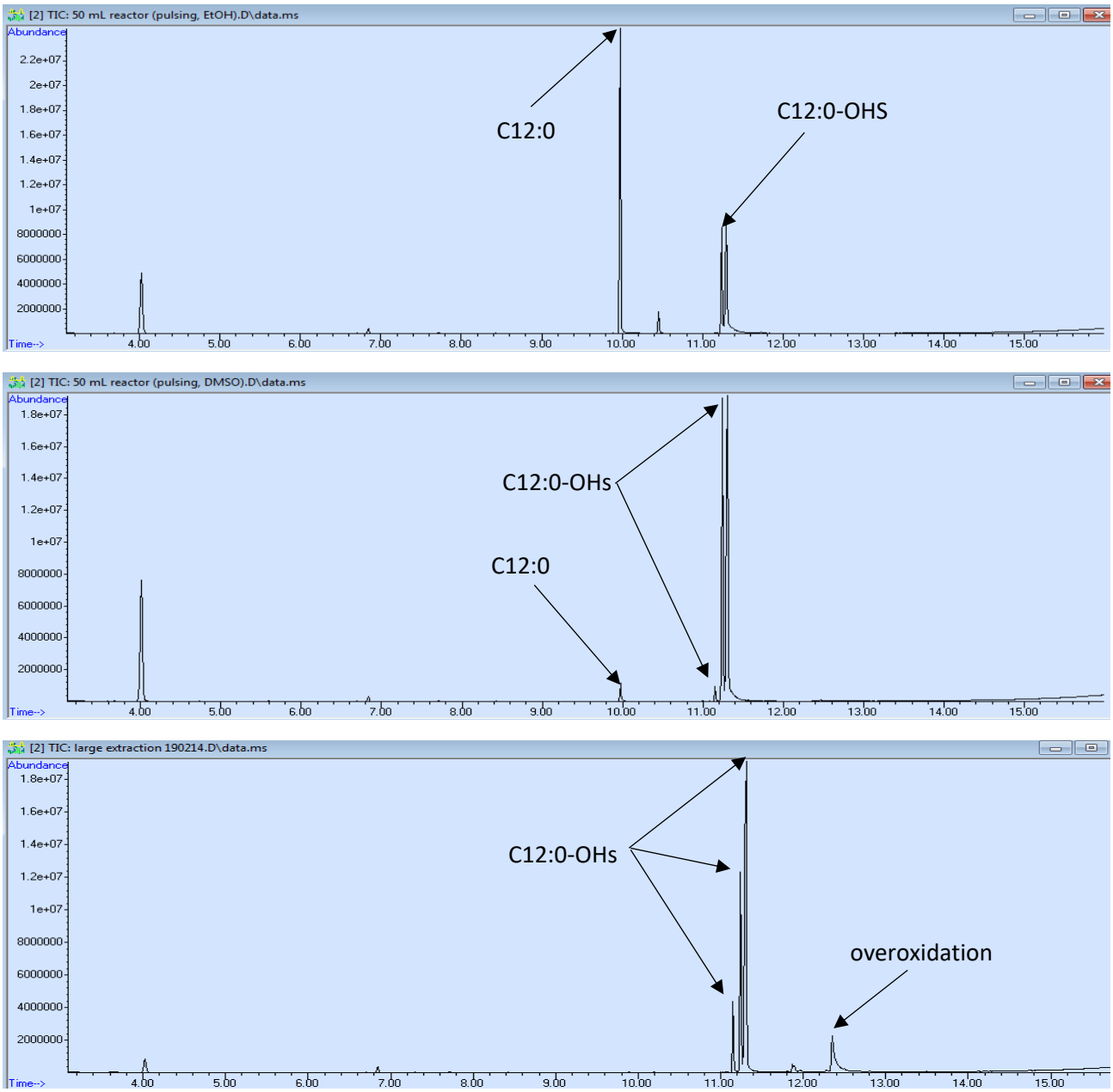

Figure 52: **Influence of the co-solvent and pulse-feeding on the conversion of C12:0 by Wt_P450 BM3 (2 µM)/Z_GDH (7 U mL^{-1}) reaction system.** The figure shows GC-MS chromatograms of the entire extracted reactions pulsed with 40 mM C12:0 in EtOH (top 5.3 h reaction time), DMSO (middle, 17.6 h reaction time) and 1:1 EtOH/DMSO (v/v, bottom, 20.2 h reaction time).

5.6 Technical summary for oxygen dependent substrate feed reactions

Table 34: **Key reaction parameters for a 40 mM C12:0 conversion with free Z_P450 BM3 (50 mL scale).**

Time (h)	KOH (mL)	Stirrer speed (rpm)	O_2 (mL min^{-1})	Feed	Loaded C12:0 (mg)
0	0	350	25		80
1.8	0.7			1st	160
3.3	1.2			2nd	240
4.7	1.5			3rd	320
5.8	---	300		4th	400
6.5	1.9				
22.2	2.3				

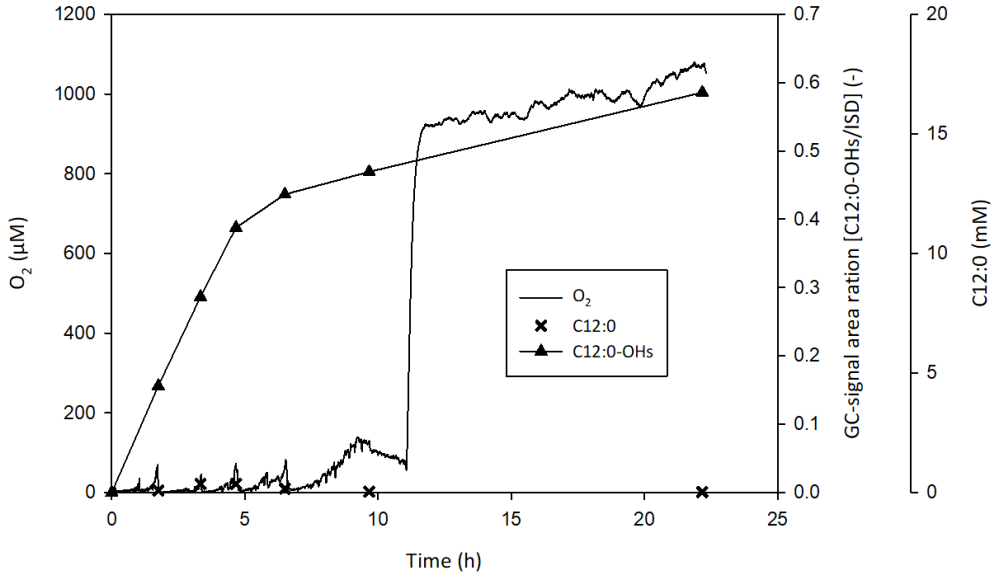

Figure 53: **Time course for the conversion of 40 mM C12:0 (here: >99%) with free Z_P450 BM3 (2 µM) and Z_GDH (10.8 U mL^{-1}).** ISD = internal standard (1-octanol).

Table 35: **Key reaction parameters for a 40 mM C12:0 conversion with co-immobilizate (50 mL scale).**

Time (h)	KOH (mL)	Stirrer speed (rpm)	O_2 (mL min^{-1})	Feed	Loaded C12:0 (mg)
0	0	350	25		80
1.1	5.7			1st	160
2.8	7.3			2nd	240
4.4	0.9			3rd	320
6.9	1.1		5	4th	400
7.5	---		2.5		
9.0	1.2				
23.0	1.4		0		

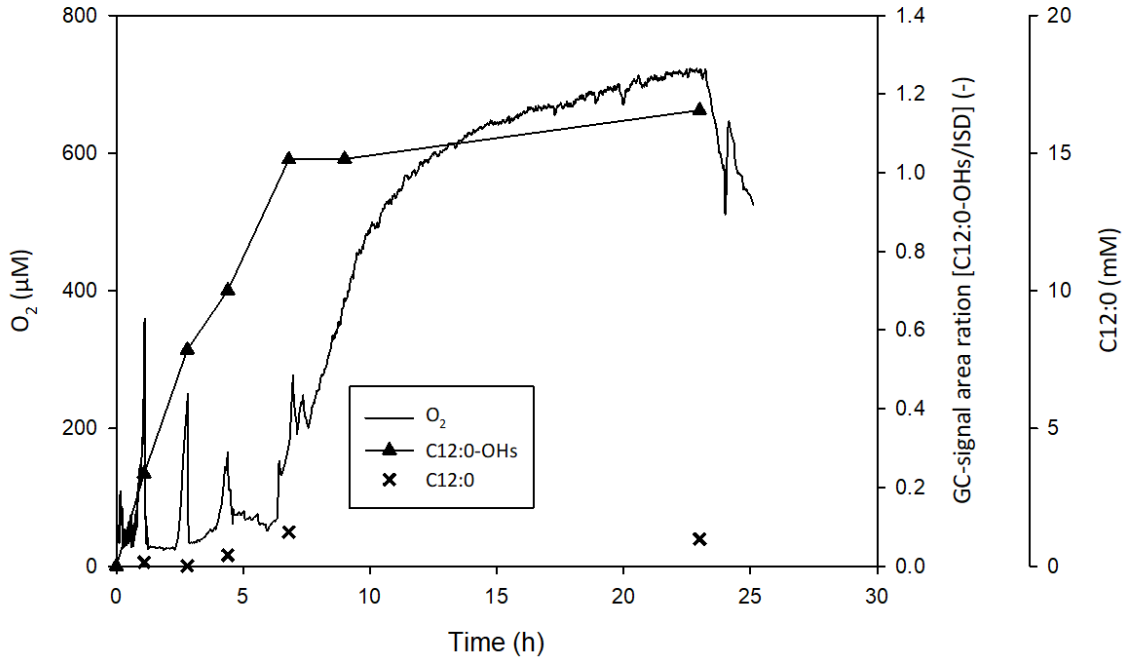

Figure 54: **Time course for the conversion of 40 mM C12:0 (here: 96.5%) with the co-immobilizate (2 µM Z_P450 BM3/10.8 U mL^{-1} Z_GDH.** Potentially, a contaminated Z_P450 BM3 CFE for immobilization was used, as a strong, uncommon smell was detectable. ISD = internal standard (1-octanol).

Table 36: **Key reaction parameters for a 48 mM C12:0 conversion with co-immobilizate (50 mL scale).**

Time (h)	KOH (mL)	Stirrer speed (rpm)	O_2 (mL min^{-1})	Feed	Loaded C12:0 (mg)
0	0	350	25		80
0.7	0.08			1st	160
1.7	0.20			2nd	240
2.8	---	250	20		
3.1	0.40			3rd	320
3.3	---	300	10		
3.8	---		5		
4.1	---		2		
5.0	0.53			4th	400
6.5	0.60			5th	480
23.5	0.63		0		

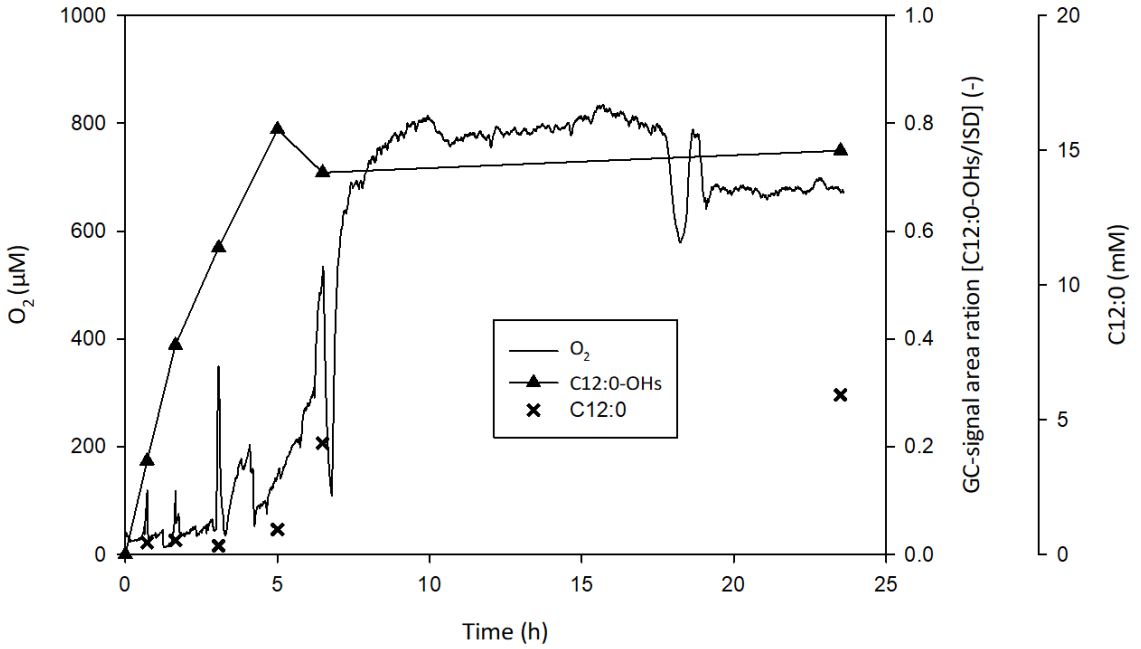

Figure 55: **Time course for the conversion of 48 mM C12:0 with the co-immobilizate (2 µM Z_P450 BM3/8.8 U mL^{-1} Z_GDH) (75% GC-area product).** ISD = internal standard (1-octanol).

Table 37: **Key reaction parameters for the conversion of 80 mM C12:0 conversion with Wt_P450 BM3 (50 mL scale).** The corresponding time course plot of the reaction is shown in Figure 35.

Time (h)	KOH (mL)	Stirrer speed (rpm)	O_2 (mL min^{-1})	Feed	Loaded C12:0 (mg)
0	0	350	25		80
0.9	0.5			1st	160
2.1	1.0			2nd	240
2.9	1.2			3rd	320
3.9	1.5			4th	400
5.1	1.7			5th	500
6.3	1.9	300		6th	600
8.5	2.1	250		7th	700
10.8	2.3		10		800
23.5	2.8				
28.0	2.9				

Table 38: **Key reaction parameters for the conversion of 80 mM C12:0 with Wt_P450 BM3 and Z_GDH (500 mL scale).** The corresponding time course plot of the reaction is shown in Figure 39.

Time (h)	KOH (mL)	Stirrer speed (rpm)	O_2 (mL min^{-1})	Feed	Loaded C12:0 (g)	total µM Wt_P450 BM3	measured µM Wt_P450 BM3	total U GDH	measured U GDH
0	0	500	50		0.8	1		3000 (Z)	
0.8	---								
1.0	1.9	550		1st	1.6				
1.7	3.8			2nd	2.4				
2.3	5.5			3rd	3.2				
2.4	---					1.2			
2.8	7.3	500		4th	4.0				
3.8	9.0			5th	5.0				
3.8	---					1.4			
4.6	10.2	400	20	6th	6.0				
5.1	---		5				0.81		
5.6	---					1.6			
7.0	1.9			7th	7.0		0.68		
9.1	12.8			8th	8.0	2			
10.0	13.4						0.95		
23.3	15.6	500	0						
24.2	---		5						0
25.2	15.9						0.87	4400 (Z)	
24.0	---		20						
26.7	19.4								
28.3	20.8							4685 (Z+DSM)	
29.5	22.3		5						
30.8	23.7						0.58		175
31.8	24.4		2						
32.5	25.0								
47.5	30.0						0.40		22

5.7 Preparative scale isolation of C12:0-OHs

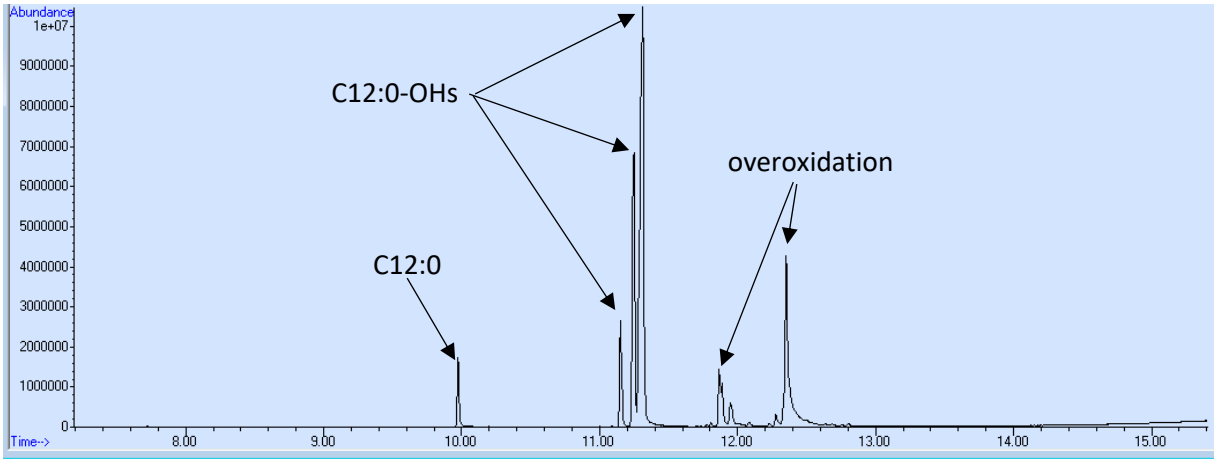

Figure 56: **GC-MS chromtogram obtained after the preparative extraction of a 36 mM C12:0 reaction (50 mL) with free Z_P450 BM3.**

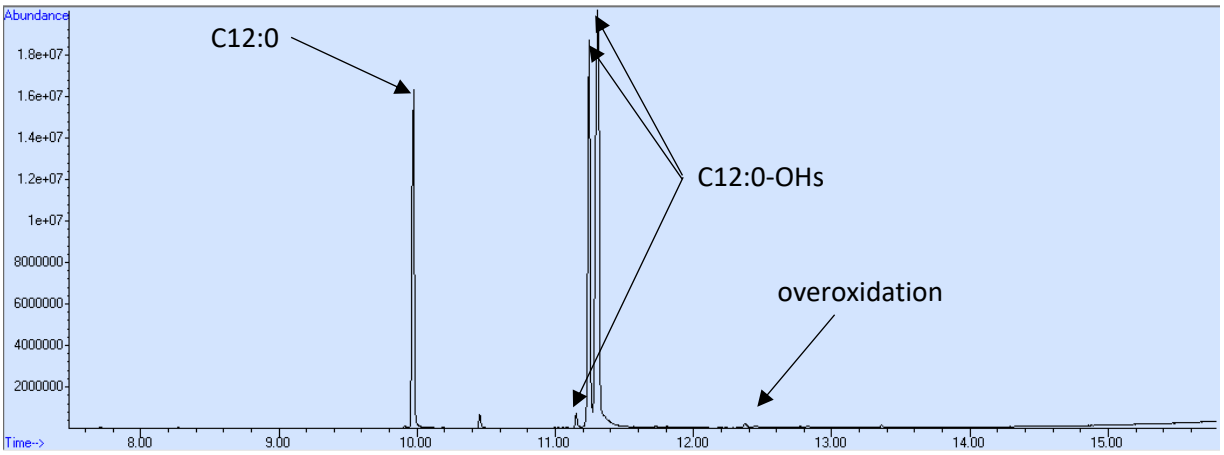

Figure 57: **GC-MS chromtogram obtained after the preparative extraction of a 40 mM C12:0 reaction (50 mL) with co-immobilizate.**

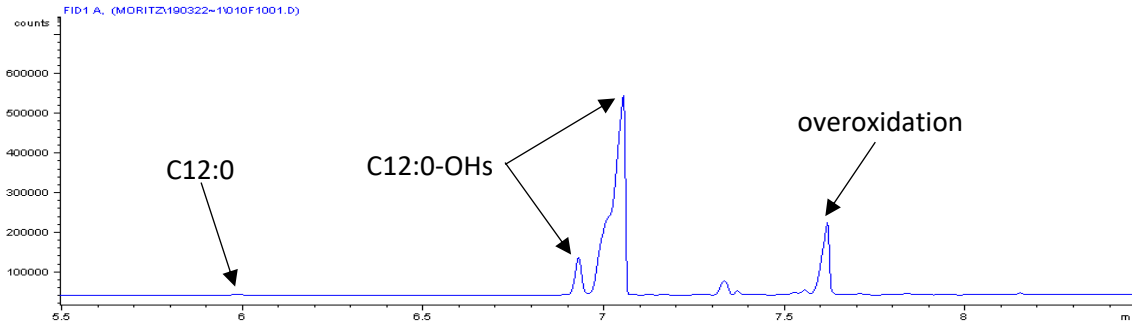

Figure 58: **GC-FID chromtogram obtained after the preparative extraction of a 40 mM C12:0 reaction (50 mL) with free Wt_P450 BM3.** The peaks for the oxeroxidation are larger compared to other reactions, as the reaction was not stopped and continued for 110 hours.

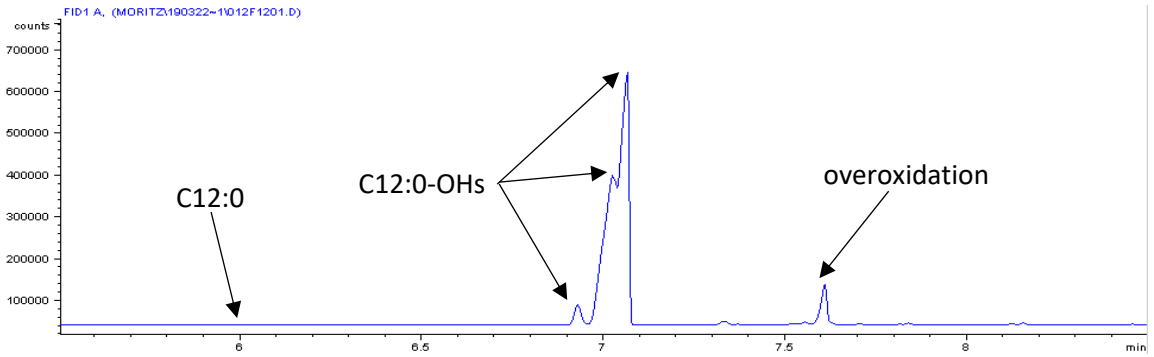

Figure 59: **GC-FID chromtogram obtained after the preparative extraction of a 80 mM C12:0 reaction (50 mL) with free Wt_P450 BM3.**

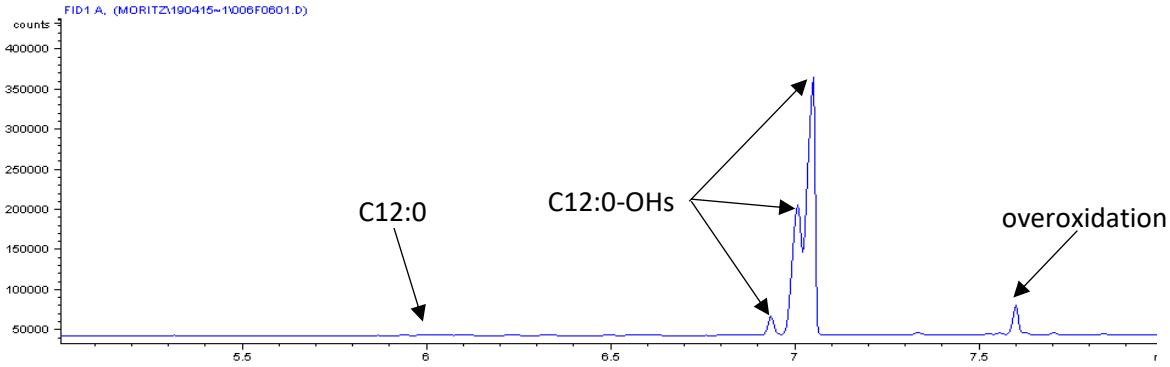

Figure 60: **GC-FID chromtogram obtained after the preparative extraction of a 40 mM C12:0 reaction (50 mL) with free Z_P450 BM3.**

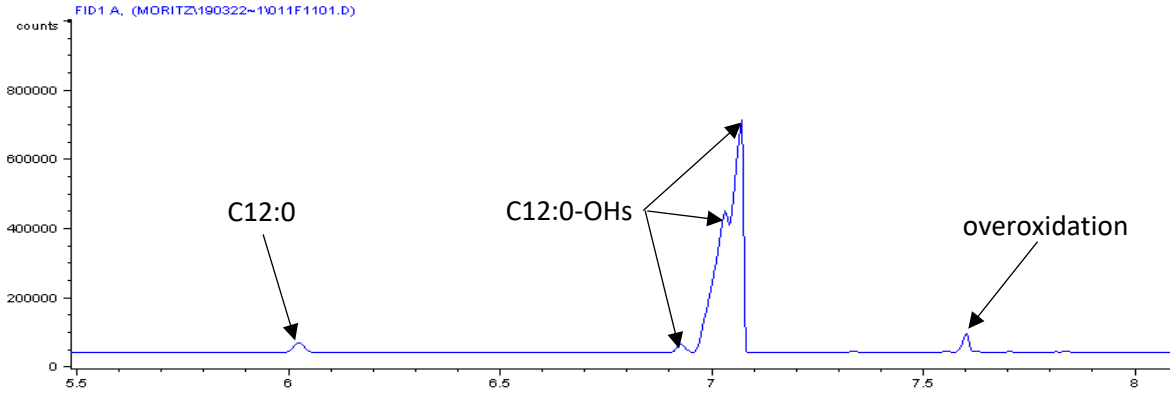

Figure 61: **GC-FID chromtogram obtained after preparative extraction of a 40 mM C12:0 reaction (50 mL) with co-immobilizate.**

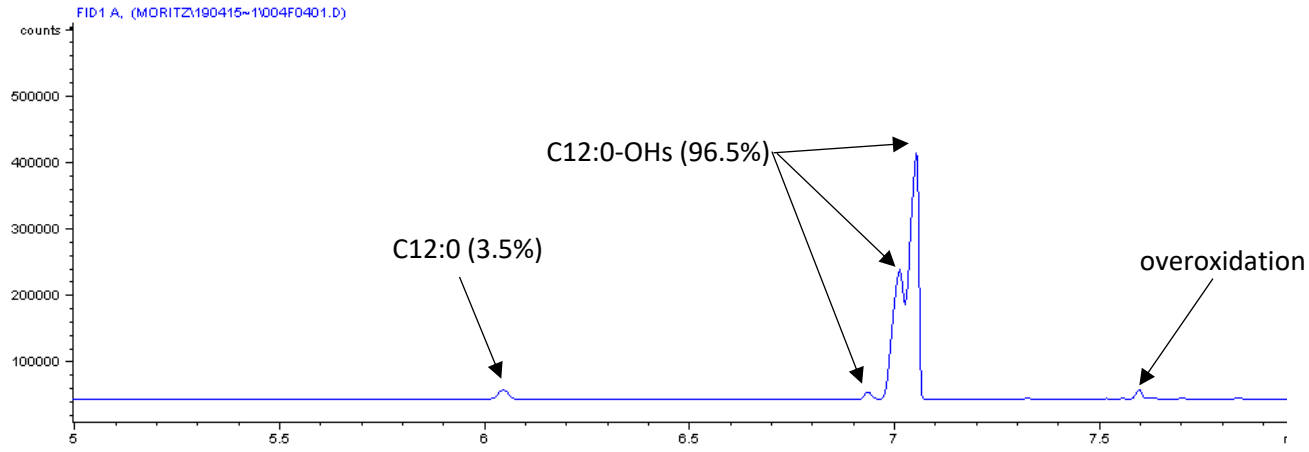

Figure 62: **GC-FID chromtogram obtained after the preparative extraction of the water phase of a 48 mM C12:0 reaction (50 mL) with co-immobilizate.**

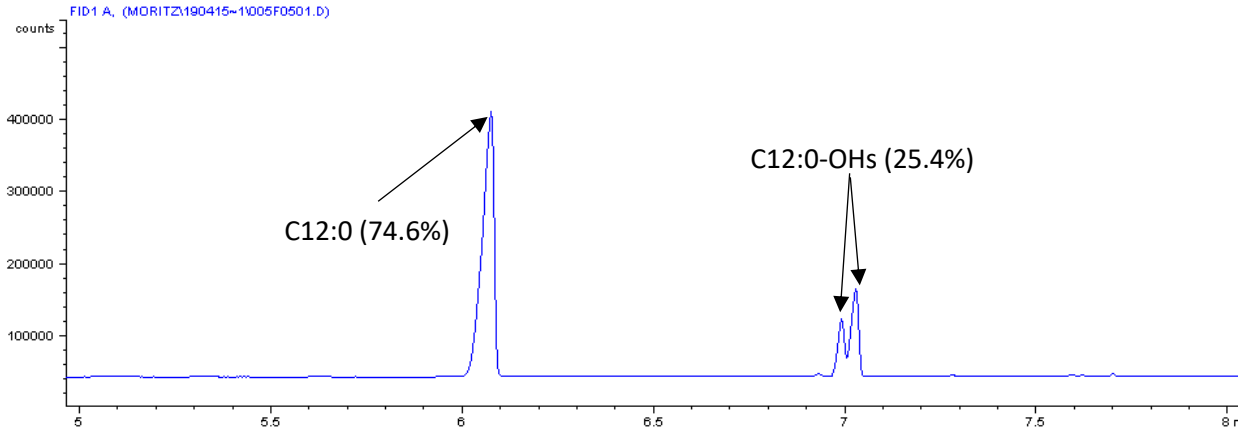

Figure 63: **GC-FID chromtogram obtained after the preparative extraction of the carrier of a 48 mM C12:0 reaction (50 mL) with co-immobilizate.**

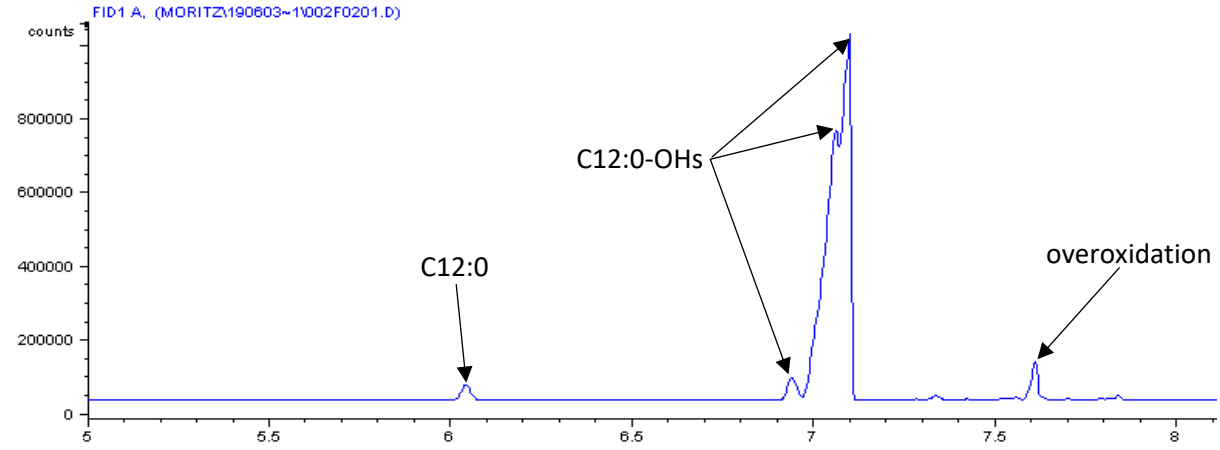

Figure 64: **GC-FID chromtogram for the preparative extraction (7 g material isolated) of the carrier of a 80 mM C12:0 reaction (500 mL) with free Wt_P450 BM3.**

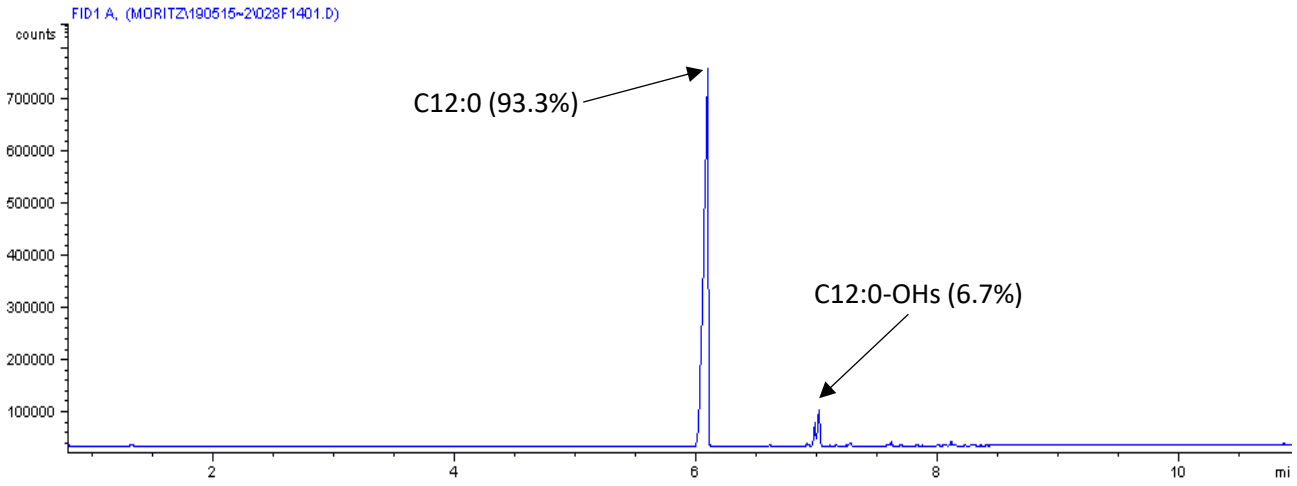

Figure 65: **GC-FID chromatogram of the removed solids from the 80 mM C12:0 reaction (500 mL).** The removed solids obtained after centrifugation were composed mainly of substrate (93.3%) and only small amount of product (6.7%).

5.8 Purification of Wt_P450 BM3 and Z_P450 BM3

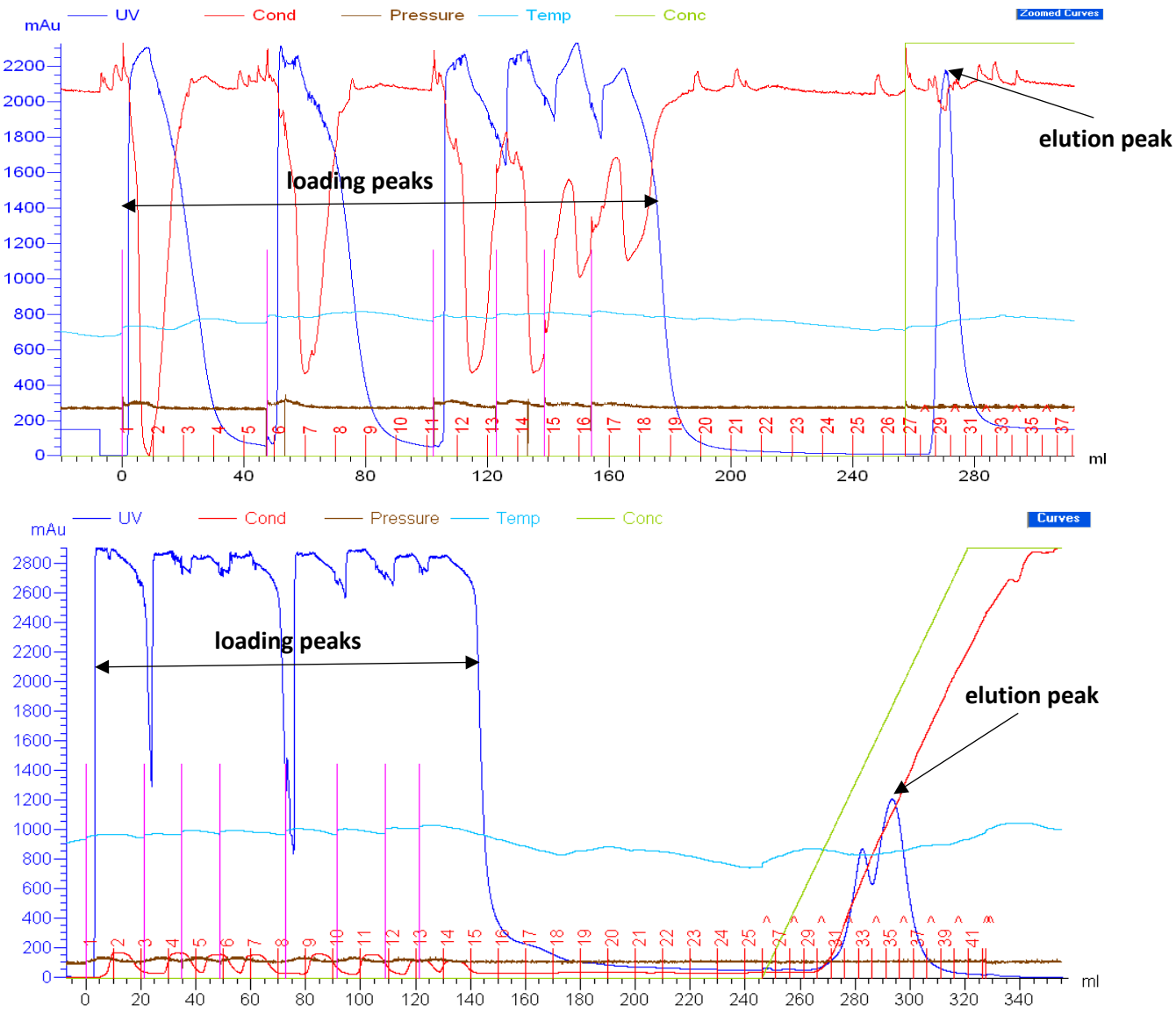

Figure 66: **Purification of Wt_P450 BM3 (top) and Z_P450 BM3 (bottom).** Wt_P450 BM3 was purified via affinity chromatography with a $NiSO_4$-His-Trap and Z_P450 BM3 via ion exchange chromatography with pre-packed HiTrap SPFF columns.

5.9 Michaelis-Menten plots

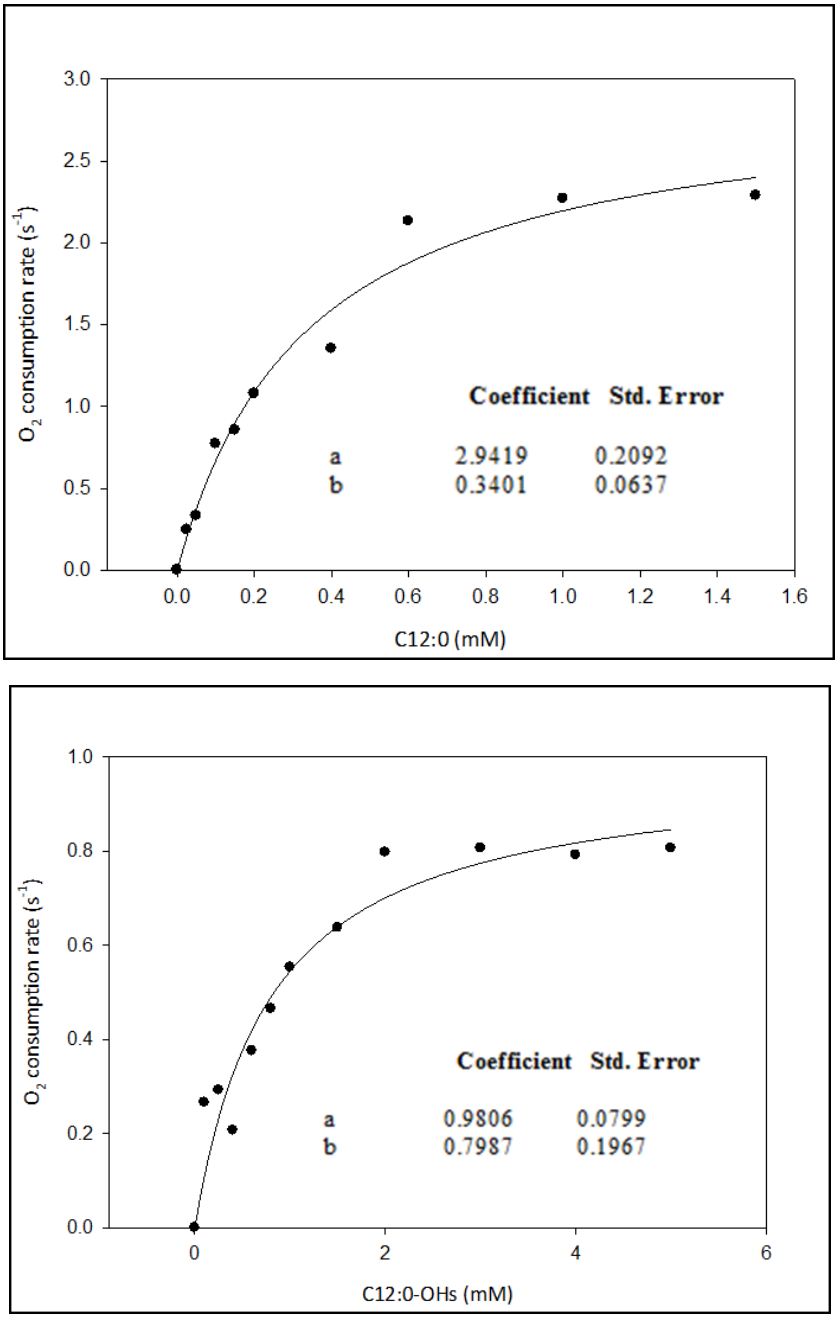

Figure 67: **Determination of the O_2 consumption rate for different C12:0 (top) and C12:0-OHs (bottom) concentrations for purified Wt_P450 BM3**. The maximal O_2 consumption rate (a) and the K_m value (b)were fitted using a hyperbolic function provided by SigmaPlot 10.0 software.

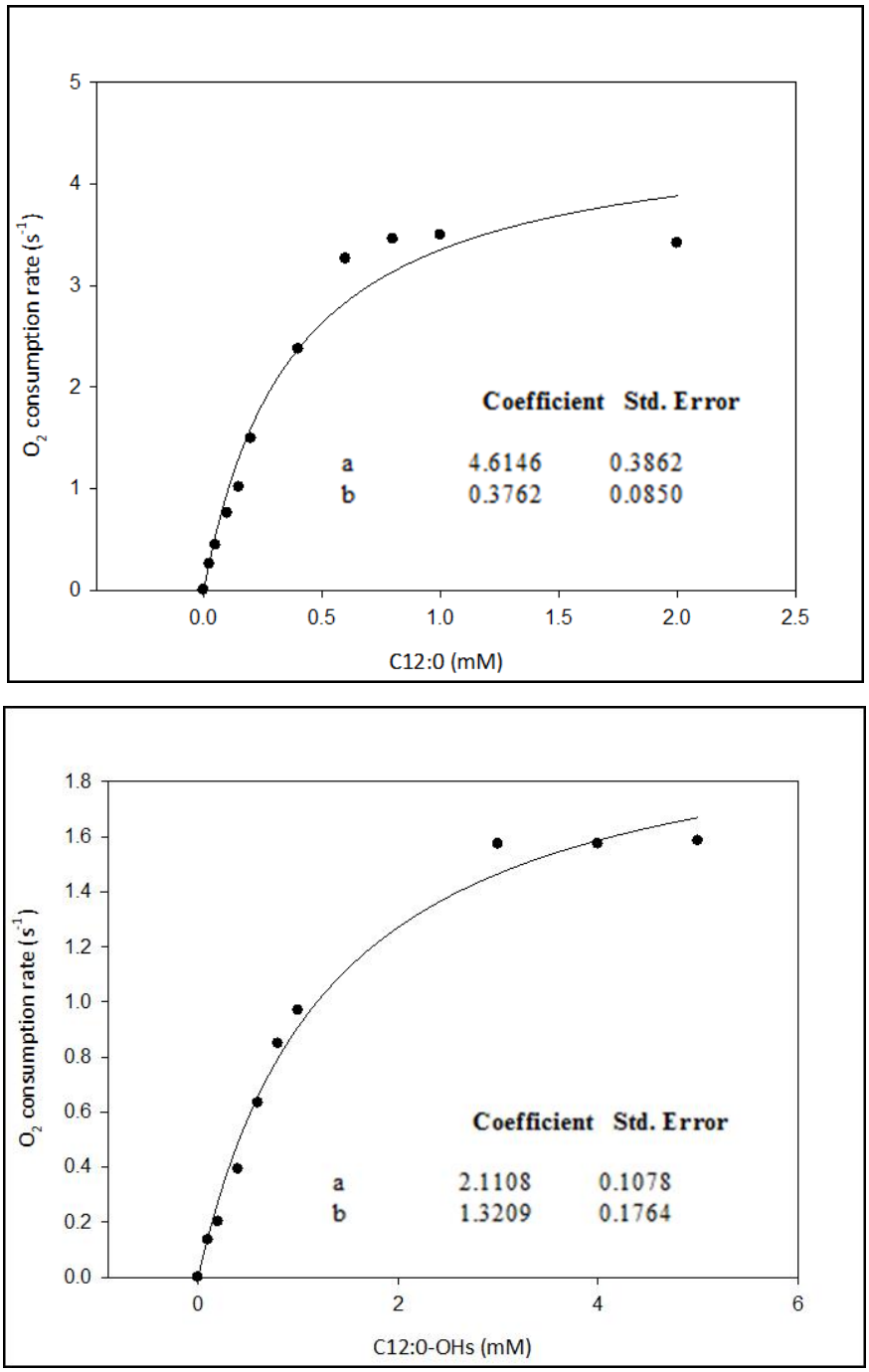

Figure 68: **Determination of the O_2 consumption rate for different C12:0 (top) and C12:0-OHs (bottom) concentrations for purified Z_P450 BM3**. The maximal O_2 consumption rate (a) and the K_m value (b)were fitted using a hyperbolic function provided by SigmaPlot 10.0 software.

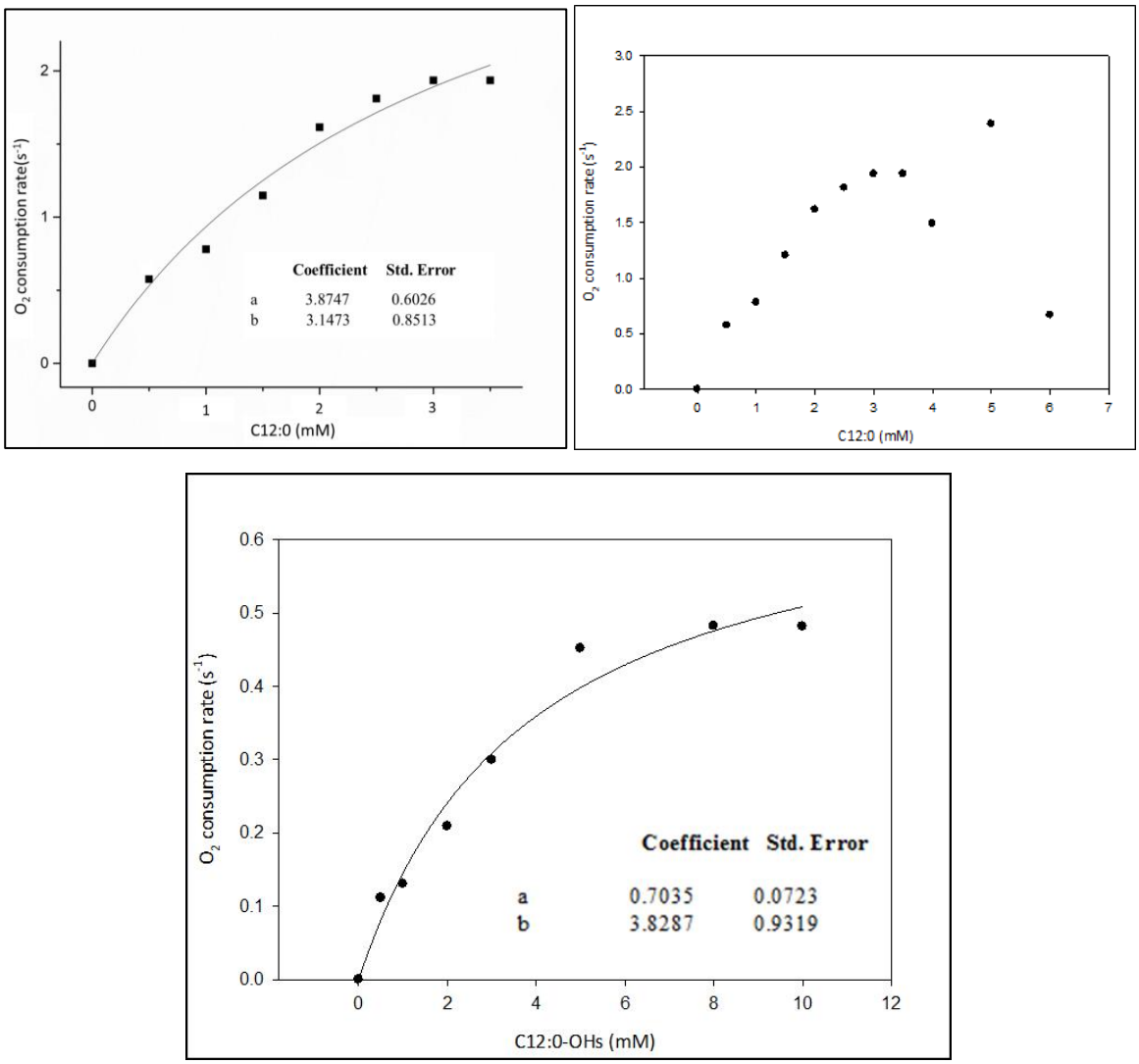

Figure 69: **Determination of the O_2 consumption rate for different C12:0 (top) and C12:0-OHs (bottom) concentrations for the co-immobilizate**. The maximal O_2 consumption rate (a) and the K_m value (b) were fitted using a hyperbolic function provided by Origin 9.0 (top) or SigmaPlot 10.0 (bottom) software. The top right diagram shows the entire measured values for C12:0 and the co-immobilizate. At a C12:0 concentration higher than 3 mM the reaction became cloudy, indicating a solubility problem.

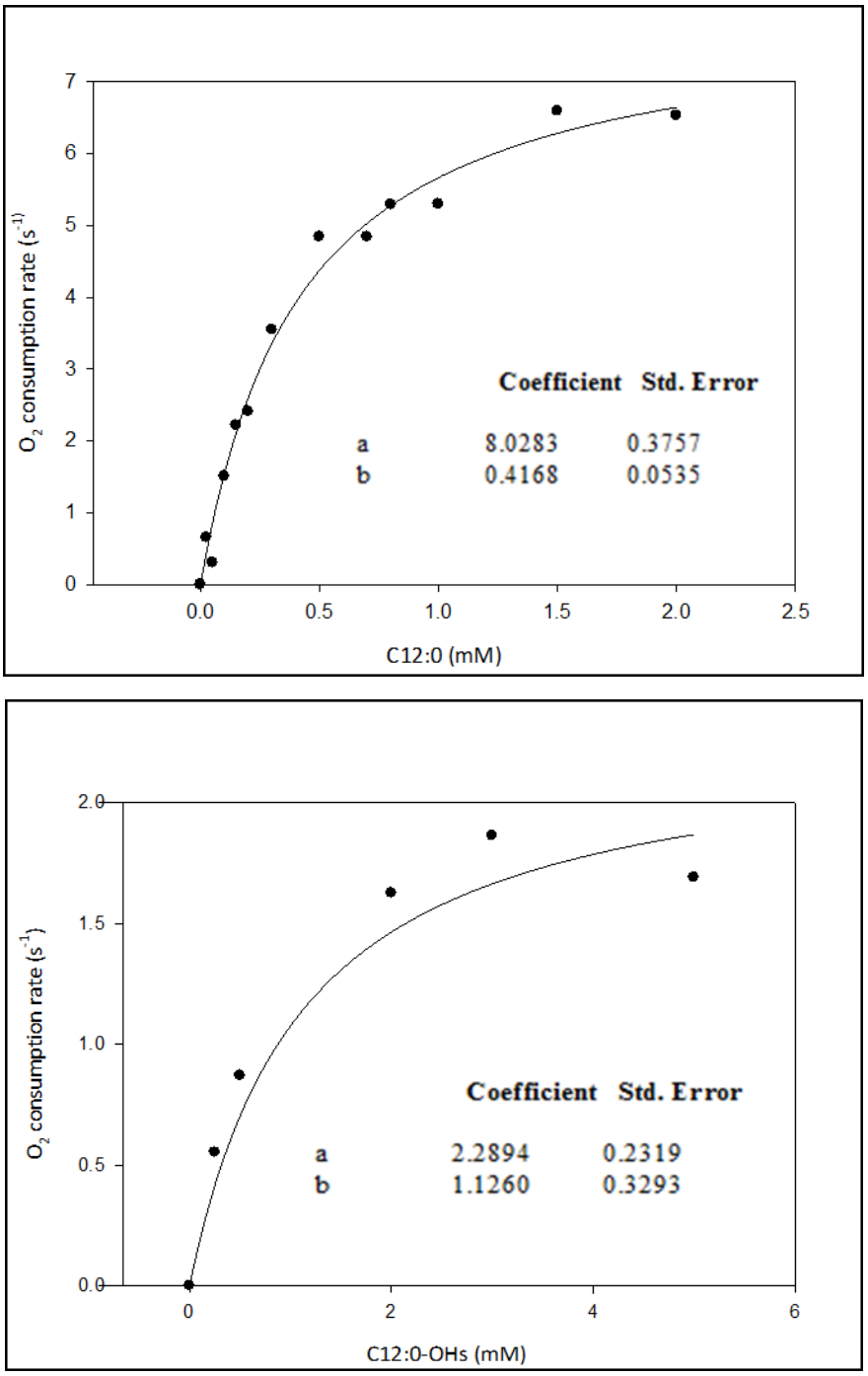

Figure 70: **Determination of the O_2 consumption rate for different C12:0 (top) and C12:0-OHs (bottom) concentrations for Wt_P450 BM3 (CFE)**. The maximal O_2 consumption rate (a) and the K_m value (b)were fitted using a hyperbolic function provided by SigmaPlot 10.0 software.

6 References

[1] Ahmed, S., Ahmed, O., Biochemistry, Lipids, StatPearls Publishing, 2018.

[2] Belitz, H.-D., Grosch, W., Schieberle, P., Lipids, in: Belitz, H.-D., Grosch, W., Schieberle, P. (Ed.). *Food Chemistry*, Springer Berlin Heidelberg, Berlin, Heidelberg, pp. 157–244.

[3] Biermann, U., Bornscheuer, U., Meier, M. A. R., Metzger, J. O. *et al.*, Oils and fats as renewable raw materials in chemistry. *Angewandte Chemie (International ed. in English)* 2011, *50*, 3854–3871, DOI: 10.1002/anie.201002767.

[4] Dennig, A., Kuhn, M., Tassoti, S., Thiessenhusen, A. *et al.*, Oxidative Decarboxylation of Short-Chain Fatty Acids to 1-Alkenes. *Angewandte Chemie (International ed. in English)* 2015, *54*, 8819–8822, DOI: 10.1002/anie.201502925.

[5] Oliw, E. H., Bylund, J., Herman, C., Bisallylic hydroxylation and epoxidation of polyunsaturated fatty acids by cytochrome P450. *Lipids* 1996, *31*, 1003–1021, DOI: 10.1007/bf02522457.

[6] Guengerich, F. P., Martin, M. V., Sohl, C. D., Cheng, Q., Measurement of cytochrome P450 and NADPH-cytochrome P450 reductase. *Nature protocols* 2009, *4*, 1245–1251, DOI: 10.1038/nprot.2009.121.

[7] Labinger, J. A., Bercaw, J. E., Understanding and exploiting C–H bond activation. *Nature* 2002, *417*, 507–514, DOI: 10.1038/417507a.

[8] Scheps, D., Honda Malca, S., Richter, S. M., Marisch, K. *et al.*, Synthesis of omega-hydroxy dodecanoic acid based on an engineered CYP153A fusion construct. *Microbial biotechnology* 2013, *6*, 694–707, DOI: 10.1111/1751-7915.12073.

[9] Hammerer, L., Winkler, C. K., Kroutil, W., Regioselective Biocatalytic Hydroxylation of Fatty Acids by Cytochrome P450s. *Chem. Commun.* 2018, *148*, 787–812, DOI: 10.1007/s10562-017-2273-4.

[10] Urlacher, V. B., Girhard, M., Cytochrome P450 monooxygenases: An update on perspectives for synthetic application. *Trends in biotechnology* 2012, *30*, 26–36, DOI: 10.1016/j.tibtech.2011.06.012.

[11] Cao, Y., Zhang, X., Production of long-chain hydroxy fatty acids by microbial conversion. *Applied microbiology and biotechnology* 2013, *97*, 3323–3331, DOI: 10.1007/s00253-013-4815-z.

[12] Kim, K.-R., Oh, D.-K., Production of hydroxy fatty acids by microbial fatty acid-hydroxylation enzymes. *Biotechnology advances* 2013, *31*, 1473–1485, DOI: 10.1016/j.biotechadv.2013.07.004.

[13] Prasad, B., Mah, D. J., Lewis, A. R., Plettner, E., Water oxidation by a cytochrome p450: Mechanism and function of the reaction. *PloS one* 2013, *8*, e61897, DOI: 10.1371/journal.pone.0061897.

[14] Meunier, B., Visser, S. P. de, Shaik, S., Mechanism of oxidation reactions catalyzed by cytochrome p450 enzymes. *Chemical reviews* 2004, *104*, 3947–3980, DOI: 10.1021/cr020443g.

[15] Larsen, B. T., Gutterman, D. D., Sato, A., Toyama, K. *et al.*, Hydrogen peroxide inhibits cytochrome p450 epoxygenases: Interaction between two endothelium-derived hyperpolarizing factors. *Circulation research* 2008, *102*, 59–67, DOI: 10.1161/CIRCRESAHA.107.159129.

[16] Girhard, M., Schuster, S., Dietrich, M., Dürre, P. *et al.*, Cytochrome P450 monooxygenase from Clostridium acetobutylicum: A new alpha-fatty acid hydroxylase. *Biochemical and biophysical research communications* 2007, *362*, 114–119, DOI: 10.1016/j.bbrc.2007.07.155.

[17] Burek, B. O., Bormann, S., Hollmann, F., Bloh, J. Z. *et al.*, Hydrogen peroxide driven biocatalysis. *Green Chem.* 2019, *21*, 3232–3249, DOI: 10.1039/C9GC00633H.

[18] Grinkova, Y. V., Denisov, I. G., McLean, M. A., Sligar, S. G., Oxidase uncoupling in heme monooxygenases: Human cytochrome P450 CYP3A4 in Nanodiscs. *Biochemical and biophysical research communications* 2013, *430*, 1223–1227, DOI: 10.1016/j.bbrc.2012.12.072.

[19] Whitehouse, C. J. C., Bell, S. G., Wong, L.-L., P450(BM3) (CYP102A1): Connecting the dots. *Chemical Society reviews* 2012, *41*, 1218–1260, DOI: 10.1039/c1cs15192d.

[20] Johnston, J. B., Ouellet, H., Podust, L. M., Ortiz de Montellano, P. R., Structural control of cytochrome P450-catalyzed ω-hydroxylation. *Archives of biochemistry and biophysics* 2011, *507*, 86–94, DOI: 10.1016/j.abb.2010.08.011.

[21] Munro, A. W., Leys, D. G., McLean, K. J., Marshall, K. R. *et al.*, P450 BM3: The very model of a modern flavocytochrome. *Trends in Biochemical Sciences* 2002, *27*, 250–257, DOI: 10.1016/S0968-0004(02)02086-8.

[22] Weckbecker, A., Hummel, W., Glucose Dehydrogenase for the Regeneration of NADPH and NADH, in: Barredo, J. L. (Ed.). *Microbial Enzymes and Biotransformations*, Humana Press, Totowa, NJ, pp. 225–238.

[23] Vrtis, J. M., White, A. K., Metcalf, W. W., van der Donk, W. A., Phosphite Dehydrogenase: A Versatile Cofactor-Regeneration Enzyme. *Angewandte Chemie (International ed. in English)* 2002, *41*, 3257–3259, DOI: 10.1002/1521-3773(20020902)41:17<3257:AID-ANIE3257>3.0.CO;2-N.

[24] Johannes, T. W., Woodyer, R. D., Zhao, H., Efficient regeneration of NADPH using an engineered phosphite dehydrogenase. *Biotechnology and bioengineering* 2007, *96*, 18–26, DOI: 10.1002/bit.21168.

[25] Bernhardt, R., Urlacher, V. B., Cytochromes P450 as promising catalysts for biotechnological application: Chances and limitations. *Applied microbiology and biotechnology* 2014, *98*, 6185–6203, DOI: 10.1007/s00253-014-5767-7.

[26] Kuper, J., Wong, T. S., Roccatano, D., Wilmanns, M. *et al.*, Understanding a mechanism of organic cosolvent inactivation in heme monooxygenase P450 BM-3. *Journal of the American Chemical Society* 2007, *129*, 5786–5787, DOI: 10.1021/ja067036x.

[27] Maurer, S. C., Kühnel, K., Kaysser, L. A., Eiben, S. *et al.*, Catalytic Hydroxylation in Biphasic Systems using CYP102A1 Mutants. *Adv. Synth. Catal.* 2005, *347*, 1090–1098, DOI: 10.1002/adsc.200505044.

[28] Maurer, S. C., Oxidationsreaktionen mittels der Cytochrom P450-Monooxygenase CYP102A1 in Enzymreaktoren, Universität Stuttgart, 2006.

[29] Kühnel, K., Maurer, S. C., Galeyeva, Y., Frey, W. *et al.*, Hydroxylation of Dodecanoic Acid and (2R,4R,6R,8R)-Tetramethyldecanol on a Preparative Scale using an NADH- Dependent CYP102A1 Mutant. *Adv. Synth. Catal.* 2007, *349*, 1451–1461, DOI: 10.1002/adsc.200700054.

[30] Cao, Y., Cheng, T., Zhao, G., Niu, W. *et al.*, Metabolic engineering of Escherichia coli for the production of hydroxy fatty acids from glucose. *BMC biotechnology* 2016, *16*, 26, DOI: 10.1186/s12896-016-0257-x.

[31] Valikhani, D., Bolivar, J. M., Dennig, A., Nidetzky, B., A tailor-made, self-sufficient and recyclable monooxygenase catalyst based on coimmobilized cytochrome P450 BM3 and glucose dehydrogenase. *Biotechnology and bioengineering* 2018, *115*, 2416–2425, DOI: 10.1002/bit.26802.

[32] Xing, W., Yin, M., Lv, Q., Hu, Y. *et al.*, Oxygen Solubility, Diffusion Coefficient, and Solution Viscosity, in: Xing, W., Yin, G., Zhang, J. (Ed.). *Rotating electrode methods and oxygen reduction electrocatalysts*, Elsevier, Amsterdam, pp. 1–31.

[33] Hoschek, A., Schmid, A., Bühler, B., In Situ O 2 Generation for Biocatalytic Oxyfunctionalization Reactions. *ChemCatChem* 2018, *10*, 5366–5371, DOI: 10.1002/cctc.201801262.

[34] Karimi, A., Golbabaei, F., Mehrnia, M. R., Neghab, M. *et al.*, Oxygen mass transfer in a stirred tank bioreactor using different impeller configurations for environmental purposes. *Iranian journal of environmental health science & engineering* 2013, *10*, 6, DOI: 10.1186/1735-2746-10-6.

[35] Garcia-Ochoa, F., Gomez, E., Bioreactor scale-up and oxygen transfer rate in microbial processes: An overview. *Biotechnology advances* 2009, *27*, 153–176, DOI: 10.1016/j.biotechadv.2008.10.006.

[36] Hoschek, A., Bühler, B., Schmid, A., Overcoming the Gas-Liquid Mass Transfer of Oxygen by Coupling Photosynthetic Water Oxidation with Biocatalytic Oxyfunctionalization. *Angewandte Chemie (International ed. in English)* 2017, *56*, 15146–15149, DOI: 10.1002/anie.201706886.

[37] Bolivar, J. M., Mannsberger, A., Thomsen, M. S., Tekautz, G. *et al.*, Process intensification for O2 -dependent enzymatic transformations in continuous single-phase pressurized flow. *Biotechnology and bioengineering* 2019, *116*, 503–514, DOI: 10.1002/bit.26886.

[38] Solé, J., Brummund, J., Caminal, G., Álvaro, G. *et al.*, Enzymatic Synthesis of Trimethyl-ε-caprolactone: Process Intensification and Demonstration on a 100 L Scale. *Org. Process Res. Dev.* 2019, DOI: 10.1021/acs.oprd.9b00185.

[39] Kaluzna, I., Schmitges, T., Straatman, H., van Tegelen, D. *et al.*, Enabling Selective and Sustainable P450 Oxygenation Technology. Production of 4-Hydroxy-α-isophorone on Kilogram Scale. *Org. Process Res. Dev.* 2016, *20*, 814–819, DOI: 10.1021/acs.oprd.5b00282.

[40] Thompson, M. P., Derrington, S. R., Heath, R. S., Porter, J. L. *et al.*, A generic platform for the immobilisation of engineered biocatalysts. *Tetrahedron* 2019, *75*, 327–334, DOI: 10.1016/j.tet.2018.12.004.

[41] Basso, A., Serban, S., Industrial applications of immobilized enzymes—A review. *Molecular Catalysis* 2019, *479*, 110607, DOI: 10.1016/j.mcat.2019.110607.

[42] DiCosimo, R., McAuliffe, J., Poulose, A. J., Bohlmann, G., Industrial use of immobilized enzymes. *Chemical Society reviews* 2013, *42*, 6437–6474, DOI: 10.1039/c3cs35506c.

[43] Bahrami, A., Garnier, A., Larachi, F., Iliuta, M. C., Covalent immobilization of cytochrome P450 BM3 (R966D/W1046S) on glutaraldehyde activated SPIONs. *Can. J. Chem. Eng.* 2018, *96*, 2227–2235, DOI: 10.1002/cjce.23208.

[44] Maurer, S. C., Schulze, H., Schmid, R. D., Urlacher, V., Immobilisation of P450 BM-3 and an NADP+ Cofactor Recycling System: Towards a Technical Application of Heme-Containing Monooxygenases in Fine Chemical Synthesis. *Adv. Synth. Catal.* 2003, *345*, 802–810, DOI: 10.1002/adsc.200303021.

[45] Solé, J., Caminal, G., Schürmann, M., Álvaro, G. *et al.*, Co-immobilization of P450 BM3 and glucose dehydrogenase on different supports for application as a self-sufficient oxidative biocatalyst. *J. Chem. Technol. Biotechnol.* 2019, *94*, 244–255, DOI: 10.1002/jctb.5770.

[46] Bolivar, J. M., Nidetzky, B., Oriented and selective enzyme immobilization on functionalized silica carrier using the cationic binding module Z basic2: Design of a heterogeneous D-amino acid oxidase catalyst on porous glass. *Biotechnology and bioengineering* 2012, *109*, 1490–1498, DOI: 10.1002/bit.24423.

[47] Wiesbauer, J., Bolivar, J. M., Mueller, M., Schiller, M. *et al.*, Oriented Immobilization of Enzymes Made Fit for Applied Biocatalysis: Non-Covalent Attachment to Anionic Supports using Zbasic2 Module. *ChemCatChem* 2011, *3*, 1299–1303, DOI: 10.1002/cctc.201100103.

[48] OMURA, T., SATO, R., THE CARBON MONOXIDE-BINDING PIGMENT OF LIVER MICROSOMES. I. EVIDENCE FOR ITS HEMOPROTEIN NATURE. *The Journal of biological chemistry* 1964, *239*, 2370–2378.

[49] Fitch, C. A., Platzer, G., Okon, M., Garcia-Moreno, B. E. *et al.*, Arginine: Its pKa value revisited. *Protein science a publication of the Protein Society* 2015, *24*, 752–761, DOI: 10.1002/pro.2647.

[50] Dennig Alexander, Engineering of cytochrome P450 monooxygenases for application in phenol synthesis, 2013.

[51] Ramachandran, S., Fontanille, P., Pandey, A., Larroche, C., Gluconic Acid: Properties, Applications and Microbial Production 2006, 185–195.

[52] Liu, X., Kong, J.-Q., Steroids hydroxylation catalyzed by the monooxygenase mutant 139-3 from Bacillus megaterium BM3. *Acta pharmaceutica Sinica. B* 2017, *7*, 510–516, DOI: 10.1016/j.apsb.2017.04.006.

[53] Nishioka, T., Yasutake, Y., Nishiya, Y., Tamura, T., Structure-guided mutagenesis for the improvement of substrate specificity of Bacillus megaterium glucose 1-dehydrogenase IV. *The FEBS journal* 2012, *279*, 3264–3275, DOI: 10.1111/j.1742-4658.2012.08713.x.

[54] Angelastro, A., Dawson, W. M., Luk, L. Y. P., Allemann, R. K., A Versatile Disulfide-Driven Recycling System for NADP + with High Cofactor Turnover Number. *ACS Catal.* 2017, *7*, 1025–1029, DOI: 10.1021/acscatal.6b03061.

[55] van der Donk, W. A., Zhao, H., Recent developments in pyridine nucleotide regeneration. *Current Opinion in Biotechnology* 2003, *14*, 421–426, DOI: 10.1016/S0958-1669(03)00094-6.

[56] Kunjapur, A. M., Tarasova, Y., Prather, K. L. J., Synthesis and accumulation of aromatic aldehydes in an engineered strain of Escherichia coli. *Journal of the American Chemical Society* 2014, *136*, 11644–11654, DOI: 10.1021/ja506664a.

[57] Domingues, M. A. F., Ribeiro, A. P. B., Kieckbusch, T. G., Gioielli, L. A. *et al.*, Advances in Lipids Crystallization Technology, in: Mastai, Y. (Ed.). *Advanced Topics in Crystallization*, InTech, [S.l.].

[58] Dennig, A., Blaschke, F., Gandomkar, S., Tassano, E. *et al.*, Preparative Asymmetric Synthesis of Canonical and Non-canonical α-amino Acids Through Formal Enantioselective Biocatalytic Amination of Carboxylic Acids. *Adv. Synth. Catal.* 2018, *361*, 1348–1358, DOI: 10.1002/adsc.201801377.

[59] Doran, P. M., *Bioprocess engineering principles,* 2nd edn., Academic Press, Waltham, MA, 2013.

[60] Bommarius, A. S., Karau, A., Deactivation of formate dehydrogenase (FDH) in solution and at gas-liquid interfaces. *Biotechnology progress* 2005, *21*, 1663–1672, DOI: 10.1021/bp050249q.

[61] Ahmed, F., Avery, K. L., Cullis, P. M., Primrose, W. U. *et al.*, An unusual matrix of stereocomplementarity in the hydroxylation of monohydroxy fatty acids catalysed by cytochrome P450 from Bacillus megaterium with potential application in biotransformations. *Chem. Commun.* 1999, 2049–2050, DOI: 10.1039/a905974a.

[62] Dennig, A., Busto, E., Kroutil, W., Faber, K., Biocatalytic One-Pot Synthesis of l -Tyrosine Derivatives from Monosubstituted Benzenes, Pyruvate, and Ammonia. *ACS Catal.* 2015, *5*, 7503–7506, DOI: 10.1021/acscatal.5b02129.

[63] Kuper, J., Tee, K. L., Wilmanns, M., Roccatano, D. *et al.*, The role of active-site Phe87 in modulating the organic co-solvent tolerance of cytochrome P450 BM3 monooxygenase. *Acta crystallographica. Section F, Structural biology and crystallization communications* 2012, *68*, 1013–1017, DOI: 10.1107/S1744309112031570.